First Annual Meeting of Kazakh Physical Society

10-13 October 2018, Nazarbayev University, Astana

NAZARBAYEV UNIVERSITY
SCHOOL OF SCIENCE AND TECHNOLOGY

Scientific Program

Chair: Prof. T. A. Kozhamkulov, President of KPS
Co-Chairs: Prof. K. A. Baigarin, Head of Astana Branch of KPS, Nazarbayev University
Prof. T. S. Ramazanov, Vice-President of KPS, Al Farabi University

Scientific Program Committee:

KazNU: T. A. Kozhamkulov, T. S. Ramazanov, A. E. Davletov, M. E. Abishev; ***NU***: K. A. Baigarin, A. Nurmukhanbetova, Z. Utegulov, A. Tikhonov, A. Desyatnikov, A. Bountis, M. Kaikanov; ***ENU***: R. Myrzakulov, A. K. Aryngazin, K. S. Zhumadilov, A. Dauletbekova; ***KBTU***: M. T. Gabdullin, ***KazNTU***: S. E. Kumekov, A. T. Mustafin; ***KazNPU***: S. K. Sakhiyev, V. N. Kosov; ***NNC***: E. G. Batyrbekov, M. K. Skakov; ***INP***: N. T. Burtebayev, T. Zholdybayev, M. Zdorovets; ***PTI***: T. K. Sadykov; ***FAPI***: L. M. Chechin; A. Zh. Bibossinov; ***II***: V. M. Somsikov; ***KSU***: N. Ibrayev

Local Organizing Committee:

Astana Branch of KPS
Physics Department, Nazarbayev University
L. N. Gumilyov Eurasian National University

Organizational and financial support

Nazarbayev University
School of Science and Technology
Support team:
- Arailym Konysbayeva
- Nazira Temirkhanova
- Kuralay Baimenova
- Gulsina Adamova
- Ainura Shakirova

Student volunteers:
- Sabina Sagynbayeva
- Yegor Polikarpov
- Tileubek Uakhitov
- Abdybek Urmanov

Venue

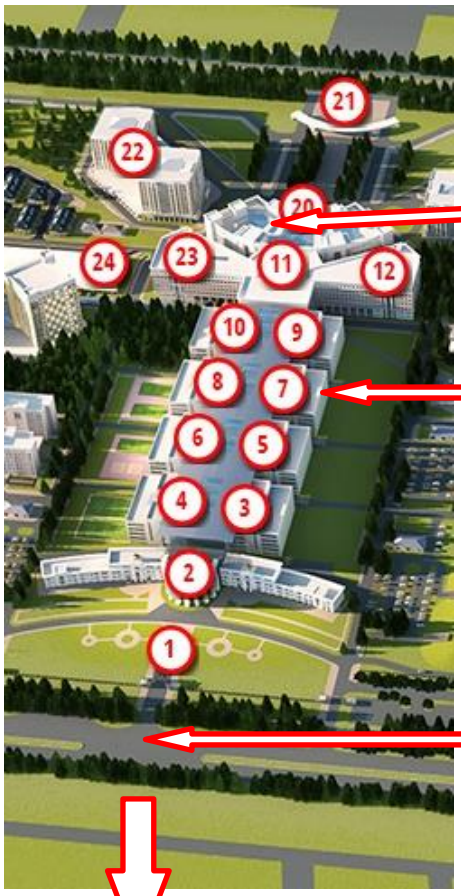

Lunch at Kunde Social Cafe, Block C-2

Block 7, Floor 3, ***Lecture Hall 7e.329***
School of Science and Technology
All presentations and coffee breaks

Main entrance, 53 Kabanbay Batyr Ave
Please bring your ID card or passport

Shopping mall “Mega Silk Way”

Time	Wednesday 10 October
8:30	Registration
9:00	Annual Meeting Opening Chair **K. A. Baigarin**, Head of Astana Branch of KPS, Nazarbayev University *Opening Remarks* by Prof. **Ilesanmi Adesida,** Provost of Nazarbayev University
9:15	**T. A. Kozhamkulov**, President of Kazakh Physical Society *Kazakh Physical Society problems and perspectives of the development*
9:30	General Assembly of Kazakh Physical Society Chair **M. Abishev**, Scientific Secretary of Kazakh Physical Society
10:00	Coffee break
	Chair: V. Kovanis, Nazarbayev University
10:40	**M. Abishev**, Al-Farabi Kazakh National University *Nonlinear electrodynamics effects in the strong magnetic field*
11:00	**A. Bountis**, Nazarbayev University *Dynamics of Classical Nonlinear Hamiltonian Lattices*
11:20	**A. E. Davletov**, Al-Farabi Kazakh National University *Thermodynamics and dust-acoustic wave dispersion in strongly coupled dusty plasmas*
11:40	**V. Dzhunushaliev**, Al-Farabi Kazakh National University *Gluon contribution to the proton spin by using the non-perturbative quantization a la Heisenberg*
12:00	Lunch and Poster Session
	Chair: A. S. Desyatnikov, Nazarbayev University
13:40	**S. E. Kumekov**, Satbayev Kazakh National Technical University *Diffuse Spectra of Photoluminescence of Carbon Quantum Dots*
14:00	**T. M. Inerbaev**, L. N. Gumilyov Eurasian National University *Non-Equilibrium Charge Dynamics in Functionalized Titania*
14:20	**Z. N. Utegulov**, Nazarbayev University *Nanosecond Laser Melting Thresholds in Refractory Metals Detected by Laser Generated Acoustic Shear Waves*
14:40	**Y. A. Ussenov**, Al-Farabi Kazakh National University *"Coulomb crystal" experiments under microgravity conditions and diagnostics of complex plasma*
15:00	Coffee break
	Chair: S. E. Kumekov, Satbayev Kazakh National Technical University
15:40	**A. B. Tazhen**, Al-Farabi Kazakh National University *Experimental modeling of dust formation in fusion reactors by pulsed plasma accelerator. Pulsed plasma diagnostics.*
16:00	**A. Tikhonov**, Nazarbayev University *Materials surface modification with pulsed ion beam: using the new INURA accelerator facility at Nazarbayev University*
16:20	**A. I. Fedosimova**, Al-Farabi Kazakh National University *Fluctuations of secondary particles at development of cascade process in thin calorimeter*
16:40	**M. U. Khasenov**, National Laboratory of Astana *Emission and Level Population in Gas Mixtures Pumped by Ionizing Radiation*

Time	Thursday 11 October
	Chair: Z. N. Utegulov, Nazarbayev University
9:00	**V. Kovanis**, Nazarbayev University *Twin Photonic Oscillators as a Unit Cell for the Next Generation of Topological Lasers*
9:20	**T. S. Ramazanov,** Al-Farabi Kazakh National University *Dynamical and transport properties of dense plasmas*
9:40	**K. N. Dzhumagulova**, Al-Farabi Kazakh National University *Dynamical properties of the dusty plasma in external magnetic field*
10:00	Coffee break
	Chair: T. S. Ramazanov, Al-Farabi Kazakh National University
10:40	**E. Batyrbekov**, Special presentation by the Director General of the National Nuclear Center of the Republic of Kazakhstan *Scientific-Technical Support of the Peaceful Use of Atomic Energy in Kazakhstan*
11:00	**O. Skrynyk**, Ukrainian Hydrometeorological Institute *Atmospheric transport, dispersion and deposition of radioactive materials released from nuclear accidents or weapons tests: the case study of the Chernobyl catastrophe*
11:20	**V. Ju. Maximov**, Al-Farabi Kazakh National University *The introduction of information and innovative technologies in the energy production processes of existing TPS of the Republic of Kazakhstan in order to address the problems of power engineering and ecology*
11:40	**M. T. Gabdullin**, Kazakh British Technical University *Thermodynamic properties of dense non-ideal plasma on the basis of effective potentials of interactions*
12:00	Lunch and Poster Session
	Chair: A. S. Desyatnikov, Nazarbayev University
13:40	**V. M. Somsikov**, Institute of Ionosphere *Deterministic Mechanism of Irreversibility and Physics of Evolution*
14:00	**Z. Sagidullayeva**, L. N. Gumilyov Eurasian National University *Integrable spin system and Hirota's method*
14:20	**Zh. Moldabekov**, Al-Farabi Kazakh National University *Multiscale approach and computation of dense quantum plasmas*
14:40	**S. Toktarbay,** Al-Farabi Kazakh National University *The stability of circular orbits of a test body in the field of two rotating massive bodies*
15:00	Coffee break
	Chair: A. E. Davletov, Al-Farabi Kazakh National University
15:40	**A. S. Desyatnikov**, Nazarbayev University *Paraxial laser beams as versatile tool for modern photonics*
16:00	**A. Mandilara**, Nazarbayev University *Quantum compiling with diffusive sets of gates*
16:20	**M. Lukac**, Nazarbayev University *Optimal Mapping of Reversible Logic Circuits to Quantum LNN Model*
16:40	**T. Yakupov**, Nazarbayev University *Evaluating performance of modern Brillouin light scattering spectrometers*

Time	Friday 12 October
	Chair: A. N. Jumabekov, Nazarbayev University
9:00	**A. Dauletbekova**, L. N. Gumilyov Eurasian National University *Synthesis of ZnO nanocrystals in a-SiO2/Si ion track templates*
9:20	**D. G. Batryshev**, Al-Farabi Kazakh National University *Obtaining of carbon nanomaterials*
9:40	**S. Kunakov**, Al-Farabi Kazakh National University *Antineutrino oscillations and energy distributions of fast particles in a fission plasma*
10:00	Coffee break
	Chair: A. Tikhonov, Nazarbayev University
10:40	**G. Yar-Mukhamedova**, Al-Farabi Kazakh National University *Physical Basic of Nano-composition Coatings Obtaining Technology*
11:00	**D. Sokolov**, Al-Farabi Kazakh National University *Properties of thin cryovacuum deposition films of organic molecules*
11:20	***A. Ng***, Nazarbayev University *A Novel Cryo-controlled Nucleation Method for High Efficiency Perovskite Solar Cells*
11:40	**A. N. Jumabekov**, Nazarbayev University *Dipole-field-assisted Charge Extraction in Metal-perovskite-metal Back-contact Solar Cells*
12:00	Lunch and Poster Session
	Chair: E. Abdikamalov, Nazarbayev University
13:40	**N. Dadhich**, Inter-University Center for Astronomy & Astrophysics, India *Understanding General Relativity after 100 years*
14:00	**V. Dzhunushaliev**, Al-Farabi Kazakh National University *Modified gravities from the nonperturbative quantization of a metric*
14:20	**G. Bauyrzhan**, L. N. Gumilyov Eurasian National University *FRW cosmology of Myrzakulov gravity with a scalar field*
14:40	**K. Boshkayev**, Nazarbayev University *Geodesics in the field of a rotating deformed gravitational source*
15:00	Coffee break
	Chair: V. Dzhunushaliev, Al-Farabi Kazakh National University
15:40	**B. J. Ahmedov**, Ulugh Beg Astronomical Institute, Uzbekistan *Optical and energetic properties of black holes*
16:00	**D. Malafarina**, Nazarbayev University *Phenomenology of bouncing black holes*
16:20	**D. Alina**, Nazarbayev University *Interstellar filaments and interstellar magnetic fields using interstellar dust polarization*
16:40	**E. Abdikamalov**, Nazarbayev University *Linear theory of shock-turbulence interaction and its application to stellar explosions*

Time	Saturday 13 October
	Special Discussion Session on Nobel Prize 2018
9:00	**A. S. Desyatnikov**, Nazarbayev University *Arthur Ashkin and optical tweezers*
9:30	**V. Kovanis**, Nazarbayev University *Compression of Amplified Chirped Optical Pulses*
10:00	Coffee break
	Chair: D. Malafarina, Nazarbayev University
10:40	**K. Myrzakulov**, L. N. Gumilyov Eurasian National University *Cosmological model of f(T,B) gravity with fermion fields via Noether symmetry*
11:00	**N. Myrzakulov**, L. N. Gumilyov Eurasian National University *f(R) gravity with fermion fields in (2+1) dimensions*
11:20	**Y. Myrzakulov**, L. N. Gumilyov Eurasian National University *FRW cosmology of Myrzakulov gravity with f-essence*
11:40	**P. Tsyba**, L. N. Gumilyov Eurasian National University *Nonlinear solution in Myrzakulov gravity model*
12:00	Closing of the Annual Meeting
12:10	Lunch
14:00 --- 16:00	Bus excursion in Astana city

Abstracts for Oral Presentations

Nonlinear electrodynamics effects in the strong magnetic field

Medeu Abishev, Saken Toktarbay, Manas Khassanov
Al-Farabi Kazakh National University, IETP, Almaty, Republic of Kazakhstan
abishevme@gmail.com

Abstract: In the work, the nonlinear effect of the magnetic field on the propagation of electromagnetic waves in the eikonal approximation of the parametrized post-Maxwell electrodynamics of the vacuum is calculated. Equations of motion for electromagnetic pulses transmitted in a strong magnetic field by two normal modes with mutually orthogonal polarization are constructed. The difference in propagation times of normal waves from the common source of electromagnetic radiation to the receiver is calculated. It is shown that the front and back parts of any hard radiation pulse due to the nonlinear electromagnetic influence of the magnetic field turn out to be linearly polarized in mutually perpendicular planes, and the remaining part of the pulse must have elliptical polarization.

1. Introduction to the style guide, formatting of main text, and page layout

According to the ideas of modern theoretical astrophysics [1-2], neutron stars have magnetic dipole fields, which on their surface reach values comparable with quantum electrodynamic induction Bq = 4.41 · 1013 Gs. In such fields, the nonlinearity of electrodynamics in a vacuum must appear, leading to the appearance of various physical effects [3]. Theoretical studies of such nonlinear electrodynamic processes use the post-Maxwellian approximation. In this approximation, the Lagrangian of the nonlinear electrodynamics of vacuum is written in the parametrized form:

$$L = \frac{1}{32\pi}\left\{2J_2 + \xi\left[(\eta_1 - 2\eta_2)J_2^2 + 4\eta_2 J_4\right]\right\} - \frac{1}{c} j^m A_m$$

Let us consider the effects of the nonlinear electrodynamic action of the magnetic quadrupole field on the electromagnetic wave.

Estimates show that when $B_0 \sim 10^{13}$ G the angle β can reach several angular seconds. However, because of the large distance between pulsars and the Earth, compared with the radii of pulsars, the angles of non-linear electrodynamic curvature of rays from the solar system can not be measured.

Further, for $\eta_{\_1} \neq \eta_{\_2}$ because of the nonlinear-electrodynamic birefringence, each electromagnetic pulse emitted at the point r0 = {q,0,z0}, splits into two pulses, one of which is carried by the first normal wave and the other by the second normal wave having orthogonal polarization. These pulses move to the receiver along different beams, spending on this way different time.

We calculate the delay time of the electromagnetic pulse carried by the first normal wave, in comparison with the propagation of the momentum carried by the second normal wave.

$$\Delta t = \frac{25\pi(\eta_1 - \eta_2)\,\xi B_0^2 R^8}{3072 x_s^7 c}\left[35 - 182 f_1 f_3 + 193 f_2^2 + 336 f_3^2\right]$$

The presence of a non-zero value of Δt leads to the appearance of unusual polarization properties for an electromagnetic pulse. These properties are a consequence of the different magnitude of the propagation velocity of two modes in an external magnetic field. Indeed, suppose that a pulse of an arbitrarily polarized hard radiation of finite duration T. Because of the birefringence of the vacuum, it splits into two modes, polarized in mutually perpendicular planes, with the leading edges of these modes coinciding at the initial instant of time. The leading edge of the faster mode will arrive at the hard radiation detector earlier than the leading edge of the slow mode, which for some time is equal to Δt. Therefore, during the time Δt, only the faster normal pulse mode will pass through the detector and the detector will detect the linear polarization of this part of the momentum.

After the time Δt, the front of the momentum transferred by another normal mode, the phase of which differs from the phase of the faster mode on ωΔt, where ω is the frequency of the wave. The addition of these orthogonally polarized normal modes in the subsequent time will create in the detector radiation with elliptical polarization that will pass through the detector for a time T − Δt.

Quite analogously, the trailing edge of the faster momentum mode will leave the detector before the trailing edge of the slow mode. Therefore, at the back of the hard radiation momentum duration Δt, the polarization will also be linear, but orthogonal to the linear polarization of the front of the momentum.

Thus, the detection of the above-mentioned polarization properties of hard pulses coming from pulsars makes it possible not only to assert the manifestation of nonlinear electrodynamics of vacuum, but also to estimate the magnitude of the induction of the magnetic field on the surface of the pulsar from the value of Δt.

[1]. M.Abishev, Y. Aimuratov Y.Aldabergenov, N.Beissen, B.Zhami, M.Takibayeva Some astrophysical effects of nonlinear vacuum electrodynamics in the magnetosphere of a pulsar. Astroparticle Physics, Volume 73, 15 January 2016, Pages 8-13
[2]. V. M. Kaspi, J. R. Lackey, J. Mattox, R. N. Manchester, M. Bailes and R. Pace, High-energy gamma-ray observations of two young, energetic radio pulsars, Astrophysical Journal 528 (2000) 445
[3]. Caniulef D. G., Zane S., Taverna R., Turolla R., Wu K., 2016, MNRAS, 459, 3585

Dynamics of Classical Nonlinear Hamiltonian Lattices

Anastasios Bountis
Department of Mathematics, Nazarbayev University, Kabanbay-Batyr 53, Astana, 010000 Republic of Kazakhstan
Author e-mail address: anastasios.bountis@nu.edu.kz

Abstract: There has been great progress in recent years in the study of dynamics and statistics of N – particle Hamiltonian lattices, in which the author has made significant contributions. In this short presentation, I will present in an introductory way, a number of methods studying and quantifying the orderly and chaotic behavior of these lattices, which generalize our knowledge of these phenomena from the case of N = 2,3,.. to the case of arbitrarily high number of degrees of freedom N.

1. Introduction

The appearance of chaotic behavior in Hamiltonian systems of few (N=2, 3,...) degrees of freedom has been the subject of intense study in the field of Nonlinear Dynamical Systems ever since the celebrated theorem of Kolmogorov, Arnol'd and Moser in the 1950's and 1960's. With the advent of computers, the implications of this and other related theorems was extensively scrutinized in many physical fields where Hamilton's equations come into play, like solid state physics, astronomy, molecular dynamics, charged particles in magnetic fields, and many others. Dynamical indicators like the spectrum of Lyapunov exponents have been extensively used to quantify the extent of ordered and chaotic motion present in such systems. In this brief talk, we will discuss the more recently proposed method of Generalized Alignment Indices (GALIs) which generalize Lyapunov exponents and are able to quantify faster and more accurately order and chaos in Hamiltonian systems of arbitrarily number of degrees of freedom N [1].

2. Equations

Starting with the example of the N = 2 degree of freedom example, whose dynamics is derived from the Hamiltonian

$$H = H_0 + \varepsilon H_1 = \frac{1}{2}(p_x^2 + p_y^2) + \frac{1}{4}(x^4 + y^4) + \varepsilon x^2 y^2 \tag{1}$$

and pictorially described by its solutions in the surface of section shown in Fig. 1 below

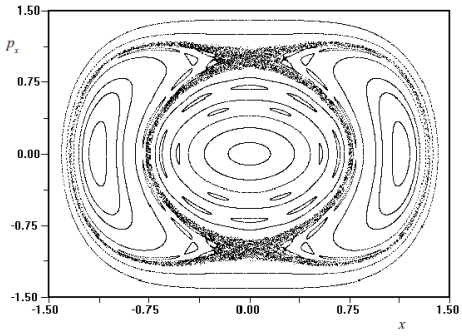

Fig. 1. Dynamics of the Hamiltonian system of N = 2 of equation (1) below for ε = 0.2

we will proceed to study its generalization to N – degree of freedom Hamiltonian systems described by the famous FPU lattice [2]:

$$H = \frac{1}{2}\sum_{j=1}^{N} p_j^2 + \sum_{j=1}^{N}\frac{1}{2}(x_{j+1} - x_j)^2 + \frac{\beta}{4}\sum_{j=1}^{N}(x_{j+1} - x_j)^4 = E \tag{2}$$

where E represents the total constant energy of the lattice. We will apply our GALI indices to (2) and demonstrate how effective they are in revealing some of the secrets of its ordered and chaotic solutions for arbitrary N [3,4].

3. References

[1] T. Bountis and H. Skokos, "Complex Hamiltonian Systems", Springer Verlag, (2012).
[2] H. Christodoulidi, T. Bountis, C. Tsallis and L. Drossos, "Chaotic Behavior of the Fermi-Pasta-Ulam Model with Different Ranges of Particle interactions", J. Stat. Mech. **12** (12) 123206 (2016).
[3] J. C. Macias Diaz, A. Bountis, "On the Transmission of Energy in β-Fermi–Pasta–Ulam Chains with Diff erent Ranges of Particle Interactions", CNSNS, vol. **63** (2018) 307–321 (2018).
[4] H. Christodoulidi, A. Bountis and L. Drossos, "The Effect of Long--range Interactions on the Dynamics and Statistics of 1D Hamiltonian Lattices with On--Site Potential", to appear in EPJST, Elsevier (2018). https://arxiv.org/abs/1801.03282

Thermodynamics and dust-acoustic wave dispersion in strongly coupled dusty plasmas

A.E. Davletov, L.T. Yerimbetova
Al-Farabi Kazakh National University, 71 Al-Farabi av., 050040 Almaty, Kazakhstan
Askar.Davletov@kaznu.kz

Abstract: The analysis, grounded on the premise that dust particles are charged hard balls, provides an original pseudopotential model of intergrain interaction in complex (dusty) plasmas [1]. This accurate model is engaged herein to consistently treat the finite-size effects from the process of dust particle charging to determination of the thermodynamic quantities and the dust acoustic wave dispersion in the strongly coupled regime. The orbital motion limited approximation is adopted to evaluate an electric charge of dust grains immersed in a neutralizing background of the buffer plasma. To account for finite dimensions of dust particles the radial distribution function is calculated within the reference hypernetted-chain (RHNC) approximation to demonstrate a well-pronounced short-range order formation at rather large values of the coupling parameter and the packing fraction. The evaluated excess pressure of the dust component is compared to the available theoretical approaches and the simulation data and is, then, used to predict the dust-acoustic wave (DAW) dispersion in the strongly coupled regime under the assumption that the dust particles charge varies in the course of propagation. In contrast to many previous investigations it is demonstrated for the first time ever that for DAW the charge variation of dust particles should necessarily be taken into account while evaluating the dust isothermal compressibility.

1. Interaction model

It was recently demonstrated that the plasma electrodynamics in the framework of the density-response formalism provides the following interaction model of dusty plasma particles [1]:

$$\varphi_{ab}(r) = \frac{Q_{ab}}{r+R_{ab}} - \frac{Q_{ab}}{r}\left(1 - \exp(-k_D r) - \frac{R_{ab}k_D}{2}B_{ab}(r)\right),$$

where the subscirpts a, b take on values of e for electrons, p for protons and d for dust grains, $Q_{ed} = -Q_{pd} = Z_d e^2$, $R_{ed} = R_{pd} = R$ and $Q_{dd} = Z_d^2 e^2$, $R_{dd} = 2R$, Z_d and R are the grain charge number and radius, respectively, e denotes the elementary charge, r stands for the distance between surfaces of interacting particles and

$$B_{ab}(r) = \exp\big(k_D(r+R_{ab})\big)\mathrm{Ei}\big(k_D(r+R_{ab})\big) - \exp\big(k_D(R_{ab}-r)\big)\mathrm{Ei}(k_D R_{ab}) + \exp\big(-k_D(R_{ab}+r)\big)\big[\mathrm{Ei}(-k_D R_{ab}) - \mathrm{Ei}\big(-k_D(r+R_{ab})\big)\big]$$

with $\mathrm{Ei}(x)$ being the integral exponential function and k_D signifying the inverse screening length.

2. Thermodynamics and dust-acoustic waves

This investigation has been generally focused on estimating the impact the finite-size effects and the screening phenomena have on the electric charge of dust particles, its thermodynamics and dust-acoustic wave dispersion.

The starting point of the whole consideration is an original intergrain interaction model that stems from the plasma electrodynamics formulated within the linear density-response formalism.

In the framework of the orbital motion limited approximation the charge number of the dust grain in a plasma has been evaluated as a function of the nonisothermicity, the density-ratio and the packing fraction parameters to show that the screening effects are responsible for the increase of the charge number as compared to the pure Coulomb interaction. It has also been verified that the Yukawa potential always predicts higher values of the dust charge than the intergrain interaction model that takes advantage of the plasma electrodynamics.

The cornerstone of the present consideration has been the self-consistent evaluation of the thermodynamic quantities of the dust component starting from the determination of the grain charge. The radial distribution function has been calculated within the RHNC scheme to take into account the finite dimension of dust particles and it has been proved that the HNC method works very well for small values of the packing fraction. Such a consistent determination of the thermodynamic characteristics has allowed us to study the dispersion of the dust-acoustic waves that accounts for variation of the dust grain charge in the dust isothermal compressibility [2].

4. References

[1] A.E. Davletov, Yu.V. Arkhipov, I.M. Tkachenko, “Electric charge of dust particles in a plasma”, Contrib. Plasma Phys. **56,** 308 (2016).
[2] A.E. Davletov, L.T. Yerimbetova, Yu.V. Arkhipov, Ye.S. Mukhanetkarimov, A. Kissan, I.M. Tkachenko, “Dust particles of finite dimensions in complex plasmas: Thermodynamics and dust-acoustic wave dispersion”, J. Plasma Phys. **84,** 905840410 (2018).

Gluon contribution to the proton spin by using the non-perturbative quantization a la Heisenberg

V. Dzhunushaliev[1,2], T. Kozhamkulov[2]
[1]*Dept. Ther. Nucl. Phys., al-Farabi KazNU, Almaty, 050040, Kazakhstan,*
[2] *IETP, al-Farabi KazNU, Almaty, 050040, Kazakhstan,*
e-mail: v.dzhunushaliev@gmail.com

Abstract: The contribution of crossed gluon fields in flux tubes connecting quarks to the proton spin is calculated. The calculations are performed following non-perturbative Heisenberg's quantization technique. In our approach a proton is considered as consisting of three quarks connected by three flux tubes. The flux tubes contain colour longitudinal electric and transversal electric and magnetic fields. The transversal fields causes the appearance of the angular momentum density. The dimensionless relation between the angular momentum and the mass of the gluon fields is obtained. The contribution to proton spin from rotating quarks and flux tubes connecting quarks is estimated. Simple numerical relation between the proton mass, the speed of light and the proton radius, which is of the same order as the Planck constant, is discussed.

The spin structure of the proton is one of the most challenging problems in modern physics. The experimental results of the European Muon Collaboration showed that only a small fraction of the proton spin is carried by the quark spin.

The proton spin can be split as

$$\frac{1}{2} = \frac{1}{2}\Delta\Sigma + \Delta G + L_q + L_G \tag{1}$$

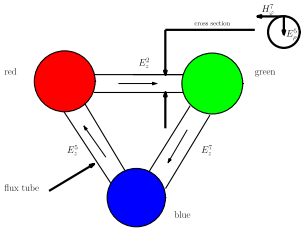

Here we use the non-perturbative methods \`{a} la Heisenberg \cite{heis} to investigate the gluon field contribution to the proton spin. We use the following model of a proton: three quarks are connected by flux tubes, see Fig.1.

The flux tube stretched between two infinitely separated quarks has the longitudinal colour electric field E_z^3 and two transversal fields: the radial colour electric field E_ρ^1 and the azimuthal colour magnetic field H_φ^2. The angular momentum density is

$$\vec{M} = \frac{1}{4\pi c}\left[\vec{r} \times \left[\overline{E^a} \times \overline{H^a}\right]\right] \tag{2}$$

There is a quantum proton state $|p\rangle$ with the properties

$$\left\langle p\middle|E_{\rho,\varphi}^{2,5} H_{\varphi,\rho}^{5,2}\middle|p\right\rangle \neq 0, \left\langle p\middle|E_{\rho}^{2,5} H_{\varphi}^{2,5}\middle|p\right\rangle \neq 0 \tag{3}$$

It allows us to calculate the expectation value of the angular momentum of the gluon field of flux tubes connecting three quarks.

$$L_G = \left(\frac{24\pi}{g'^2} l r_0 \phi_0^2 \overline{\overline{M_\perp}}\right)\frac{\hbar}{2} \tag{4}$$

For the rough estimation of L_G we have: $\frac{L_G}{\left(\frac{\hbar}{2}\right)} \approx 4\%$.

References

[1] V. Dzhunushaliev, "Calculation of gluon contribution to the proton spin by using the non-perturbative quantization \`{a} la Heisenberg", Physics of Particles and Nuclei Letters, 14, no. 6, 836 (2017); [arXiv:1611.02697 [hep-ph]].

Diffuse Spectra of Photoluminescence of Carbon Quantum Dots

S.E.Kumekov, N.K.Saitova
Kazakh National Technical University named K.I.Satbayev,Almaty, Satbayev str. 22, Kazakhstan, 050013
skumekov@mail.ru

Investigation of the photoluminescence properties of carbon quantum dots (CQD) have revealed a number of unique features: a wide structure less band, the dependence of the photon energy at the maximum of the band and its short-wave edge on the energy of the excitation quantum, the fluorescent kinetics of the luminescence decay, and the independence of the long-wavelength edge of the band on the excitation quantum energy. Different mechanisms of photoluminescence (PL) in the CQD were discussed in the literature: the quantum size effect, fluorophores with various degrees of π - conjugation, recombination of electron-hole pairs localized within small sp^2 carbon clusters embedded within a sp^3 matrix, defects and surface states, surface groups, and surface passivation [1].

A common structural feature of CQDs is the existence of carbon sextets-aromatic rings connected by Van der Waals forces. This representation of the structure made it possible in the present work to develop a dimer-excimer model of radiative processes in the CQD.

We believe [2] that the crystalline structure of graphite clusters contains graphene-like monomer layers that form dimer-like structures. Similar structures are described in [3]. Physical dimer contains two benzene like monomer that created sandwich structure. In these structures, the monomers are linked together in the direction of the **c**-axis of the crystal by weak long-range Van der Waals forces. The Van der Waals forces compensate for the repulsive forces. The repulsive forces exist due to the exchange and Coulomb interactions between the graphene-like layers. These circumstances lead to a stable ground state of the dimer with an insignificant potential barrier

The excited state of the dimer, which represents the excimer state, also corresponds to a stable state due to the Coulomb interaction, but at distances between layers in the excited dimer R_e that are smaller than in the stable ground state of the dimer R_d ($R_e < R_d$). The Hamiltonian of the physical dimer H can be written [4,5]

$$H = H_1 + H_2 + V_{12} \quad (1)$$

Where H_1 and H_2 are the Hamiltonians of the individual monomers and V_{12} (R) is the interaction energy between the monomers, depending on the distance between the monomers R. Figure 1 illustrates the scheme for calculating the width of the diffuse spectrum Δ of the luminescence [6]. Here E_1 and E_2 are energies of ground and excited states of excimer.

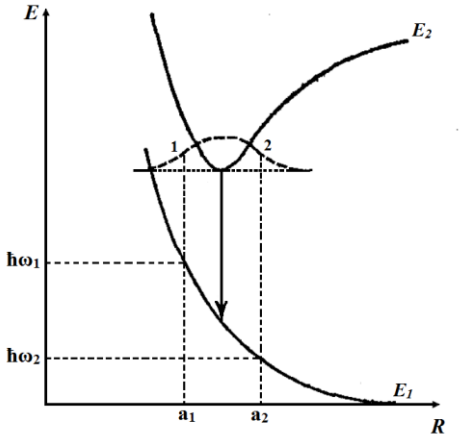

Fig. 1. The creation of the diffuse spectrum. R – Distance between monomers, a_1, and a_2 – coordinates of zero vibrational level.

For the transitions from zero vibrational level, we find the wide of the spectrum

$$\Delta = \hbar\omega_1 - \hbar\omega_2 = (a_1 - a_2) \cdot \frac{dE_1}{dR} \quad (2)$$

The width of the spectrum is defined by slope of curve $E_1(R)$. Based on the concept of structural features of CQD, the dimer-excimer model of radiative processes in the CQD is developed. In addition, a part of the absorbed quantum of light is determined, which is dissipated due nonradiative channel of energy relaxation as a function of the energy of the excitation quantum. The independence of the long-wave edge of PL on the energy of the excitation quantum is explained.

[1] Y. Wang, A. Hu, "Carbon quantum dots: synthesis, properties and applications J. Mater. Chem. C 2, 6921-6939 (2014)
[2] S.E.Kumekov, N.K.Saitova, "Relaxation of the energy of optically excited states in the carbon quantum dots", Eurasian Chem.Tech.J. 20, 3 (2018)
[3] J. Guillet, "*Polymer photophysics and photochemistry*", Cambridge university press, 1987, p. 414.
[4] M.Pope, Ch.Swenberg, "*Electronic processes in organic crystals*", Oxford, N -Y, 1982, p. 1360.
[5] J.B. Birks, "Excimers", Phys. Rep. Prog. 38, 1975, p.903-974
[6] E.V. Shpolskii, "Diffuzionniye spectry i himicheskiye problemi", Uspehy fizicheskih nauk 13, p.325-366, (1933) [in Russian]

Non-Equilibrium Charge Dynamics in Functionalized Titania

Talgat M. Inerbaev
L.N. Gumilyov Eurasian National University
talgat.inerbaev@gmail.com

Abstract: Atomistic modeling of light driven electron dynamics are important in studies of photoactive materials. Spin-resolved electronic structure calculations become necessary when dealing with transition metal, magnetic, and even some carbon materials, intermediates, and radicals. An approximate treatment can be pursued in the basis of spin-collinear density functional theory. Most transition-metal compounds exhibit open shell nonsinglet configurations, necessitating special treatment of electrons with α/β spin projections. By separate treatment of electronic states with the α/β spin components one is able to describe a broader range of materials, identify new channels of relaxation and charge transfer, and provide knowledge for rational design of new materials in solar energy harvesting and information storage. For this methodology, named spin-resolved electron dynamics, spin-polarized DFT is used as the basis to implement nonadiabatic molecular dynamics. At ambient temperatures, the thermal lattice vibrations results in orbital and energy fluctuations with time. Nonadiabatic couplings are then calculated, which control the dissipative dynamics of the spin resolved density matrix.

1. Introduction

Titanium dioxide (TiO_2) is a promising semiconducting material for photocatalysis, but it suffers several drawbacks on large scale practical applications. At first, its wide band gap (3.2 eV) restricts the photocatalytic property to UV radiation, making it ineffective for visible light. Second, the relatively high rate of electron and hole recombination in TiO_2 tends to decrease its photocatalytic efficiency. Therefore, to address these two main issues, a great deal of attention has been paid to the functionalization of titania by (i) varying size, shape, and surface or introducing a mesoporous form of titania, (ii) by sensitization titania surface with dyes, including metalorganic dyes, and by (iii) introduction of mid band gap cationic or anionic dopants into the TiO_2 crystal structure. In this respect, transition metals, rare earth metals, and nonmetals were examined as dopants that improve the visible light photoresponse.

In present report, the spin-resolved nonadiabatic excited state dynamics of transition metal doped anatase TiO_2 structures are investigated by the reduced density operator formalism to elucidate electron-transfer pathways together with energy losses due to lattice induced charge carrier relaxation. Electron−phonon coupling controls nonradiative relaxation dynamics of the photoexcited electron−hole pair in semiconductor nanostructures. We attempt to provide an insight on relaxation rate dependence on excitation energy for models with different charge and spin states.

2. Results

By separate treatment of electronic states with the α/β spin components one is able to describe a broader range of materials, identify new channels of relaxation and charge transfer, and provide knowledge for rational design of new materials in solar energy harvesting and information storage. For this methodology, named spin-resolved electron dynamics, spin-polarized DFT is used as the basis to implement nonadiabatic molecular dynamics. At ambient temperatures, the thermal lattice vibrations results in orbital and energy fluctuations with time. Nonadiabatic couplings are then calculated, which control the dissipative dynamics of the spin resolved density matrix. Different initial excitations are then analyzed and used to calculate relaxation dynamics. Spin-resolved electronic dynamics approach is applied to study vanadium (IV) substitutionally doped bulk anatase in a doublet ground state. Spin-resolved charge transfer dynamics at the interface of a $Co(NH_3)_2$ -doped (001) anatase TiO_2 nanowire and liquid water calculations based on density functional theory and density matrix formalism are considered. Three models with the same stoichiometry but different electronic structure are explored. While one model had no change to electron count and spin count (neutral model), the other two models were assigned a charge of 2+, one in a doublet and the other a quartet spin configuration. Co^{2+} is the most probable state for dopant in all models and Co acts as an electron acceptor. The results show that a difference in the electronic structure for α and β spin components determines consequences in optical excitations and electronic dynamics pathways experienced by electrons with α and β spin projections. The slower non-radiative relaxation rate of α-excitations is rationally explained as a consequence of difference of electronic structure for α and β spin projections and specific pattern of energy levels contributed by doping. Specifically, excitations involving orbitals with α-projection of spin experience transitions through larger sub-gaps in the conduction band compared to the ones experienced by similar excitations involving orbitals with β-projection of spin.

[1] S. J. Jensen, T. M. Inerbaev, and D. S. Kilin, "Spin Unrestricted Excited State Relaxation Study of Vanadium (IV)-Doped Anatase," J. Phys. Chem. C **120,** 5890 (2016).
[2] S. J. Jensen, T. M. Inerbaev, and D. S. Kilin, "Spin Unrestricted Nonradiative Relaxation Dynamics of Cobalt- Doped Anatase Nanowire" ," J. Phys. Chem. C **121,** 16110 (2017).

Nanosecond Laser Melting Thresholds in Refractory Metals Detected by Laser Generated Acoustic Shear Waves

A. Abdullaev[1,*] B. Muminov[1,2,*] A. Rakhymzhanov[1,3,4,*] N. Mynbayev[1,3,4,*] and Z. N. Utegulov[1,3]

[1]*Department of Physics, School of Science and Technology, Nazarbayev University, Astana 010000, Kazakhstan*
[2]*Department of Mechanical Engineering, University of California Riverside, CA, USA*
[3]*Center for Energy and Advanced Material Science, National Laboratory Astana, Nazarbayev University, Astana 010000, Kazakhstan*
[4]*L.N.Gumilyov Eurasian National University, Astana 010008, Kazakhstan*
** These authors have made equal contribution*
Presenting author's e-mail address: zhutegulov@nu.edu.kz

The laser-based generation and detection of ultrasound have been widely used to characterize materials remotely and non-destructively. Due to noncontact nature of these measurements, the use of laser-based techniques for non-contact, *in-situ* control of materials and processes present in harsh environments has found numerous research and industrial applications. Considering above mentioned advantages, this technique can be also used for advanced examination of refractory materials used for nuclear fuels and supersonic vehicles during fast laser-induced melting regime.

There has been a number of works devoted to laser pulsed generation of acoustic waves in thermoelastic and ablative regimes in metals. However, limited attention has been paid to laser ultrasonic regime when the laser pulse energy is sufficient to *melt solids but not enough to ablate them*. Previously few researchers have investigated signal amplitude changes for shear acoustic waves in stainless steel and for surface acoustic waves in silicon under nanosecond laser-induced melting. Recently we have examined epicentral waveform for laser ultrasound in the surface melting regime of tungsten without automated control of incident laser pulse energy [1] and performed numerical simulations based on elastodynamic Green's functions and finite element methods for calculation of epicentral displacement [2].

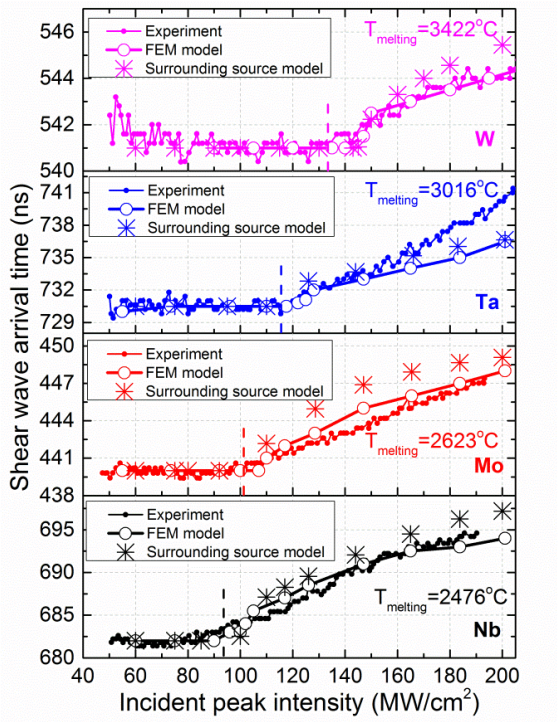

In the present work [3] we have introduced automated control of laser pulse energy-induced melting to improve measurement accuracy by studying dynamic thermomechanical properties in thermoelastic regime, at and above melting in several refractory metals such as (niobium, molybdenum, tantalum and tungsten) with various bulk shearing behavior, by actually measuring nanosecond laser melting thresholds in these metals. From the real-time measurements performed using two-wave mixing photorefractive interferometry we consistently observed an increase in the propagation time of acoustic shear waves with the increase of the incident laser peak power density. Obtained melting threshold values were found to be scaled with corresponding melting point temperatures of investigated materials displaying dissimilar shearing behavior. Compared to our previous results [1, 2] in the present work we have improved quantitative convergence between our experimental results on peak intensity-dependent shear wave arrival time and the finite element model (FEM) solving coupled elastodynamic and thermal conduction governing equations with solid-melt phase transition using *apparent heat capacity method* [4]. Developed model shows that laser-induced surface melting and corresponding complete loss of rigidity (i.e. vanishing of shear modulus) within molten pool along with rapid radially spreading molten mass results in the shear wave arrival delay, which was found to be due to generation of surface and volumetric thermoelastic sources from the heated zone surrounding the molten pool.

For above-melting regime, measured transit time delay of shear waves was more pronounced in metals having lower melting points which were attributed to faster rate of molten mass formation in the plane of laser irradiated metal surfaces. This rate was an order of magnitude higher than effective shear wave velocity of studied metals. In these low-T_{melt} metals shearing behavior (due to increased Poisson's ratio) in their bulk becomes substantially enhanced not just in terms of risen delay of shear wave arrival times across metals bulk at the onset of laser-induced surface melting, but also in terms of enhanced shear ultrasonic energy deposited to the bulk metal during both laser-induced thermoelastic and above-melting regimes.

Funding from MES RK grant AP05130446 and state-targeted program BR05236454 is acknowledged.

References

[1] S. J. Reese, Z. N. Utegulov F. Farzbod, R. S. Schley, and D. H. Hurley, *Ultrasonics*, 53(3), 799 (2013)
[2] A. G. Every, Z. N. Utegulov and I. A. Veres, *Journal of Applied Physics*, 114 (20), 203508 (2013).
[3] A. Abdullaev, B. Muminov, A. Rakhymzhanov, N. Mynbayev, Z. N. Utegulov "Examination of Nanosecond Laser Melting Thresholds in Refractory Metals by Shear Wave Acoustics", *AIP Advances*, 7, 075203 (2017)
[4] H. Hu, and S. A. Argyropoulos, Modelling and Simulation in Materials Science and Engineering, 4(4), 371 (1996)

"Coulomb crystal" experiments under microgravity conditions and diagnostics of complex plasma

Y. A. Ussenov[2,6], T. S. Ramazanov[1], K. N. Dzhumagulova[1], M. K. Dosbolayev[1,2], L. G. D'yachkov[1,3], , M. T. Gabdullin[2], Zh. A. Moldabekov[1,6], O. F. Petrov[3], M. M. Vasiliev[3], M. I. Myasnikov[3], V. E. Fortov[3], S. F. Savin[4], T. A. Musabayev[5], Zh. Sh. Zhantayev[5] and A. A. Aimbetov[5].

[1] IETP, Al Farabi Kazakh National University - Al Farabi av., 71, Almaty, Kazakhstan
[2] NNLOT, Al Farabi Kazakh National University - Al Farabi av., 71, Almaty, Kazakhstan
[3] Joint Institute for High Temperatures, RAS - 125412 Moscow, Russia
[4] S.P. Korolev Rocket-Space Corporation "Energia" - 141070 Korolev, Moscow region, Russia
[5] National Center of Space Research and Technology, KazCosmos - Almaty, Kazakhstan
[6] Institute of Applied Science and Information Technology - Shashkina str. 40, Almaty, Kazakhstan
e-mail: yerbolat@physics.kz

Abstract: In this contribution the results of series of experiments on complex plasmas at laboratory and microgravity conditions were presented. The modernized "Coulomb crystals" setup on board of the International Space Station (ISS) was performed. Formation of a cluster of charged and uncharged particles was observed. Excitation and damping of cluster oscillations, as well as its destruction in the high electric field were investigated. The results of studying of the electron temperature of buffer and complex plasmas by Langmuir probe in mixtures of noble gases (helium + argon) in capacitive coupled radiofrequency (CCRF) discharge at laboratory conditions are presented. An alternative method for the determination of the buffer plasma parameters in DC glow discharge was developed by measuring the dust-free region area around the probe.

1. Introduction

Complex plasma - a plasma containing charged micron and submicron size particles of condensed matter, various active radicals and ions. Nowadays, an experimental and theoretical study of complex plasma is actively carried out not only in terrestrial and laboratory conditions, but also in microgravity. A striking example is the international projects "Plasma Kristall (PK-4 experiments at ISS)" and "Coulomb Crystal" experiments. Also, despite the fact that the study of complex plasma has been conducted for the last several decades, until now the diagnosis of such complex systems by conventional methods requires further study and improvement. This paper presents the results of complex plasma experiments in "Coulomb Crystal" setup, which is carried out in microgravity conditions during the flight of third Kazakh cosmonaut to ISS and study and diagnosis of complex plasma parameters at laboratory conditions.

2. Results and conclusions

The properties of strongly interacting spatially ordered structures consisting of micron-size charged particles have been studied in the framework of the experiment "Coulomb crystals" on board of the International Space Station (ISS) [1,2]. Unlike plasma-dust structures in gas discharges, used for this purpose before, our method allows to form stable three-dimensional structures of charged particles in non-ionized gas or in a vacuum. This is an alternative to the plasma-dust structures in gas discharges usually used for the study of Coulomb structures. The main idea of the experiment was to hold charged particles by the forces different from the electrostatic ones causing interactions between them. In this experiment, a cusp magnetic trap for diamagnetic particles was used. Some results obtained in previous experiments are confirmed using simpler methods. The destruction of the cluster with the gradual increase in voltage at the center electrode of up to 150V was observed. Estimations of the charges of the particles based on their observed velocities have been made. The interpretation of the obtained results is presented. It is shown that graphite particle autoadhesion can be important during cluster formation and destruction.

The electron temperature of the dust and the buffer gas discharge plasma in mixtures of inert gases (helium and argon) in CCRF discharge at laboratory conditions was studied [3]. The probe method was used to measure the axial distribution of the electron temperature in the buffer plasma of RF discharge in helium and mixtures of helium and argon. The results of measurements show an increase in the temperature of electrons in the near-electrode regions compared to the area of a homogeneous plasma characterized by a relatively normal distribution of the electron temperature. Also, the method for the diagnostics of the buffer plasma based on the study of the dust-free region was proposed [4]. The main deal is only measuring the dust-free region and then applying the special software which calculates the temperature and numerical density of dust, and the electron temperature and numerical density.

4. References

[1] T. S. Ramazanov, L. G. D'yachkov, K. N. Dzhumagulova and et. al., " Experimental investigations of strongly coupled Coulomb systems of diamagnetic dust particles in a magnetic trap under microgravity conditions", Europhysics Letters, **116** 45001 (2016).
[2] L.G. D'yachkov , T.S. Ramazanov and et. al., "Structure of a Coulomb cluster in the cusp magnetic trap under microgravity conditions ", Contirb. to Plasma Phys. , DOI: 10.1002/ctpp.201700103 (2018).
[3] S. A. Orazbayev, Y.A Ussenov, T. S. Ramazanov, M. K. Dosbolayev, and A.U. Utegenov, "A Calculation of the Electron Temperature of Complex Plasma of Noble Gases Mixture in CCRF Discharge", Contrib. Plasma Phys. **55(5),** 428 – 433 (2015).
[4] Y. A. Ussenov, T. S. Ramazanov, K. N. Dzhumagulova and M. K. Dosbolayev, "Application of dust grains and Langmuir probe for plasma diagnostics ", Europhysics Letters, **105** 15002 (2014) .

Experimental modeling of dust formation in fusion reactors by pulsed plasma accelerator. Pulsed plasma diagnostics.

M.K. Dosbolayev, A.B. Tazhen, A.U. Utegenov, Zh. Rayimkhanov, T.S. Ramazanov
Institute of Experimental and Theoretical Physics, Al-Farabi Kazakh National University, Almaty, Kazakhstan
merlan@physics.kz

Abstract: In this paper, the results of an experimental investigation of dust formation in a pulsed plasma accelerator, which is formed due to the interaction of a pulsed plasma flow with the candidate material of the thermonuclear reactor, are presented. Dynamic and optical properties of a pulsed plasma flow are considered. Several diagnostic methods were also used in this work to determine pulsed plasma parameters. The results of the synergetic analysis by the Raman spectrometer of the target surface after irradiation with plasma are also presented. It was revealed that after interaction with the plasma, the surface of the graphite target becomes amorphous. Materials with fractal surfaces, similar to the materials formed in Tokamaks under the action of erosion, were obtained experimentally.

1. Introduction

The interaction of hot plasma with the reactor components, placed inside the chamber, represents a complex problem in the physics of thermonuclear reactors. Investigation of the interaction processes is important for selecting materials of the wall of the thermonuclear reactor, as well as for its correct operation, taking into account the constraints imposed by the interaction with the wall. Although active research in this area has cleared up a large number of questions related to the interaction of plasma with solids, it has left a lot of unsolved problems. To date, we can identify the following main problems playing a key role in the interaction of plasma with the material of the front wall of the reactors: Working resource of materials facing the plasma; formation of dust as a result of erosion of materials; accumulation of tritium in the materials of the vacuum chamber [1].

It is known that dust formation in Tokamaks is caused by various processes in the chamber of the thermonuclear installation. For instance, in many papers various mechanisms of formation of dust particles in thermonuclear devices, including erosion of walls, ion-molecular reactions and coalescence of dust particles into large-sized particles, were considered. The particle sizes typically vary over a very wide range from nanometers to hundreds of micrometers.

The composition of the particles includes materials used for the plates of the divertor, the first wall and other internal structural elements, which are usually graphite, titanium, tungsten, beryllium, and steel. This work is devoted to the study of dust formation in the interaction of an accelerated pulsed plasma flow with the graphite plates and the dynamics of the flow itself. To simulate and study this process, a plasma accelerator of the coaxial type was used.

The accelerator is powered by capacitor banks with a total capacitance of 100 μF. The principle of operation of the installation is based on the acceleration of the plasma bunch formed in the inter-electrode space by an electric arc discharge in the intrinsic magnetic field [2,3].

2. Results and Discussion

During the interaction of a pulsed plasma flow with a graphite plate, a “plasma-dust” cloud is formed. Optical-emission properties of the plasma-dust formation near the graphite target correspond carbon lines and can provide qualitative evidence that after interaction with the surface, the pulsed plasma turns into a dusty-plasma. Synergetic analysis of irradiated graphite target showed that surface becomes smoother, roughness disappear and surfaces with fractal structures appear after interaction with the pulsed plasma flow. Graphite plates were studied using a Raman spectrometer NT-MDT NTegra Spectra with a laser wavelength of 473 nm. The results of spectrum of the original sample revealed that graphite has some defects. The sizes of the obtained particles are different. Most particles have a rough surface, and the particle size varies within the range of ~0,5–50 μm. The motion of the pulsed plasma beam was recorded using a high-speed Phantom camera version v2512 with a rate of 470,000 frames per second. The speed of the pulsed plasma bunch and the diameter of the plasma cord were determined: 23 km/s and 4 cm. It is important to know pulsed plasma parameters. To this purpose following diagnostic equipments: Faraday cup, wire calorimeter, magnetic probe, Rogowski coil were used [4,5].

References

[1] J.C. Flanagan, M. Sertoli, M. Bacharis et al., "Characterising dust in JET with new ITER-like wall", Plasma physics and controlled fusion, Vol. **57**, P. 014037 (2015).
[2] M.K. Dosbolayev, A.U. Utegenov, A.B. Tazhen, T.S. Ramazanov, "Investigation of dust formation in fusion reactors by pulsed plasma accelerator", Laser and Particle Beams, **35**, Pp. 741-749 (2017).
[3] M.K. Dosbolayev, A.U. Utegenov, A.B. Tazhen, T.S. Ramazanov, M.T. Gabdullin, "Dynamic properties of pulse plasma flow and dust formation in the pulsed plasma accelerator", News of the Natnl. Acad.Sci. RK. **6(310)**, Pp. 59–66 (2016).
[4] A.B. Tazhen, A.U. Utegenov, M.K. Dosbolayev, T.S. Ramazanov, M.I. Kaikanov, A.V. Tikhonov, "Definition of the density of energy of a pulsed plasma flow using a wire calorimeter" J. PEOS. Is. **18**, Vol. 2, Pp. 40-44 (2016).
[5] S.A. Orazbayev, Y.A Ussenov, T.S. Ramazanov, M.K. Dosbolayev, A.U. Utegenov, "A Calculation of the Electron Temperature of Complex Plasma of Noble Gases Mixture in CCRF Discharge" Contrib. Plasma Phys. **55**, No. 5, Pp. 428 – 433 (2015).

Materials surface modification with pulsed ion beam: using the new INURA accelerator facility at Nazarbayev University

M. Kaikanov[1], G. Remnev[2], M. Zhuravlev[2], I. Koryashov[2], R. Sazonov[2], W. Waldron[3], J. Kwan[3], E. Henestroza[3], A. Kozlovskiy[1,4], A. Urazbayev[1], F. Bozheev[1], K. Baigarin[1], A. Tikhonov[1]

[1]Nazarbayev University, Astana, Kazakhstan
[2]Tomsk Polytechnic University, Tomsk, Russia
[3]Lawrence Berkeley National Laboratory, Berkeley, USA
[4]Astana Branch of Institute of Nuclear Physics, Astana, Kazakhstan
atikhonov@nu.edu.kz

We are currently installing at Nazarbayev University a new accelerator facility, to use in fundamental plasma and beam physics experiments as well as in materials modification research. A new single gap pulsed ion accelerator [1], Nazarbayev University Research Accelerator (INURA), is based on pulsed-power technology to generate a high-current up to 10 kA pulsed ion beam with a duration of less than 100 ns. Ion beam (protons) will reach a high current density 100 A/cm2 at focal spot ~5 cm diameter, enabling experiments in the fields of high energy densities physics, plasma and ion beam physics, and material science.

At high power density of the beam it is possible to modify near-surface layer of a various solid materials: refractory alloys, high-temperature ceramics, etc. Irradiation of metals (semiconductors)with short pulse of ion beam leads to rapid heating of the near surface which is immediately followed by rapid cooling and re-solidification, resulting in defects migration and annealing, structural modification and recrystallization and changing of grain size.

Applying smaller current densities of less than 10 A/cm2 we able to modify and fabricate of nanomaterials: 2D materials, metallic nanotubes, silver nanowires, nanosized powders (nano-oxides). Some of our recent results include modification of Ni.nanotubes [2-3], defects engineering for 2-D materials (WS_2) for optical properties enhancement [4], modification of refractory metals, fabrication of conductive transparent and flexible electrodes with Ag nanowires networks.

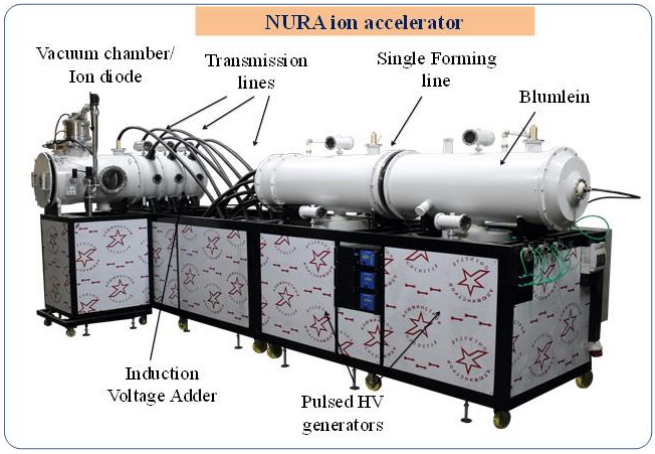

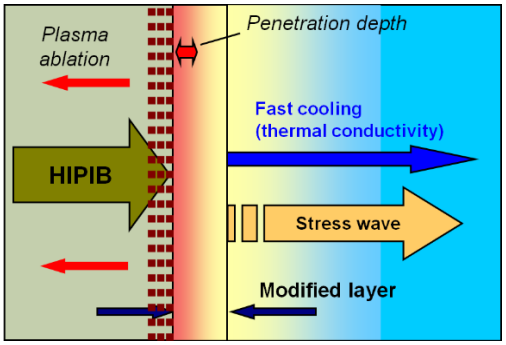

Future plans of INURA facility development include developing capabilities for electron and X-ray high intensity short ~80 nsec beam, with further applications in plasm-chemistry nano-powder synthesis, agricultural and biology applications.

[1] 1. M. Kaikanov, K Baigarin, A Tikhonov, A Urazbayev, J W Kwan, E Henestroza, G Remnev, B Shubin, A Stepanov, V Shamanin and W L Waldron. "An accelerator facility for WDM, HEDP, and HIF investigations in Nazarbayev University"/ Journal of Physics: Conference Series 717 012099 (2016).
[2] A. Kozlovskiy, M. Kaikanov, A. Tikhonov, I. Kenzhina, D. Ponomarev and M. Zdorovets "Radiation modification of Ni nanotubes by electrons"/ Materials Research Express, 4, 105042 (2017).
[3] G. Kalkabay, A. Kozlovskiy, M.A. Ibragimova, D.I. Shlimas, M.Zdorovets, D. Borgekov, A.Tikhonov, "Ni nanotubes reaction activity in media with different pH" / Crystallography Reports, Vol. 63, No. 1, pp. 90–95 (2018).
[4] F. Bozheyev, D. Valiev, R. Nemkayeva, V. An, A. Tikhonov, G. Sugurbekova "Pulsed cathodoluminescence of WS2 nanocrystals at various electron excitation energy densities: Defect induced sub-band gap emission" / Journal of Luminescence, 192, 1308 (2017).

Fluctuations of Secondary Particles at Development of Cascade Process in Thin Calorimeter

A. I. Fedosimova and T. A. Kozhamkulov
Al-Farabi Kazakh National University, Almaty, Kazakhstan

Researches of the characteristics of cosmic rays (CR) on the basis of "direct" measurements outside the atmosphere on the spacecrafts or high-altitude balloons can allow solving many problems of particle physics, cosmic ray physics and astrophysics. Consequently, this region has a significant interest and dynamism to the development of theoretical and experimental studies worldwide [1].

Direct experiments on high-altitude balloons: JACEE and RUNJOB, which were aimed to studying the elemental composition of cosmic rays, gave very similar spectra of protons, but very different spectra of helium nuclei. Data on heavier nuclei have weak statistics due to the relatively high energy threshold of the applied methodology. Great hopes were pinned on experiments ATIC and CREAM, however, contradictory data were obtained from the spectral indices of the basic elements of cosmic rays, which do not provide a consistent picture of the processes occurring in the sources of cosmic rays and their propagation to the Earth.

The main advantage of direct experiments is the ability to measure the charge of the incident particle. It is much harder to use outside the atmosphere a energy detector for particles with energies of E >1012 eV. The best option, for energy measurements of different nuclei in a wide energy range (at E>1012 eV) at present, remains only the method of ionization calorimeter [2]. The main problem with this method of energy measurement is massive installation because the calorimeter must have a sufficiently depth to build the cascade curve. This greatly complicates the possibility of using such a device in the space industry.

In this regard, a more promising approach for the determination of the energy on the basis of direct measurements of CR, is the use of thin calorimeter. In a thin calorimeter the entire cascade of secondary particles is not fixed, and it is recorded only the beginning. The energy is determined on the basis of the analysis of the size of the cascade, because the number of particles in the cascade is almost proportional to the energy of the primary particle.

In present work the technique of measurement of energy of primary cosmic particles on the basis of correlation research of development of cascade process in consistently located layers of a thin calorimeter, is developed. The method is tested on the basis of computer calculations. Simulation of development of the cascade processes, initiated by primary particles of various masses and energies, has been performed on the basis of software package GEANT4.

The method is based on universality in development of cascade processes. For measurement of primary energy of cosmic particles, the correlation analysis of dependence of number of secondary particles, Ne, at observation level and the relation of number of particles, dN, at two levels, divided by an absorber layer, is used.

It is shown, that use of correlation curves (log Ne versus dN) allows to reduce essentially errors of definition of energy of the primary particle, which are connected with uncertainty of a primary nucleus and with fluctuations in development of cascade process. Uncertainties of energy reconstruction on the base of the correlation curves methodology, is less than 10 percent.

Further for possible technical realization of the project of a thin calorimeter it will be necessary to solve problems connected with calculation of installation response, optimization of the information gathering, etc. However, now the basic result is received: on the basis of computer simulation the correlation parameters, which allow to define the energy of a primary nuclei on an ascending branch of a cascade curve, are found out.

[1] Sparvoli R., *Direct measurements of cosmic rays in space* // Nucl. Phys. B – Proc. Suppl. V. 239-240, 2013, P. 115-121
[2] A. I. Fedosimova, P. B. Kharchevnikov, I. A. Lebedev, A. T. Temiraliev, *Applying universality in development of cascade processes for study of high energy cosmic particles in space experiments* // Eur. Phys. J. WC **145**, 10004 (2017)

Emission and Level Population in Gas Mixtures Pumped by Ionizing Radiation

Khasenov M.U., Batyrbekov E.G., Gordienko Yu.N., Amrenov A.K.
[1] Nazarbayev University, National Laboratory Astana PI, Astana, 010000, Kazakhstan
[2] National Nuclear Center of the Republic of Kazakhstan, Kurchatov, 071100, Kazakhstan
mendykhan.khassenov@nu.edu.kz

Abstract: Research of the luminescence of the noble gases and their mixtures are conducted at the different ways of excitation: by electron and ion beams, products of nuclear reaction in the core of nuclear reactor. The population mechanisms of levels of atoms and heteronuclear ionic molecules under the ionizing pumping are discussed. At first time products of $^{6}Li(n,\alpha)^{3}H$ nuclear reaction were used for the excitation of gases in the core of nuclear reactor.

Research on light emission of gas mixture plasma created in the active zone of a nuclear reactor is of interest from the perspective of producing ionizing radiation detectors, devices of direct transformation of the energy of nuclear reactions into light and also diagnostics of high-temperature plasma in thermonuclear reactors. Kinetics of processes at the excitation of gases by electron and ion beams or products of nuclear reaction will be the same that allow modelling processes at nuclear pumping by using particle accelerators.

Research is conducted at DC-60 heavy ions accelerator, nuclear reactor IVG1.M, compact nanosecond electron accelerator. The possibility of using products of $^{6}Li(n,\alpha)^{3}H$ nuclear reaction for excitation of gases in the core of nuclear reactor was investigated [1, 2]. The effective luminescence of lithium in the mixtures with noble gases was highlighted at the extremely low pressure of lithium vapors (10^{-6}-10^{-8} Pa). The presence of bright lines of atoms of lithium, and also of sodium and potassium, contained in the form of impurities in lithium, is explained by the sputtering of the lithium layer by products of nuclear reaction, as well as by excited atoms and ions of buffer gas.

Luminescence of the noble gases and their mixtures was investigated under the excitation by the products of nuclear reaction, by electron and ion beam [2-5]. The continuous spectra of pure gases were presented by the "third continuum" of Ar, Kr and Xe, the weak band was observed in neon in the range of 200-370 nm. Strong bands of transitions of $ArXe^{+}$ (with maxima at 329 and 506 nm), $KrXe^{+}$(491 nm), $ArKr^{+}$(642 nm) were observed in the binary mixtures of noble gases, having said that transitions from lower levels of heteronuclear ion molecules are absent. Intensity of bands of heteronuclear ionic molecules under the excitation by the powerful electron beam (W~1 MW/cm^3) relatively atomic lines was several times less, than under the excitation by an ion beam or products of nuclear reaction (W~0.1-1 W/cm^3). Apparently this is associated with the mixing of the levels of ion molecule at the high density of electrons.

In helium were observed bands of first negative system of nitrogen, 706.5 and 667.8 nm lines comparable with them in intensity and weaker 501.6 nm, 587.5 nm, 706.5 nm, 728.1 nm lines. In other noble gases prevail lines of 2p-1s transitions (Paschen notations). Distribution of radiation intensity among atomic 2p-levels differs noticeably from the distribution of flow of the dissociative recombination of molecular ions among levels given at [6]. In less degree it is related to neon, the distribution of intensity is more uniform there. The significant part of the flow of Ar_2^{+} dissociative recombination refers to the $2p_9$ level in argon, while about half of the radiation refers to $2p_2$ level. The half of radiation occurs from $2p_5$ level in xenon, there is only 4% of the flow of Xe_2^{+} ion recombination at this level. Apparently, population of atomic 2p-levels of noble gases happens in cascade transitions from d-levels [7], and the dissociative recombination of molecular ions with electrons is not the major process in population of 2p atomic levels of noble gases.

The work is performed within the Programs: "Development of nuclear energy in Kazakhstan" and "NU-Berkeley Program: 2014-2018 Strategic Research Program on critical state of substance, non-conventional materials and energy sources".

References

[1] E.G. Batyrbekov, Yu.N. Gordienko, Yu.V. Ponkratov et all., "Development of the reactor lithium ampoule device for research of spectral-luminescent characteristics of nuclear-excited plasma", Fusion Engineering and Design **117**, 204 (2017).

[2] Yu.N. Gordienko, M.U. Khasenov, E.G. Batyrbekov et all., "Emission of noble gases and their mixtures with lithium excited by products of $^{6}Li(n,\alpha)^{3}H$ nuclear reaction", Laser and Particle Beams, accepted for publication (2018).

[3] M.U. Khasenov, "Emission spectra of noble gases and their mixtures under ion beam excitation", Laser and Particle Beams **34**, 655 (2016).

[4] Yu.N. Gordienko, M.U. Khasenov, E.G. Batyrbekov et all., "Luminescence of noble gases and their mixtures under nanosecond electron beam excitation", J. Appl. Spectroscopy **85**, 545 (2018).

[5] E.G. Batyrbekov, Yu.V. Gordienko, M.U. Khasenov, Yu.V. Ponkratov, "Method of Measuring the Efficiency of the Conversion of Nuclear Energy into Optical Energy", Science and Technology of Nuclear Installations, Article ID 161535 (2015).

[6] V.A. Ivanov, "Dissociative recombination of molecular ions in noble-gas plasmas", Soviet Physics Uspekhi **35**, 17 (1992).

[7] M.U. Khasenov, "Mechanisms of level population in gas lasers pumped by ionizing radiation", Laser and Particle Beams **32**, 501 (2014).

Twin Photonic Oscillators as a Unit Cell for the Next Generation of Topological Lasers

Vassilios Kovanis
vassilios.kovanis@nu.edu.kz Department of Physics, Nazarbayev University,
Astana, Republic of Kazakhstan

In this talk, I will review and dramatize legacy topics of phased arrays of optically coupled semiconductor lasers, including experiments, accompanied by refined numerical, asymptotic and continuation methods. Recoding and dissecting the optical power spectrum of two coupled lasers, optically injected lasers and feedback configurations has guided us to a third order Adler type phase equation, as the minimal model of optically coupled diode systems. Based on these findings, we have been promoting a differentially pumped two diode laser configuration as a good candidate for the unit cell of next generation topological lasers [1]. The spectra in the vicinity of Hopf points and Exceptional Points [2] for such systems will be analyzed and computed. The modulation function will be evaluated, leading to the conclusion even in the twin system we can have resonances that exist 100GHz speeds.

All these findings and observations about the photonic Meta-Atom will be also reviewed as possible candidate for sharp, highly tunable and ultrafast photonic chip scale oscillators, with no need from the expensive optical isolators. In addition, two new proposals will be made about how to observe and dissect Photonic Chimera States in large arrays of diode lasers. Such observations will be connected to the elusive Synchronous Sisyphus effect in external cavity lasers as a path towards the super-radiant emitter. In addition, coexistence of coherent and incoherent modes in the optical comb generated by a passively mode-locked quantum dot laser, will be interpreted as Chimera State paving the way to generators for on-demand Optical Diverse Waveforms.

References

(1) Stefano Longhi, Yannis Kominis, and Vassilios Kovanis, Presence of temporal dynamical instabilities in topological insulator lasers, Europhysics Letters, 122 14004 (2018).

(2) Yannis Kominis, Kent D. Choquette Anastassios Bountis and Vassilios Kovanis, Exceptional points in two dissimilar coupled diode lasers, Applied physics Letters, 113, 081103 (2018).

Dynamical and transport properties of dense plasmas

T. S. Ramazanov[1], S. K. Kodanova[1], M. K. Issanova[1], S. Amirov[1], Zh. Moldabekov[1,2]
[1]*Institute for Experimental and Theoretical Physics, Al-Farabi Kazakh National University, 71 Al-Farabi Str., 050040 Almaty, Kazakhstan*
[2]*Institut fuer Theoretische Physik und Astrophysik, Christian-Albrechts-Universitaet zu Kiel, Leibnizstraße 15, 24098 Kiel, Germany*
ramazan@physics.kz

We present the results of an extensive research on studying of the stopping power and the transport properties of dense plasmas [1, 2]. In the former case, the main idea is to use a cold plasma model with thermal and quantum effects taken into account in a screened pair interaction potential, where screening is due to partially or totally degenerate (possibly non-ideal) electrons [3]. By comparison with other more involved calculations, which clearly shows a very good agreement at low velocities, the applicability range of the model is discussed. The main advantage of the model is that the strong ion-electron scattering is treated accurately and, hence, applicable for the description of the stopping power at the critical velocity, i.e. when the stopping power has its maximum value. The Coulomb logarithm obtained within this model is used for the computation of the dynamical and transport properties of dense plasmas. In the range of the applicability of the model, our data is in close agreement with the DFT-MD and OFDFT-MD results. Therefore, our model makes the calculation of the aforementioned effects much easier and sheds a light on the most important plasma features which govern a relevant microscopic process. In addition we presents the results on investigation of an electron scattering on an atom in dense plasmas [4]. Further, the recent results of the investigation of the dynamical screening of an ion in the case of a plasma with an electronic streaming [5, 6] (see Fig. 1) and in the case of plasma with the electrons oscillating in an external alternating field are presented [7].

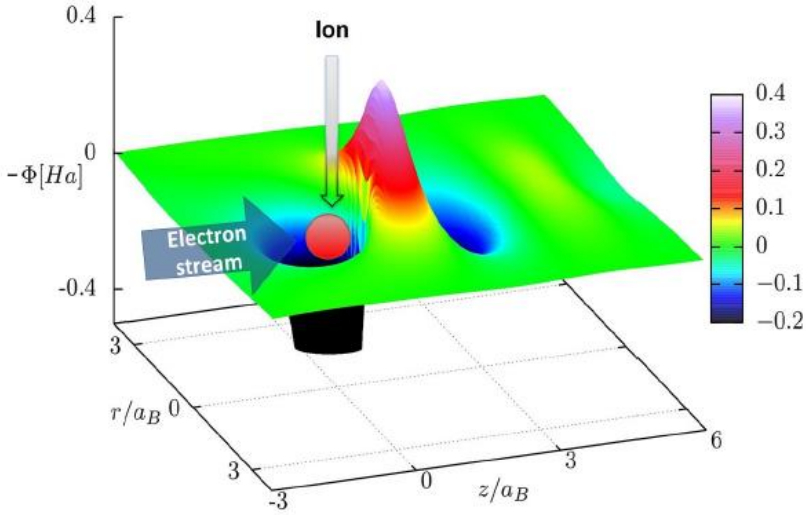

Fig. 1. Considering a nonideal plasma far from equilibrium, the total potential of a single classical ion in electron stream is calculated via a high-resolution three dimensional Fourier transformation.
For the sake of illustration the potential values have been inverted (i.e., multiplied by -1).
[*Cover Picture: Contrib. Plasma Phys. 56, issues 3–4, 2016: doi:10.1002/ctpp.201690004*]

References

[1] S.K. Kodanova, M. K. Issanova , S. M. Amirov , T. S. Ramazanov , A. Tikhonov, Zh. A. Moldabekov, "Relaxation of non-isothermal hot dense plasma parameters", Matter and Radiation at Extremes 3, 40-49 (2018)
[2] M.K. Issanova, S.K. Kodanova, T.S. Ramazanov, N.Kh. Bastykova, Zh.A. Moldabekov, "Classical scattering and stopping power in dense plasmas: the effect of diffraction and dynamic screening", Laser and Particle Beams 34, 457–466 (2016).
[3] Z. Moldabekov, T. Schoof, P. Ludwig, M. Bonitz, T. Ramazanov, "Statically screened ion potential and Bohm potential in a quantum plasma", Physics of Plasmas 22, 102104 (2015).
[4] T. S. Ramazanov, S. M. Amirov, Zh. A. Moldabekov, "Impact of quantum non-locality and electronic non-ideality on e–He scattering in a dense plasma", Contrib. Plasma Phys. 58, 155 (2018).
[5] Z. Moldabekov, P. Ludwig, M. Bonitz, T. Ramazanov, "Ion potential in warm dense matter: wake effects due to streaming degenerate electrons" Phys. Rev. E 91, 023102 (2015).
[6] Z. Moldabekov, P. Ludwig, M. Bonitz, T. Ramazanov, "Notes on anomalous quantum wake effects", Contrib. Plasma. Phys. 56, 442 (2016).
[7] T.S. Ramazanov, Zh. A. Moldabekov, M.T. Gabdullin, "Impact of single particle oscillations on screening of a test charge", Eur. Phys. J. D 72, 106 (2018).

Dynamical properties of the dusty plasma in external magnetic field

K.N. Dzhumagulova [1*], R.U. Masheyeva [1], T.S. Ramazanov [1], Z. Donkó [2]
[1] *IETP, al Farabi, Kazakh National University, 71, al Farabi av., Almaty, 050040, Kazakhstan*
[2] *Institute for Solid State Physics and Optics, Wigner Research Centre for Physics, Hungarian Academy of Sciences, Budapest, Hungary*
[*] *dzhumagulova.karlygash@gmail.com*

A number of our last papers have been devoted to the study of the dynamic properties of strongly coupled systems of charged particles interacting through the Yukawa potential and located in an external magnetic field. The studies were carried out on the basis of computer simulation of the system by the molecular dynamics method. The equation of motion (given here for particle *i*) is written as follows:

$$m\ddot{\mathbf{r}}_i(t) = \sum_{i \neq j} \mathbf{F}_{ij}(r_{ij}) + Q[\mathbf{v}_i \times \mathbf{B}], \tag{2}$$

where the first term on the right hand side gives the sum of inter-particle interaction forces, the second is the Lorentz force.

Particular attention was paid to the study of the so-called "cage correlation functions" [1]. Many of the properties of the strongly coupled complex plasmas are strongly related to one of its outstanding features, the quasi-localization of the particles in these systems: the particles oscillate in the local wells of the potential surface, which changes due to the diffusion of the particles on a timescale that can be significantly longer as compared with the timescale of oscillations. Cage correlation functions quantify the duration of the localization.

In [2-3], a mathematical model for calculating the directional cage functions of the 3-dimensional Yukawa liquid was constructed and applied for simulation. The possibility of estimating the diffusion coefficient on the basis of the decorrelation time of the cage correlation function was also shown.

Of great interest was also the investigation of the dynamic properties of a system of charged particles in an external medium, which affects the dynamics of particles by means of friction force. Such a system, in particular, is a dusty plasma, where solid dust particles of large size ($\sim 1\mu m$) and electric charge ($\sim (10^4 - 10^5)e$) move in the background plasma. The cage correlation functions of such a plasma without an external magnetic field were obtained in [4], and the diffusion coefficient in [5]. In work [6], we investigated the simultaneous effects of a static homogeneous external magnetic field and the background gas environment on the dynamical properties of dust particles in strongly coupled two-dimensional Yukawa systems. We use the Langevin dynamics computer simulation method. The equations of motion of the particles with taking into account both effects mentioned above, can be rewritten as:

$$m\ddot{\mathbf{r}}_i(t) = \sum_{i \neq j} \mathbf{F}_{ij}(r_{ij}) + Q[\mathbf{v}_i \times \mathbf{B}] - \nu m \mathbf{v}_i(t) + \mathbf{F}_{Br}, \tag{2}$$

Here the third term represents the friction force (proportional to the particle velocity), is due to of the presence of the background gaseous environment, while the fourth term accounts for a randomly fluctuating "Brownian" force that is caused by the random kicks of the gas atoms on the dust particles. To integrate the equations of motion (2), a new numerical scheme is used, in which the time step is not limited by the magnitude of the magnetic field [7]. This scheme was obtained similarly to the scheme proposed in Ref. [8], but takes into account the friction force as well. Both the presence of the magnetic field and the friction originating from the background gas, when acting alone, increase the caging time. When present simultaneously, however, we find that their effects combine in a non-trivial manner and act against each other within a window of the parameter values.

References

[1] K. N. Dzhumagulova, R. U. Masheeva, T. S. Ramazanov, and Z. Donkó, "Effect of magnetic field on the velocity autocorrelation and the caging of particles in two-dimensional Yukawa liquids," Phys.Rev. 89, 033104 (2014)
[2] K. N. Dzhumagulova, R. U. Masheyeva, T. Ott, P. Hartmann, T. S. Ramazanov, M. Bonitz, and Z. Donkó, "Cage correlation and diffusion in strongly coupled three-dimensional Yukawa systems in magnetic fields," Phys.Rev. E **93**, 063209 (2016)
[3] К.Н. Джумагулова, Т.С. Рамазанов, Р.У. Машеева, З. Донкó, М.Н. Калимолдаев, " Модель для исследования локализации заряженных частиц при наличии внешнего магнитного поля," Мат. Моделирование **30**, 135-146 (2018)
[4] K. N. Dzhumagulova, T. S. Ramazanov, and R. U. Masheeva, **"**Diffusion coefficient of three-dimensional Yukawa liquids," Phys. Plasmas **20**, 113702 (2013)
[5] K.N. Dzhumagulova, R.U. Masheyeva, T. S. Ramazanov, and Z. Donkó, "Effect of buffer gas induced friction on the caging of particles in a dusty plasma," Contrib. Plasma Phys. **56**, No. 3-4, 215 – 220 (2016)
[6] K.N. Dzhumagulova, R.U. Masheyeva, T.S. Ramazanov, G.Xia, M.N. Kalimoldayev, Z. Donkó,"Simultaneous effect of an external magnetic field and gas-induced friction on the caging of particles in two-dimensional Yukawa Systems," Contrib. Plasma Phys. 58, 217-225 (2018)
[7] K.N. Dzhumagulova and T.S. Ramazanov, "Sustainable numerical scheme for molecular dynamics simulation of the dusty plasmas in an external magnetic field," IOP Conf. Series: Journal of Physics: Conf. Series **905**, 012022(2017)
[8] Q. Spreiter and M. Walter, "Classical molecular dynamics simulation with the Velocity Verlet algorithm at strong external magnetic fields,**"** J. Comp. Phys. **152**, 102–119 (1999).

Scientific-Technical Support of the Peaceful Use of Atomic Energy in Kazakhstan

Erlan Batyrbekov
National Nuclear Center of the Republic of Kazakhstan, Kazakhstan, Kurchatov, 071100, 2 Krasoarmeyskaya st.
batyrbekov@nnc.kz

In 1991, in spite of all political, social and financial difficulties, President N.A. Nazarbayev took the decision to close the Semipalatinsk Test Site (STS) which was one of three largest world nuclear test sites, that provided development and improvement of nuclear weapon.

After Semipalatinsk Test Site closure and since Kazakhstan independence, Kazakhstan faced a number of issues that had to be solved by young independent State. Namely: Elimination of nuclear weapon testing infrastructure and its consequences on the territory of STS; Conversion of the former military and industrial complex of STS and use of its scientific and technical potential in peaceful purposes; Sensitive issue was the monitoring of nuclear weapon tests performed at other operating testing sites of the world; and development of scientific-technical, technological and staff base for nuclear power development in the Republic of Kazakhstan.

To solve all these issues, on May 15, 1992 the National Nuclear Center of the Republic of Kazakhstan (NNC) was established by Presidential Decree.

Today NNC is a leading scientific and research organization engaged in nuclear industry in the Republic of Kazakhstan. The enterprise contributes essentially in science development, solves tasks on nuclear safety enhancement, reduction of WMD proliferation risks, and provides scientific and technical support to the civil nuclear power [1].

Report will give the information about the activity of NNC on the area of scientific-technical support of the peaceful use of atomic energy in the Republic of Kazakhstan.

Reference

[1] N.A. Nazarbayev, V.S. Shkol'nik. E.G. Batyrbekov et al. Carrying-Out Scientific, Technical and Engineering Works to Bring the Former Semipalatinsk Test Site to a Safe Condition (in three volumes) // RSE "National Nuclear Center of RK" Ministry of Energy RK. Kurchatov. – 2016. - Vol 1 – p. 320. Vol 2 – p. 448. Vol 3 – p. 596.

Atmospheric transport, dispersion and deposition of radioactive materials released from nuclear accidents or weapons tests: the case study of the Chernobyl catastrophe

Oleg Skrynyk[1,2] and Sergiy Bubin[2]
[1]*Ukrainian Hydrometeorological Institute, Kyiv, Ukraine*
[2]*Nazarbayev University, Astana, Kazakhstan*
skrynyk@uhmi.org.ua, sergiy.bubin@nu.edu.kz,

Abstract: In this work we have modelled the atmospheric transport, dispersion and deposition of Chernobyl Cs-137 aerosol particles on a regional spatial scale (up to 1000 km from the source) by means of the well-known dispersion model CALPUFF. We have performed our simulations using two different parameterizations of the source term. The calculated air concentration and surface contamination have been compared with the available pollution measurements. Based on this analysis we have identified the physical mechanisms responsible for the formation of the observed surface contamination patterns. We have also investigated the suitability of the CALPUFF model for simulations of radionuclide dispersion and deposition that take place after nuclear weapons tests.

1. Introduction

Accidents at nuclear power plants and other hazardous facilities with releases of radioactive materials into the atmosphere, unfortunately, do happen (Fukushima is the latest example). For this reason, numerical simulations of the atmospheric transport, dispersion and depositions of radioactivity are essential for mitigating the consequences and assessing damage caused to population and nature. In this study we have simulated the fate of Cs-137 aerosol particles released from the 1986 Chernobyl nuclear power plant accident (CNPPA) on a regional spatial scale. This case is of special interest because of its spatial scale and fair amount of measured pollution data available. Our simulations have been carried out in the framework of the CALPUFF dispersion model. We have investigated the performance of this model in predicting the level of radioactive pollution after the CNPPA [1] and estimated its suitability for predicting fallouts after nuclear weapons tests, such as the ones that took place repeatedly at the Semipalatinsk test site.

2. Data and methods

CALPUFF is a Lagrangian puff modelling system that simulates the effects of time- and space-varying meteorological conditions on pollutant fate. It is recommended by the US Environmental Protection Agency for long-range dispersion regulatory applications. In our numerical tests we adopted two different schemes for temporal evolution and vertical distribution of Cs-137 emissions in the CNPPA [2, 3]. The modeling domain covered the whole territory of Ukraine with the grid resolution of 15 km (98×75 grid points total). As meteorological input for the CALPUFF model, we used a dataset of time series recorded at 211 surface stations, 194 precipitation stations and 14 upper air stations located in the domain. The Cs-137 daily air concentration and daily deposition data measured at 2 sites during the event and cumulative deposition data sampled at 410 sites after the accident were used for the verification of our model.

3. Results

We have performed a large number of simulations by varying the types of source parameterizations, computational algorithms for dry deposition of aerosol particles, and CALPUFF's control parameters. The comparison with available measurements of the Cs-137 pollution was based on using several statistical tests/indices. Our calculations have demonstrated that the CALPUFF model can capture the main features of the total deposition pattern on the domain. The main radioactive traces (western, eastern and southern) were reproduced fairly well. However, the accuracy of the calculated data is rather sensitive to the accuracy of the meteorological information input. We have found a strong dependence of the simulated contamination pattern on the emission source parameterization. Additionally, we have found that the resistant model for the dry deposition velocity of Cs-137 aerosol particles significantly underestimated the depositions and the best agreement with measurements was obtained with the constant deposition velocity of 0.005 m/s. Based on our simulations we identified the physical mechanisms (dry deposition and/or wet removal) responsible for the formation of the local maxima of the observed surface contamination patterns. We have also performed numerical simulations of the radionuclide dispersion and deposition that would occur after nuclear explosion in the same domain.

4. Conclusion

This work has confirmed the applicability of the CALPUFF model for simulating the air transport, dispersion and deposition of radioactive aerosol particles on a regional spatial scale.

[1] Giaiotti D., Oshurok D., Skrynyk O., "The Chornobyl nuclear accident Cs-137 cumulative depositions simulated by means of the CALMET/CALPUFF modeling system", Atm. Pol. Res. **9,** 502-512 (2018).
[2] Brand J., Christensen J.H., Frohn L.M., "Modeling transport and deposition of caesium and iodine from the Chornobyl accident using the DREAM model", Atm. Chem. Phys. **2**, 397-417 (2002).
[3] Talerko N., "Mesoscale modeling of radioactive contamination formation in Ukraine caused by the Chornobyl accident", J. Env. Rad. **78**, 311-329 (2005)

The introduction of information and innovative technologies in the energy production processes of existing TPS of the Republic of Kazakhstan in order to address the problems of power engineering and ecology

A.S. Askarova
Al-Farabi Kazakh National University, 71, Al-Farabi ave., Almaty, Kazakhstan
Aliya.Askarova@kaznu.kz
S.A. Bolegenova
Al-Farabi Kazakh National University, 71, Al-Farabi ave., Almaty, Kazakhstan
Saltanat.Bolegenova@kaznu.kz
S.A. Bolegenova
Scientific Research Institute of Experimental and Theoretical Physics, 71, Al-Farabi ave., Almaty, Kazakhstan
bolegenova.symbat@kaznu.kz
V.Ju. Maximov
Al-Farabi Kazakh National University, 71, Al-Farabi ave., Almaty, Kazakhstan
valeriy.maximov@kaznu.kz
A.O. Nugymanova
Aizhan.Nugymanova@kaznu.kz

Abstract: The computational experiments using the "Overfire Air" (OFA) technology at the coal dust torch combustion in the combustor of existing TPS of the Republic of Kazakhstan have been conducted. The results show a possibility of reaching a reduction of the emission of noxious nitrogen oxides NO_x and minimizing the energy losses. The results of numerical experiments on the influence of the additional air supply on the main characteristics of heat and mass transfer are presented.

1. Introduction

The share of power engineering enterprises in the total volume of the ambient medium pollution by the fuel combustion products is high. The enterprises of heat-and-power engineering, ferrous and non-ferrous metallurgy, oil and gas branches, and machine-building are the most harmful for ecology. Such substances as the carbon oxide, nitrogen oxide, nitrogen dioxide, dust, lead, sulfur dioxide, etc., are exhausted into the atmosphere in Kazakhstan, which harm substantially the living organisms [1].

In connection with the fact that the thermoelectric power stations operating on solid fuel are one of the main sources of the atmospheric air pollution by harmful gaseous and dust emissions, the development of the fuel combustion technologies with minimum emissions of the NO_x, SO_x, and ash particles becomes urgent.

The problem of minimizing noxious substance emissions into the atmosphere by power engineering enterprises can be solved only by basing on the physical, mathematical, and chemical modeling. In this connection, the numerical experiment becomes one of the most economical and convenient techniques for a detailed analysis of complex physical and chemical phenomena occurring in the furnace chamber. The use of the efficient equipment and advanced program complexes enables the solution of these tasks for specific power plants and for any power-plant fuel [2].

2. Methodology of the research

The authors of this article used information and innovation technologies of 3D modeling to the energy production processes of operating heat stations in Kazakhstan to solve the problems of heat and power engineering and ecology.

The FLOREAN application package was used for simulation and determination of various parameters of combustion using "clean" coal dust combustion technology – Over Fire Air Technology.

The OFA method, which is also termed the "Overfire Air" method, involves the supply of the entire air volume for (primary and secondary) combustion in two stages: 70-90 % of air is fed to the burners, and the remaining amount of air is supplied to the furnace facility above the burner by the over fire air technology. When the fuel is mixed in the burner with a controlled air flow a combustion zone with a relatively low-temperature, with vitiated air, and enriched with fuel is created in the lower part of the furnace facility, which helps to reduce the formation of the NO_x from the nitrogen contained in fuel (the fuel NO_x) [3].

The results of the conducted numerical modeling of the coal dust torch combustion in the boiler of the thermoelectric power station using the "Overfire Air" method enable us to propose for heat-and-power engineers the newest technologies of a coal pure combustion and reduction of noxious emissions of the nitrogen oxides NO_x.

[1] R. Leithner, A. Askarova, S. Bolegenova, V. Maximov, "Computational modeling of heat and mass transfer processes in combustion chamber at power plant of Kazakhstan" , MATEC Web of Conferences **76**, 06001 (2016).
[2] R. Leithner, H. Müller, "CFD studies for boilers", in: Second M.I.T. Conf. on Computational Fluid and Solid Mechanics, Cambridge, 2003.
[3] A.S. Askarova, S.A. Bolegenova, V.Yu. Maximov, "Reduction of noxious substance emissions at the pulverized fuel combustion in the combustor of the BKZ-160 boiler of the Almaty heat electropower station using the «Overfire Air» technology", Thermophysics and Aeromechanics **23**, 125 (2016).

Thermodynamic properties of dense non-ideal plasma on the basis of effective potentials of interactions

M.T. Gabdullin[1], T.S. Ramazanov[2], Zh.A. Moldabekov[2], T.N. Ismagambetova[2]
[1]*KBTU, Kazakh British Technical University, Almaty, 050000, Kazakhstan*
[2]*IETP, al-Farabi Kazakh National University, Almaty, 050040, Kazakhstan*
gabdullin@physics.kz

Abstract: In this work the thermodynamic properties of a dense non-ideal plasma were studied. The method of effective potentials (pseudopotentials) was used to construct the corresponding models and to study the fundamental properties of a non-ideal plasma. The effective potentials used in this work take into account both the collective nature of particle interaction in plasmas (screening) at large distances between particles, and the quantum mechanical effects of diffraction and symmetry at small distances [1]. The difference between temperatures of electrons and ions can significantly influence plasma properties. The electron-ion temperature in this work was used in the form $T_{\alpha\beta} = \sqrt{T_\alpha T_\beta}$ [2].

The following effective screened interaction potentials taking into account the quantum-mechanical effect of diffraction were used [1]:

$$\Phi_{\alpha\beta}(r) = \frac{Z_\alpha Z_\beta e^2}{r} \frac{1}{\gamma^2\sqrt{1-\left(2k_D/\lambda_{ee}\gamma^2\right)^2}} \times \left(\left(\frac{1/\lambda_{ee}^2 - B^2}{1 - B^2\lambda_{\alpha\beta}^2} \right) \exp(-Br) - \left(\frac{1/\lambda_{ee}^2 - A^2}{1 - A^2\lambda_{\alpha\beta}^2} \right) \exp(-Ar) \right) - \quad (1)$$

$$- \frac{Z_\alpha Z_\beta e^2}{r} \frac{(1-\delta_{\alpha\beta})}{1+C_{\alpha\beta}} \exp(-r/\lambda_{\alpha\beta}),$$

where $k_D^2 = k_e^2 + k_i^2$ is the screening parameter taking into account the contribution of electrons and ions, $\gamma^2 = k_i^2 + 1/\lambda_{ee}^2$, $A^2 = \frac{\gamma^2}{2}\left(1+\sqrt{1-\left(\frac{2k_D}{\lambda_{ee}\gamma^2}\right)^2}\right)$, $B^2 = \frac{\gamma^2}{2}\left(1-\sqrt{1-\left(\frac{2k_D}{\lambda_{ee}\gamma^2}\right)^2}\right)$, $C_{\alpha\beta} = \frac{k_D^2\lambda_{\alpha\beta}^2 - k_i^2\lambda_{ee}^2}{\lambda_{ee}^2/\lambda_{\alpha\beta}^2 - 1}$.

The thermodynamic properties of a two-component plasma were calculated on the basis of effective potentials and radial distribution functions. The results for the correlation energy and equation of state agree with the results of computer simulations at small values of coupling parameter. The difference appearing with increasing coupling parameter is due to change in a plasma composition; i.e., the concentration of atoms in the system rises and concentration of free charges decreases. The results of this work can be used in promising applied fields of applications, such as thermonuclear energy, new-generation rocket engines, astrophysics. Also, in works [3-5] various effective potentials of dense non-ideal plasma were obtained. To study how the oscillations of electrons induced by an external field change the inter-particle interaction, the impact of the single particle oscillations on the screening of the test charge has been analyzed using the polarization function in the long wavelength limit [3]. In work [4], it has been shown that the screened Cornell type interaction potential between ions can be realized in the hot dense plasma. The potentials describing interactions of dipole-dipole and charge-dipole pairs in a classical non-degenerate plasma as well as in degenerate quantum and semiclassical plasmas were derived using multipole expansion method in work [5].

References

[1] T.S. Ramazanov, Zh.A. Moldabekov, and M.T. Gabdullin, Physical Review E **92**, 023104 (2015).
[2] R. Bredow, Th. Bornath, W.-D. Kraeft, R.Redmer, Contrib. Plasma Phys. **53**, 276 (2013).
[3] T.S. Ramazanov, Zh.A. Moldabekov, and M.T. Gabdullin, Eur. Phys. J. D. **72**, 106 (2018).
[4] T. S. Ramazanov, Zh. A. Moldabekov, and M. T. Gabdullin, Phys. Plasmas **23**, 042703 (2016).
[5] T. S. Ramazanov, Zh. A. Moldabekov, M. T. Gabdullin, Phys. Rev. E **93**, 053204 (2016).

Deterministic Mechanism of Irreversibility and Physics of Evolution

Vyacheslav M. Somsikov
Institute of Ionosphere, Almaty, Kazakhstan
E-mail: vmsoms@rambler.ru

Abstract: The first attempts of a design of physics of evolution on the basis of the received earlier determined mechanism of irreversibility (DMI) are discussed. Key ideas which formed the basis of DMI and fundamental concepts used at creation of mechanics of systems are explained. Examples of possible application of DMI in some departments of physics are given.

The steps in the construction of the physics of evolution are submitted. These steps based on of the deterministic mechanism of irreversibility (DMI) of the system's dynamics. The DMI was obtained in the frame of the laws of the classical mechanics basing on the fact that the body's motion equations were taking into attention of the body's structure. According to this equation the external energy is transformed into the system's motion energy and internal energy.

The motion equation for the system consisting from the N potential interaction of the material points (MP) has a form [1]:

$$M_N\dot{V}_N = -\sum_{i=1}^{N} F_i^0 - \frac{V_N}{NV_N^2}\sum_{i=1}^{N-1}\sum_{j=i+1}^{N} v_{ij}(m\dot{v}_{ij} + F_{ij}^0 + NF_{ij})$$

Here F_i^0 -is external force, acted on i-th MP; F_{ij}- is interaction force i and j MP; $m_i = m_j = 1 \forall i, j$; $i, j = 1,2,...N$, $V_N = 1/N\sum_{i=1}^{N} v_i$; $M_N = Nm = N, m = 1$, $M_N = Nm = N; m = 1.$

The first term on the right-hand side of equation is the force which applied to the center of mass of the system. It determines the system's motion as a whole. The second term depends on the micro - and macro variables (micro-variables are determined the motion of MP in relative to the center of mass of the system. The macro-variables determined the system's motion in the space). The symmetry of the system's motion equation differs from the symmetry of Newton's motion equation for MP because of the presence of the second term, which determined the change of the internal energy. That is, the motion energy for the system, in contrast to the motion energy for MP, in the general case is no invariant. This means the possibility of breaking the symmetry of time.

As can be seen from equation, the work of external forces in the general case does not coincide with the work on the displacement of the system, because part of this work is transformed into internal energy.

It was shown that when N>>1 and when the gradient of external forces are exists, the irreversibility of the system's dynamic have a place. It allowed introducing of the concept of D-entropy into the mechanics of systems, having defined it as the relation of value of an increment of internal energy to its full value. With the help of DMI and D-entropy, it was shown how the laws of the thermodynamics and statistical physics can be following from the mechanics laws.

The basic concepts of physics of evolution were introduced. One of these concepts is the principle of duality of the symmetries. According to this principle, the body dynamics determined not only by the symmetry of space, as in the case of a MP, but by the body's symmetries also.

It was shown how the laws of system dynamics are determined on the basis of the dynamics laws of their elements. The principles of constructing a hierarchical world picture based on the laws of the physics were submitted [3]. It was explained based on these principles how the laws of evolution of systems are following from the knowledge of laws of evolution of their elements.

It was shown that infinite divisibility of matter follows from the laws of classical mechanics. The concept of evolutionary nonlinearity, which responsible for the violation of symmetry of system dynamics was introduced [2]. The extended Schrodinger equation was obtained. This equation is applicable to describe the interaction and evolution of quantum systems was submitted [4].

References.

1. Somsikov V.M. 'To the basics of the physics of evolution". Almaty. (2016).
2. Somsikov V.M. Non-Linearity of Dynamics of the Non-Equilibrium Systems. World Journal of Mechanics..11.(2017)
3. Somsikov V.M. Irreversibility and physics of evolution. *Chaotic Modeling and Simulation (CMSIM).* 10th Chaotic Modeling and Simulation International Conference. Barcelona/ Selected paper. 47-61, (2018).
4. Somsikov V.M. Extension of the Schrodinger equation. EPJ Dubna Web of Conferences Baldin ISHEPP XXIII. (2017).

Integrable spin system and Hirota's method

Zh. Sagidullayeva, G. Nugmanova
Eurasian International Center for Theoretical Physics,
L.N. Gumilyov Eurasian National University, Astana, Kazakhstan
Author e-mail address: sagidullayeva.zh@gmail.com

Abstract: In this work we consider an integrable generalization of the Landau-Lifshitz equation with self-consistent potential. Also by generalizing Hirota's method we found exact solutions and defined an interaction between the potential and soliton.

Solitons are structurally stable solitary waves propagating in a nonlinear medium. Due to their special properties, solitons behave like particles (particle-like waves): when interacting with each other or with some other perturbations, they do not collapse, but continue to move, keeping their structure unchanged. This property can be used to transmit data over long distances without interference, which opens up huge opportunities for the use of solitons. Solitons manifest themselves in completely different areas: in hydrodynamics, optics, magnetism and etc.

In this work we investigate the spin model which describes nonlinear wave processes in ferromagnets - the generalized Landau-Lifshitz (GLL) equation with self-consistent potential [1,2], which reads as

$$iS_t + \frac{1}{2}[S, S_{xx}] + \frac{1}{a}[S, W] = 0, \quad (1)$$

$$iW_x + a[S, W] = 0, \quad (2)$$

where $a = const$, $S = \Sigma_{j=1}^{3} S_j(x, y, t)\sigma_j$ is a matrix analogue of the spin vector, W - potential with the matrix form $W = \Sigma_{j=1}^{3} W_j(x, y, t)\sigma_j$, and σ_j are Pauli matrices.

Waves of magnetic ordering irregularities in ferro-, antiferro- and ferrimagnets are called spin waves. The spins of the atoms in these substances and the magnetic moments associated with them in the ground state are ordered. The deviation of the magnetic moment from the preferred direction is not localized on the atom, but in the form of a wave propagates in the medium. The corresponding spin systems with self-consistent potentials can be made in the general class family of integrable nonlinear evolution equations with the additional potential fields. We have proved the integrability of the equation with vector potential, so it is a soliton equation and describes the process of magnetization in ferromagnetic. An important result of this work was establishing a consistent interaction between the spin and potential vector fields [3]. Further work on this research is to establish the exact form and to determine the behavior of two- and more layers of the spin system, the so-called multilayer system with potentials and their physical applications.

References

[1] Myrzakulov R., Mamyrbekova G. K., Nugmanova G.N., Yesmakhanova K.R. “Integrable Motion of Curves in Self-Consistent Potentials: Relation to Spin Systems and Soliton Equations” Phys. Lett. A **378**, 2118-2123, (2014).
[2] Myrzakulov R., Mamyrbekova G., Nugmanova G., Lakshmanan M. “Integrable (2+1)-Dimensional Spin Models with Self-Consistent Potentials” Symmetry **7**, 1352 (2015).
[3] Nugmanova G., Sagidullayeva Zh., Myrzakulov R. “Hirota's method for a spin model with self-consistent potential” J. of Phys. Conf. Series **804**, 012035 (2017).

Multiscale approach and computation of dense quantum plasmas

Zhandos Moldabekov[1,2], Michael Bonitz[1], Tlekkabul Ramazanov[2]

[1]*Institut fuer Theoretische Physik und Astrophysik, Christian-Albrechts-Universitaet zu Kiel, Leibnizstraße 15, 24098 Kiel, Germany*
[2]*Institute for Experimental and Theoretical Physics, Al-Farabi Kazakh National University, 71 Al-Farabi Str., 050040 Almaty, Kazakhstan*
zhandos@physics.kz

Abstract: A large scale simulation of quantum plasmas with correlated electrons is challenging and, currently, a formidable task. Ab initio methods such as Quantum Monte-Carlo and Kohn-Sham density functional theory (DFT) are severely limited by the number of electrons and ions which can be simulated [1]. The main problem here is the vastly different time scales of electrons and ions resulting from their different masses. A possible solution of this dilemma is a multi-scale approach based on assumption that a plasma can be considered as a combination of two subsystems: electrons moving in the field of inert ions, and ions moving in the electronic medium. Hence, for the modeling of electronic component, orbital-free formulation of DFT for dense plasmas and warm dense matter has undergone rapid development in recent years [1]. However, the OFDFT is limited to the static case. Therefore, in this work, we present our recent result on the development of quantum hydrodynamics (QHD)–within multiscale approach–of correlated electrons in dense plasmas; which e.g., can be used for the description of the dynamics of the electrons around a mean distribution obtained from the OFDFT and, thereby, can be a reliable tool for a large scale simulation of a quantum plasma dynamics [2]. We have derived the closure relations which allow to go beyond of previously used QHD models. The main features of the developed QHD theory are the following: it can be used at finite temperatures, the agreement with the random phase approximation is guarantied in the non-interacting limit, the effect of correlations is taken into account via the local filed corrections, and can be used for the weakly non-uniform case. The non-ideality effect is discussed for both static and dynamic cases employing local field corrections [2,4]. Finally, the extension to the case of a quantum plasma in an external magnetic field is presented.

As mentioned before, within multiscale approach ions are considered moving in an electronic medium. Recently, going beyond the random phase approximation, we have performed an analysis of the screened ion potential in the case of non-ideal quantum electrons by making use of local field corrections which are determined on the basis of the Singwi–Tosi–Land–Sjölander approximation (STLS) [5] and Quantum Monte Carlo data [6]. From the analysis of the structural properties of strongly coupled ions on the basis of different screened ion potentials, the region of densities and temperatures where the STLS description of screening by partially (or totally) degenerate electrons can be used for the calculation of the structural properties of ions were determined [7]. It was found that correlations (non-ideality) of the electrons result in a larger isothermal compressibility of the ions due to the stronger screening of the ion charge. Additionally, calculations using different screened potentials clearly show that strongly coupled ions can be very sensitive to the shape of the pair interaction potential and, therefore, to the approximation used for the description of screening by electrons. Further, we have extended our considerations by computing the dynamic ionic structure factor. We found that, in contrast to the static structure factor, the dynamical structure factor of ions at small values of the wave-number can be correctly described using the Yukawa potential, but with a properly adjusted screening length. We found a significant redshift in the ionic dispersion relation due to the electronic exchange-correlation effects.

References

[1] F. Graziani, M.P. Desjarlais, R. Redmer, and S.B. Tricke, "Frontiers and Challenges in Warm Dense Matter", (Springer, 2014); T. Sjostrom and J. Daligault, "Nonlocal orbital-free noninteracting free-energy functional for warm dense matter" Phys. Rev. B 88, 195103 (2013); V. Karasiev, T. Sjostrom and S. B. Trickey, "Generalized-gradient-approximation noninteracting free-energy functionals for orbital-free density functional calculations" Phys. Rev. B 86, 115101 (2012).

[2] Zh.A. Moldabekov, M. Bonitz, T.S. Ramazanov, "Theoretical foundations of quantum hydrodynamics for plasmas" Phys. Plasmas 25, 031903 (2018)

[3] H. Reinholz, R. Redmer, G. Roepke, and A. Wierling, "Long-wavelength limit of the dynamical local-field factor and dynamical conductivity of a two-component plasma" Phys. Rev. E 62, 5648 (2000).

[4] Z. Moldabekov et al., "Ion potential in warm dense matter: wake effects due to streaming degenerate electrons" Phys. Rev. E 91, 023102 (2015); "Statically screened ion potential and Bohm potential in a quantum plasma" Phys. Plasmas 22, 102104 (2015); "Notes on anomalous quantum wake effects", Contrib. Plasma. Phys. 56, 442 (2016); "Ion potential in non-ideal dense quantum plasmas" Contrib. Plasma Phys. 57, 532 (2017).

[5] S. Tanaka, S. Ichimaru, J. Phys. Soc. Jpn. 55, 2278 (1986).

[6] M. Corradini, R. D. Sole, G. Onida, M. Palummo, Phys. Rev. B 57, 14 569 (1998).

[7] Zh.A. Moldabekov, S. Groth, T. Dornheim, H. Kählert, M. Bonitz, T.S. Ramazanov, "Structural properties of strongly coupled ions in quantum plasmas" Phys. Rev. E 98, 023207 (2018).

The stability of circular orbits of a test body in the field of two rotating massive bodies

Medeu Abishev[1,2], Saken Toktarbay[1], Aigerim Abylayeva[1], Amanhan Talkhat[1]

[1]*Department of Theoretical and Nuclear Physics, Al-Farabi Kazakh National University, Almaty 050040, Kazakhstan*

[2]*Institute of Gravitation and Cosmology, Peoples Friendship University of Russia (PFUR), Moscow 117198, Russia*

saken.yan@yandex.com

Abstract: We consider the problem of orbital stability of a test particle motion in the restricted three-body problem where all bodies have their own rotation. We show that it is possible to get some insight into the stability properties of the motion of test particles, without knowing the exact solutions of the motion equations.

The orbital stability of two rotating bodies investigated in [1, 2]. As well as, the orbital stability problem of circular motion of a test body in the restricted three-body problem with the relativistic corrections investigated in [3], where the appropriate conditions are

$$U_1 \ll c^2, U_2 \ll U_1 \tag{1}$$

where U_1, U_2 are the potentials of central and second bodies respectively. All the bodies do not have their own rotation. The resting position of the central body (the first body) coincides with the reference point of coordinates while the second body moves along the circle around the central body and is not subjected to the disturbance. The test body moves in a perturbed circular orbit. This problem belongs to the class of quasi-keplerian, the orbital stability investigated in GR mechanics by the adiabatic theory of motion, which was developed by academician M.M. Abdildin [4].

According to the adiabatic theory, the evolutionary motion of the test body (third) describes the average change of its orbital momentum. Therefore, we write down the orbital angular momentum of the test body

$$\vec{M} = [\vec{r}\vec{P}], \tag{2}$$

and the time derivative from it

$$\dot{\vec{M}} = \left[\dot{\vec{r}}_i, \vec{p}_i\right] + \left[\vec{r}_i, \dot{\vec{p}}_i\right] \tag{3}$$

where

$$\dot{\vec{r}}_i = \frac{\partial H}{\partial \vec{p}_i}; \quad \dot{\vec{p}}_i = -\frac{\partial H}{\partial \vec{r}_i}; \tag{4}$$

are found by means of the equations of Hamilton from the Hamilton function of the system.

In [3,5], Abishev et al., the relativistic equation of translational motion of a test body in the field of two bodies in the mechanics of general relativity is investigated by the asymptotic methods of the adiabatic theory through the process of averaging the corresponding equations using the vector elements $\vec{M}$ (the orbital moment) and $\vec{A}$ (the Laplace vector). It is shown that in this case the orbit of the test body is stable in the form of circular orbit.

The Lagrange's function of translational and rotational motion for the three rotating bodies without interior structure can be represented in this form:

$$L = L^{(0)} + L^{(*)} \tag{5}$$

Consequently, the Hamiltonian function can be represented in this form:

$$H = H^{(0)} + H^{(*)} \tag{6}$$

where (0) term is for the three point like masses and it's explicit form was presented in the work [3] by Abishev at al., and $(*)$ is the additional term which related to the rotation of the body.

According to the adiabatic theory, in order to obtain the evolutionary equations of motion one needs to integrate the equation (3) for the repetition period of system configurations T (synodic period of the test body):

$$\bar{\dot{M}}^{(*)} = \frac{1}{T}\int_0^T \dot{M}^{(*)} dt = 0; \; T = \frac{2\pi}{\omega_2 - \omega_3} \tag{7}$$

In fact, the preliminary results show that it is possible to find the time derivative of the angular momentum, and then integrate the equation to find the average change in the orbital angular momentum.

The resulting equation was integrated (averaged) by the synodic period of the test body, which eliminates perturbations, leaving only evolutionary effects. The result of the integral is confirmed that the circular motion will be stable if the spins of all bodies are collinear within a plane. The quasi-circular orbits of the test body will be analyzed in a forthcoming works.

References

[1]Abdil'din M.M., AbishevM.E., BeissenN.A.GravitationandCosmologyV15,141(2009).

[2]BrumbergA.A. *Relativistic celestial mechanics* (Nauka,1972),382p.

[3]AbishevM.E., Toktarbay,S., ZhamiB.A. GravitationandCosmology.V20,149 (2014).

[4]AbdildinM.M. *Mechanins of Einstein theory of gravity* (Alma-Ata:Nauka,1988),198p.

[5] Abishev, Medeu; at al., EPJ Web of Conferences, Volume 168, id.04001. (2018)

Paraxial laser beams as versatile tool for modern photonics

Tileubek Uakhitov, Alfarabi Issakhanov, Nurdaulet Ozat, and Anton S. Desyatnikov
Department of Physics and Center of Excellence for Fundamental and Applied Physics,
School of Science and Technology, Nazarbayev University
anton.desyatnikov@nu.edu.kz

Abstract: Longitudinal paraxial dynamics of laser beams is described by a Schrödinger-type equation with the potential term proportional to the changes in the refractive index of the optical medium. This modulation can be pre-fabricated in the material, in the form of a single or multiple coupled optical waveguides, thus creating photonic lattices. The change in the refractive index can be also self-induced by a laser beam via nonlinear Kerr-type effect, thus supporting spatial optical solitons. We describe several applications of laser beams in singular and nonlinear photonics.

1. Introduction

Laser beams are distinguished by a narrow spectrum around central frequency ω, or quasi-monochromaticity, as well as strong directivity, forming a narrow "pencil" of light in the direction of propagation, say z. Both these properties are taken into account in the expression for electric field of the light wave $E(\boldsymbol{r},t)=\psi(\boldsymbol{r})\exp(ikz-i\omega t)$, here k is the wavenumber. The envelope of the wave $\psi(\boldsymbol{r})$ is slowly varying in the direction of z, i.e. $|\partial^2\psi/\partial z^2| \ll k|\partial\psi/\partial z|$. In this so-called paraxial approximation, the Helmholtz wave equation is reduced to

$$i\frac{\partial\psi}{\partial z}=-\frac{1}{2k}\Delta_\perp\psi-\frac{k\Delta n}{n_0}\psi\ , \tag{1}$$

here $\Delta_\perp=\partial_x^2+\partial_y^2$ is transverse Laplacian, n_0 is unperturbed refractive index of the medium, and $\Delta n \ll n_0$ is refractive index modulation. The analogy with the Schrödinger equation in quantum mechanics is established by allowing the spatial coordinate z play a role of "time" for a two-dimensional wavepacket $\psi(x,y;z)$ in the potential $\sim -k\Delta n/n_0$.

2. Photonic lattices

Photonic lattices, or two-dimensional arrays of weakly coupled optical waveguides, are formed by a periodic modulation of the refractive index $\Delta n(x,y)$ in Eq. 1, see Fig. 1(a). A light wave propagates in a photonic lattice similar to an electron wavepacket in a two-dimensional material, such as graphene. Engineering the geometry of photonic lattices allows tailoring the topology of energy-momentum spectrum. For example, instead of "fermionic" Dirac cones in photonic graphene, the Lieb lattice in Fig. 1(a) reveals "bosonic" intersection with a flat band and integer pseudospin [2], see Fig. 1(b). In short, laser beams in photonic lattices allow for direct observation of fundamental phenomena of solid state and relativistic physics.

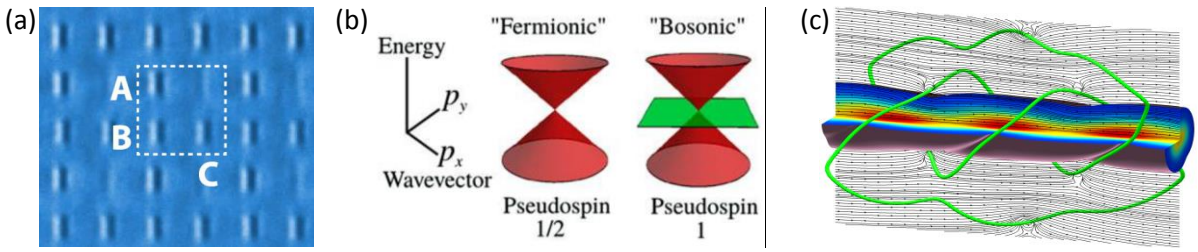

Fig. 1. (a) Example of a photonic lattice: phase contrast image of the fabricated refractive index profile for two-dimensional photonic Lieb lattice in fused silica; dashed line shows one unit cell with the three sublattices labelled A, B, C [1]. (b) Conical intersections of energy bands for two different orders with pseudospin s: the 'fermionic' (half-integer s) Dirac cone and 'bosonic' (integer s) intersection [2]. (c) Trefoil knot of an optical vortex line (green) around spatial optical soliton in saturable medium [4].

3. Spatial solitons and optical vortices

The nonlinear modulation of the refractive index $\Delta n(|\psi|^2)$ in Eq. 1 supports formation of spatial optical solitons [3] as well as nonlinear interaction between different waves. At the same time, in any system with multiple-wave interference, the so-called optical vortices appear naturally, revealing twisted light and optical orbital angular momentum. In three dimensions vortex lines emerge as "threads of darkness"; these threads can be closed in loops and knots; an example [4] of a trefoil knot around a spatial optical soliton in saturable nonlinear media is shown in Fig. 1(c). It is the nonlinear phase of the self-trapped light beam that breaks the wave front into a sequence of optical vortex loops which tangle on propagation to form links and knots. We discuss here the interplay between geometry and nonlinearity which leads to spontaneous linking and knotting of optical vortex lines and may be found as a universal feature of waves whose phase front is twisted and nonlinearly modulated, including superfluids and trapped matter waves.

[1] F. Diebel, D. Leykam, S. Kroesen, C. Denz, and A. S. Desyatnikov, *Conical diffraction and composite Lieb bosons in photonic lattices*, Physical Review Letters **116**, 183902 (2016)
[2] D. Leykam and A. S. Desyatnikov, *Conical intersections for light and matter waves*, Advances in Physics: X **1**, 101 (2016)
[3] A. S. Desyatnikov, Yu. S. Kivshar, and L. Torner, *Optical Vortices and Vortex Solitons*, Progress in Optics **47**, 291 (2005)
[4] A. S. Desyatnikov, D. Buccoliero, M. R. Dennis, and Yu. S. Kivshar, *Spontaneous knotting of self-trapped waves*, Scientific Reports **2**, 771 (2012)

Quantum compiling with diffusive sets of gates

Y. Zhiyenbayev, V. M. Akulin, A. Mandilara
Department of Physics, School of Science and Technology, Nazarbayev University, 53, Kabanbay batyr Av., Astana, 010000, Republic of Kazakhstan
Aikaterini.mandilara@nu.edu.kz

Abstract: Given a set of quantum gates and a target unitary operation, the most elementary task of quantum compiling is the identification of a sequence of the gates that approximates the target unitary to a determined precision ε. The Solovay-Kitaev theorem provides an elegant solution which is based on the construction of successively tighter `nets' around the unity comprised by successively longer sequences of gates. The procedure for constructing the nets, according to this theorem, requires accessibility to the inverse of the gates as well. In this work, using the theory of random walks we propose a method for constructing nets around unity without this requirement. The algorithmic procedure is applicable to sets of gates which are diffusive enough, in the sense that sequences of moderate length cover the space of unitary matrices in a uniform way. We prove that the number of gates sufficient for reaching a precision ε scales as $O(\log(\frac{1}{\varepsilon})^{\log 3 / \log 2})$ while the pre-compilation time is increased as compared to the Solovay-Kitaev algorithm by the polynomial factor 3/2.

Introduction

Approximation up to a given accuracy of an arbitrary unitary transformation by a series of standard transformations (gates) is an important ingredient of programming of quantum computers, which was formulated and solved [1] in the case where the set of M predetermined standard transformations contains both direct operations and their inverses. The so called Solovay-Kitaev (SK) theorem provides the proof of existence together with the method for constructing the solution. Based on the elements in the proof of the SK theorem, the Dawson-Nielsen (DNSK) algorithm [2] provides the exact steps for identifying a series of length L, which scales with the required accuracy ε as $O(\log(\frac{1}{\varepsilon})^{3.97})$ and with running time as $O(\log(\frac{1}{\varepsilon})^{2.71})$.

Here we address the question [2] whether is possible to generalize the results of SK theorem onto the case where the set of the predetermined operations does not contain the inverses. In view of the fast development of quantum technologies, this problem has theoretical but mostly practical interest since experimentalists often do not have access to inverse operations-- they are restricted to semigroup rather than group operations. In [3] progress on answering this question has been reported and our answer [4] is also positive and conditional on a specific property of the given set. We require that sequences of gates of moderate length (composed by ~15-20 gates) cover the space of unitary matrices in a uniform way. More specifically, we propose an algorithmic procedure that is based on diffusion process and justified by the theory of random walks. This method achieves an improved scaling of the length L with the required accuracy $O(\log(\frac{1}{\varepsilon})^{\log 3 / \log 2})$.

The improvement in the scaling of length is justified by an observed polynomial counter-increase in pre-compilation time by a factor 3/2, as this compares to DNSK algorithm. This confirms an expected interplay between the relations characterizing algorithmic procedures solving similar problems. When the inverses are included in the set, the notion of diffusive sets converges to the notion of ` efficiently computational sets' introduced in [5] and our results partially fulfill the predictions of that work concerning the considerable improvement of the scaling of length with accuracy. Finally, we present explicit examples of compilation of phase rotation gates, demonstrating the applicability of the proposed algorithm.

[1] A. Y. Kitaev, Russ. Math. Surv. 52, 1191 (1997).
[2] C. M. Dawson and M. A. Nielsen, Quant. Inf. Comp. 6, 81 (2006).
[3] I. S. B. Sardharwalla, T. S. Cubitt, A. W. Harrow and N. Linden, arXiv:1602.07963
[4] Y. Zhiyenbayev, V. M. Akulin and A. Mandilara, Phys. Rev. A 98, 012325 (2018)
[5] A. W. Harrow, B. Recht, and I. L. Chuang, J. Math. Physics 43, 4445, (2002).

Optimal Mapping of Reversible Logic Circuits to Quantum LNN Model

Martin Lukac

Department of Computer Science, Nazarbayev Univerzity, Kazakhstan

Abstract

In this paper an analytic approach to the mapping of reversible logic circuits to the Linear-Nearest Neighbor requirement of certain quantum technologies is presented. An optimal sift of reversible gates (multi-control single-target reversible gates) and qubits with a linear number of steps of computation is demonstrated. The algorithm allows to insert a minimal amount of SWAP gates for transforming a reversible circuit into an Linear Nearest Neighbor (LNN) model. The method is verified on experimental data and results are compared to the state of the art algorithms for the design of LNN circuits.

1 Introduction

In current Gated Quantum Computers (GQC) as well as in other technologies such as Ion Trap, NMR, etc., one major constraint is that only a directly connected qubits can interact. Several methods insert these constraints into automated design of quantum and reversible circuits [1, 3]. In this paper we provide an optimal method based on variable weighting, gate weighting and variable sifting [2]. The proposed method outperforms other proposed approaches on any 1D quantum computer architecture.

2 From Reversible to Quantum to LNN

A reversible logic function can be directly mapped to quantum computer using pure states as input and output bases via the design of reversible logic circuits. In order to make arbitrary reversible circuit implementable on

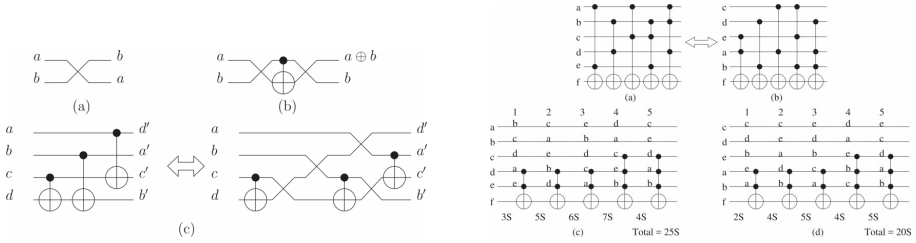

Figure 1: I: (a) SWAP gate, (b) using SWAP to invert CNOT, (c) using SWAP gates to design LNN circuit. II: (a), (b) variable ordering and (c)(d) required number of SWAP gates.

LNN quantum computer, SWAP gates must be inserted as shown in Figure 1. We show an optimal method how to insert swap gates, Illustrated in Figure 1I. The proposed method, computes qubit and gate weight and then reorders both the reversible gates as well as the qubit by minimizing the total cost. The minimization have been proven possible using an iterative approach in linear time [2]. In average the proposed method decreases the number of inserted SWAP gates by up to 45% as compared to [3] while the most computation intensive circuit required only 12 second to minimize.

3 Conclusion

In the future and currently under work a generalization based on graph flattening is developed to allow design of optimal circuits on N dimensional circuits such as IBM Q.

References

[1] Mohammad AlFailakawi, Laila AlTerkawi, Imtiaz Ahmad, and Suha Hamdan. Line ordering of reversible circuits for linear nearest neighbor realization. *Quantum Information Processing*, 12(10):3319–3339, Oct 2013.

[2] M. Lukac, P. Kerntopf, and M. Kameyama. An analytic sifting approach to optimization of lnn reversible circuits. In *2017 International Conference on Information and Digital Technologies (IDT)*, pages 240–245, July 2017.

[3] M. M. Rahman, G. W. Dueck, A. Chattopadhyay, and R. Wille. Integrated synthesis of linear nearest neighbor ancilla-free mct circuits. In *2016 IEEE 46th International Symposium on Multiple-Valued Logic (ISMVL)*, pages 144–149, May 2016.

Evaluating performance of modern Brillouin light scattering spectrometers

Zachary Coker[1], Maria Troyanova-Wood[1], Andrew J. Traverso[1], Talgat Yakupov[2], Zhandos N. Utegulov[2], and Vladislav V. Yakovlev[1]

[1]Texas A&M University, College Station, Texas 77843, USA
[2]Department of Physics, School of Science and Technology, Nazarbayev University, Astana 010000, Kazakhstan
Corresponding authors e-mail addresses: talgat.yakupov@nu.edu.kz, zhutegulov@nu.edu.kz

Brillouin light scattering spectroscopy and imaging have experienced a renaissance in recent years seeing vast improvements in methodology and increasing number of applications. With this resurgence has come the development of new virtual phased array (VIPA)-based Brillouin instruments that often tout superior performance in terms of data acquisition speed, while scanning tandem Fabry-Perot interferometers (TFPIs) are unmatched in terms of signal contrast. The performance of these new systems often goes unexplored, however, as applications often take precedence in reports. We therefore present evaluation of three modern Brillouin spectrometers: two VIPA-based spectrometers with wavelength-specific notch filters and one scanning 6-pass TFPI.

1. Introduction

In this report, we present the performance assessment of three Brillouin spectrometers across a range of acquisition times [1] with the purpose to provide a detailed look at the understanding how each spectrometer design (either static, dispersive VIPA-based design, or scanning TFPI) impacts performance and applicability to a wide range of potential investigations.

2. Methods, materials, and analysis

The performance of the following three Brillouin spectrometers was analyzed in this investigation: scanning 6-pass TFPI with a single photon counter and two custom-built VIPA-based spectrometers. We have examined the accuracy and spectral resolution of Brillouin measurements acquired from acetone against a range of spectral acquisitions times. We repeated each data acquisition cycles 50 times per acquisition time ranging from 0.01 to 1 and 100 seconds for the 780 nm VIPA-systems and from 0.512 to 102.4 seconds for the 532 nm TFPI and VIPA systems.

3. Experimental results and discussion

We analyzed Brillouin spectra acquired by three modern Brillouin spectrometers using the same analysis methods across all data sets to eliminate extra variables between system types. Results of spectra analysis are discussed below. The first data set for this investigation was acquired with the TFPI system and Verdi-G2 single longitudinal mode (SLM) laser at 532 nm. The averaged Brillouin line shift for acetone was measured to be 5.92 ± 0.007 GHz at 0.512 second acquisition time. These measurements are in agreement with the expected value of 5.936 GHz [2].The averaged Brillouin linewidth was measured to be 394 ± 29 MHz. Optimal acquisition time was determined to be between 2 and 3 seconds.

The first VIPA-based spectrometer, designed around excitation wavelength of 780 nm, was also tested with two laser sources (ECDL and iTLA). With the ECDL laser source, the averaged Brillouin shift for acetone was measured as 4.09±0.003 GHz. The Brillouin linewidth was measured to be 692±5 MHz. These measurements are in agreement to within 1% of the expected value of 4.039 GHz as calculated from the average index of refraction and speed of sound in acetone [3]. The optimal acquisition time for the 780 nm VIPA-based system with ECDL source was between 70 and 100 ms.

With the iTLA source at 0.5 seconds acquisition time, the averaged Brillouin shift for acetone was measured as 4.10±0.003 GHz. The Brillouin linewidth was measured to be 511±5 MHz. Optimal acquisition time for the 780 nm VIPA-based system with iTLA source was between 20 and 50 ms, faster than any previous reports for single-point acquisition for spontaneous Brillouin scattering. In fact, longer acquisition times than this did not provide for any improvements in accuracy or spectral resolution. With the 532 nm VIPA-based spectrometer, the averaged Brillouin shift for acetone was measured as 6.05 ± 0.032 GHz, with a linewidth of 905 ± 44 MHz at 0.512 second acquisition time. Optimal acquisition time for this spectrometer was determined to be between 1 and 2 seconds.

4. Conclusion

By evaluating the performance of our spectrometers, we were successful in identifying and correcting for specific issues and achieved improvements in overall performance, even reporting the fastest signal acquisition times to date for a single-point acquisition of Brillouin spectra.

5. References

[1] Z. Coker, M. Troyanova-Wood, A. J. Traverso, T. Yakupov, Z. N. Utegulov, and V. V. Yakovlev, “Assessing performance of modern Brillouin spectrometers”, Optics Express, Vol. 26, No. 3 (2018).
[2] M. J. Weber, *Handbook of Optical Materials* (2003), Vol. 23.
[3] J. Rheims, J. Köser, and T. Wriedt, "Refractive-index measurements in the near-IR using an Abbe refractometer," Meas. Sci. Technol. **8**, 601–605 (1999).

Synthesis of ZnO nanocrystals in a-SiO_2/Si ion track templates

A. Dauletbekova[1], A. Kozlovskyi[2], A. Akilbekov[1], A. Seitbayev[1,2], A. Alzhanova[1]
[1]L.N. Gumilyov Eurasian National University, 2 Satpayev str., 010008 Astana, Kazakhstan
[2]AB Institute of Nuclear Physics, 1/ 2 Ablaikhan ave., 010008, Astana, Kazakhstan
alma_dauletbek@mail.ru

Zn-based nanoparticles have been precipitated into nanoporous *a*-SiO_2/Si templates using chemical and electrochemical deposition. Nanoporous SiO_2 layer on Si was created by irradiation with swift Xe ions at cyclotron DC-60 (Astana, Kazakhstan) and further etching in 4% aqueous HF solution [1, 2]. Zn-based nanoparticles have been precipitated into created nanoporous *a*-SiO_2/Si templates using chemical (CD) and electrochemical (ECD)l deposition. ECD (fig. 1) of Zn in SiO_2/Si template were carried out in the potentiostatic mode at voltage of 0,7 and 1.0 V at pH = 3 using electrolyte ($ZnSO_4 \cdot 7H_2O$ - 360 g/l; NH_4Cl - 30 g/l; $3H_2O \cdot CH_3COONa$ - 15 g/l; ascorbic acid - 120 g/l) [3]. The formation of hydrogen in the process of precipitation can interfere with pores filling. To avoid it the constant pH level was supported by addition of solution of ascorbic acid.

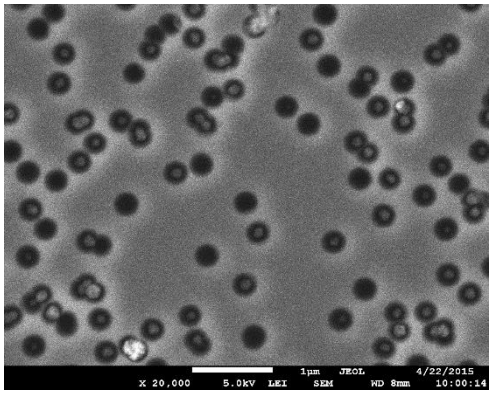

Fig. 2 SEM image of Zn-based precipitates deposited into etched tracks by ECD, time of deposition is 1 minute. SiO_2/Si sample was irradiated with Xe (133 MeV, $\Phi=6\times10^9$ ions/cm^2)

It was shown that it takes long time to fill pores of template using chemical precipitation technique (up to 7 days). The electrochemical precipitation is more convenient and reproducible for Zn-based precipitation in *a*-SiO_2/Si templates.

Analysis of PL data allows us to suppose a creation of zinc oxide nanocrystals in nanopores of SiO_2. The analysis of PL spectra shows that V_{Zn} are predominant native defects in Zn-based nanoclusters deposited in *a*-SiO_2/Si templates using CD and ECD techniques. X-ray diffraction analysis confirmed our assumption of the formation of ZnO nanocrystals in track templates using CD and ECD methods.

[1] A.Alzhanova, A.Dauletbekova, F.Komarov, L.Vlasukova, V. Yuvchenko, A. Akilbekov,, M. Zdorovets , "Peculiarities of latent track etching in SiO2/Si structures irradiated with Ar, Kr and Xe ions" Nucl, . Instr. and Meth. B, 374, 121 (2016).
[2] L. Vlasukova, F. Komarov, V. Yuvchenko, L. Baran, O. Michailin , A. Dauletbekova., A. Alzhanova, A. Akilbekov, "Etching of latent tracks in amorphous Si_2 and Si_3N_4: Simulation and experiment" Vacuum,129, 137 (2016)
[3] A. Kaur, R.P.Chauhan, "Effect of gamma irradiation on electrical and structural properties of Zn nanowires", Rad. Phys. and Chem..100, 59 64 (2014).

Obtaining of carbon nanomaterials

Batryshev D.G., Yerlanuly Ye., Ramazanov T.S., Gabdullin M.T.
LEP, IETP, NNLOT al-Farabi Kazakh national university, al-Farabi ave. 71, Almaty, 050040, Kazakhstan
e-mail address: batryshev@physics.kz

In this work a synthesis of carbon nanomaterials (CNMs) by CVD and PECVD methods and investigation their properties are considered. CVD method with different orientation of synthesis reactor was used for obtaining of carbon nanotubes [1] and their composite for using as a strain gauge. PECVD method was used for synthesis of carbon nanoparticles (CNPs), carbon nanofibres (CNFs) and nanotubes (CNTs), carbon nanowalls (CNWs, figure 1), multilayered graphene sheets and composites [2- 5].

The obtained samples were analyzed by using of analytical equipment such as: Quanta 3D scanning electron microscope (FEI, USA), NThegra Spectra Raman spectroscopy and Leica optical microscope.

It was concluded that among the tested methods of CNTs formation, the most convenient one is pyrolysis of ferrocene and ethanol aerosol generated by ultrasonic spraying. This method allows manufacture of both SWCNTs and MWCNTs in substantial quantities, and at the same time to separate SWCNTs from MWCNTs. Also, a composite material of SiO_2 fibers covered with multi-walled CNTs was obtained by CVD method in fixed bed reactor and it was found that the electric conductance of composite is quite sensitive to the external pressure. Besides, the obtained experimental results of CNTs synthesis process in fluidized bed reactor indicate that dispersity of the powdered catalyst carrier plays an important role in the growth process of CNTs and the powdered catalyst carrier with higher dispersion is more preferable for high yield of carbon nanotubes [1].

There are a different types of CNMs were obtained by PECVD method in the plasma of radio-frequency (RF) discharge and it was found that, depending on synthesis parameters in particular, temperature, discharge power, gas pressure, percentage of gas mixture and etc., a various carbon nanomaterials are synthesized. The obtained results show that synthesis (nucleation and growth) time of carbon nanoparticles depends on plasma parameters: RF power and gas temperature. It was shown that with increasing of gas temperature from 25 ^{0}C (room temperature) up to 100 ^{0}C nucleation time increases 4 times and with decreasing the temperature from 25 ^{0}C to -20 ^{0}C the time decreases twice. Also, it was shown that with increasing of RF power and at constant values of gas temperature and pressure, different CNMs (CNFs, CNWs and graphene sheets) can be synthesized. It was found that by increasing discharge power, carbon nanowalls are agglomerated into nanoclusters with the formation of defects in the structure. SEM analyses show that the growth process of CNWs on the surface of a silicon substrate with a thin catalyst nickel nanolayer gives better result than on the surface of copper wafer. Whereas estimated ratio of intensities of *D* and *G* modes from Raman spectra of obtained samples corresponds to the same quality of synthesized CNWs.

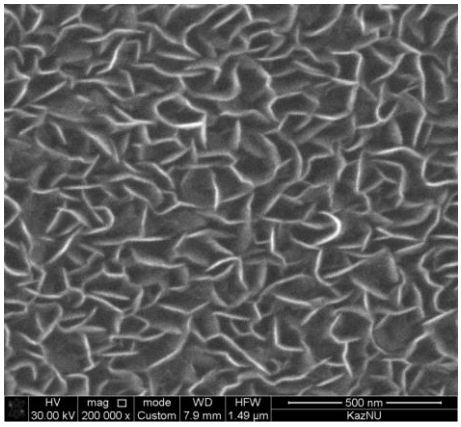

Fig. 1. Carbon nanowalls, obtained at a discharge RF power of 15 W and a temperature of 500^{0}C

[1] Batryshev D. G., Yerlanuly Ye., Ramazanov T. S., Gabdullin M. T., Abdullin Kh. A., "Influence of dispersion of catalytic carrier for growth mechanism of carbon nanotubes", J. Materials Today-Proceedings, Vol. 5, No. 9, pp. 17447-17452 (2018).
[2] Batryshev D.G., Yerlanuly Ye., Ramazanov T.S., Dosbolayev M.K., Gabdullin M.T., "Elaboration of carbon nanowalls using radio frequency plasma enhanced chemical vapor deposition", J. Materials Today-Proceedings, MATPR6365 (2018).
[3] Batryshev D. G., Ramazanov T. S., Dosbolayev M.K., Gabdullin M. T., Yerlanuly Ye, "Synthesis of Microparticles With Narrow Size Distribution in the Plasma of Arc and Radio-Frequency Discharges" J. Transactions on Plasma Science, Vol. 44, No. 5, pp. 870-873 (2016).
[4] Batryshev D.G., RamazanovT.S., DosbolayevM.K., Gabdullin M.T., "A Method of Separation of Polydisperse Particles in the Plasma of Radio-Frequency Discharge", J. Contributions to Plasma Physics, Vol. 55, No. 5, pp. 407-412 (2015).
[5] Batryshev D.G., Ramazanov T.S., Dosbolayev M.K., Gabdullin M.T., Yerlanuly Ye., "Method of Obtaining a Composite Material Based on Small-Dispersed Particles", J. of Nano- and Electronic Physics, Vol. 8, No. 3, pp. 03053 (2016).

Antineutrino oscillations and energy distributions of fast particles in a fission plasma

Sandybeck Kunakov[1], Aigerim Shapiyeva[2], Edward Son[3]
Al-Farabi Kazakh National University, Almaty, al-Farabi ave, 71, Kazakhstan,
Moscow Institute of Physics and Technology, Institutskiy Pereulok 9, Dolgoprudny, Moscow Region 141700,
Russia Joint Institute for High Temperatures of the Russian Academy of Sciences, Izhorskaya 13,Bldg. 2, Moscow 125412, Russia,
sandybeck.kunakov@gmail.com

Abstract: Any particle released out of nucleus with energy around of MeV's order (as it was theoretically and experimentally shown are bearing enormous kinetic energy due to the internal bounding energy transformation caused by transition of quarks under the influence of neutrino and antineutrino. Radioactive decay and nuclear fission are resulting fast particle, among them beta β - electrons and their immanent satellite antineutrino. It is also evident that such type of energy transformation may cause not only release fast electrons, but also fast protons or probably more compound nucleuses. In the present paper the detailed mathematical theory of function of energy distribution of fast particles based on system of Boltzmann equations is presented applied to the nuclear reaction of helium-3 isotope $^3He+n\rightarrow p+T+0.76MeV$.

1. Introduction

The present theory of energy degradation of fast particles in nuclear induced plasma generally based on and tributed to the work of Chapman and Cowling. Considering the transition of neutron to proton, β-electron and antineutrino the following might be assumed:

$$n\rightarrow p^{+}+e^{-}+\upsilon, \tag{0.1}$$

$$\left[\frac{u}{d}\frac{}{d}\right]\rightarrow\left[\frac{u}{d}\frac{u}{}\right]+e^{-}+\upsilon, \tag{0.2}$$

and one more reaction

$$^3H\rightarrow{}^3He+e^{-}+\upsilon. \tag{0.3}$$

In this reaction, quarks transitions are possible interacting as follows:

$$\left(\begin{pmatrix}u&\\d&d\end{pmatrix}\ \begin{pmatrix}u&\\d&d\end{pmatrix}\ \begin{pmatrix}u&u\\d&\end{pmatrix}\right)\rightarrow\left(\begin{pmatrix}u&\\d&d\end{pmatrix}\ \begin{pmatrix}u&u\\&d\end{pmatrix}\ \begin{pmatrix}u&u\\d&\end{pmatrix}\right)+e^{-}+\upsilon. \tag{0.4}$$

According to the quarks transitions, the reaction $^3He+n\rightarrow p+T+0.76MeV$ might be presented with antineutrino participation:

$$\left(\begin{pmatrix}u&\\d&d\end{pmatrix}\ \begin{pmatrix}u&u\\&d\end{pmatrix}\ \begin{pmatrix}u&u\\&d\end{pmatrix}\right)\rightarrow\begin{pmatrix}u&u\\&d\end{pmatrix}+e^{-}+\upsilon+\left(\begin{pmatrix}u&u\\&d\end{pmatrix}\ \begin{pmatrix}u&\\d&d\end{pmatrix}\ \begin{pmatrix}u&\\d&d\end{pmatrix}\right). \tag{0.5}$$

2. Conclusion

Appearance of any particle with energy comparable with energy of beta electrons strongly connected with antineutrino interference into any fission process, including strong interactions.

3. References

[1] S. K. Kunakov, E. Ye. Son, “Probe Diagnostics of Nuclear Excited Plasma of Uranium Hexafluoride”, ISSN 0018,151, High Temp., Vol. **48**, No. 6, pp. 789–805 (2010)

Physical Basic of Nano-composition Coatings Obtaining Technology

Gulmira Yar-Mukhamedova, Kanat Mukashev, Abyl Muradov
Al-Farabi Kazakh National University
Gulmira.Yar-Muhamedova@kaznu.kz

Solving the applied problems in extending a range of functional materials predetermines interest in the electrolytic multi-component alloys. Special attention is paid to the co-deposition of iron triad metals with refractory elements [1]. Such coatings are interesting by the possibility of combining functional properties that exceed alloying metals. Spheres of multi-component coatings application are replacement of electrolytic toxic chromium and hardening of the surface [2], corrosion protection [3], magnetic films with increased microhardness [4], catalytic materials for heterogeneous red-ox processes [5] and for electrodes in fuel cells (FC) and various red-ox flow batteries (RFB) [6]. Utilization of the electrochemical methods for thin alloy coatings synthesis displays interactions in the chain "process parameters – composition and structure of the material – properties – functions – application". It should be noted that publications mainly reflect the binary Fe(Ni, Co)-Mo(W) alloys deposition and properties, but there are some positive results of the multi-component alloys deposition from the gluconate-chloride [4], citrate and citrate-ammonia, pyrophosphate , sulfate-citrate [7] electrolytes in galvanostatic and non-stationary mode.

Principles of Fe-Co-W alloys electrodeposition from complex Fe (III) based citrate electrolytes are discussed. It is shown, that deposition of ternary alloys proceeds through competitive reduction of cobalt and tungsten with iron. Increasing concentration of citrate ions in solution at fixed Fe^{3+} content that's what expectedly increases the electrolyte pH. The protonation of citrate anions decreases with pH, as well as degree of Fe^{3+} hydrolysis increasing, therefore ionic forms of complexing agents and ligand in the electrolytes are different. Consequently, the composition of particles discharged at the electrode varies, which effect the composition of coatings. Cathodic reduction of separate metals in Fe-Co-W alloy occurs by competition between Iron, Cobalt and Tungsten. The order of competition depends on the ratio of alloying components' concentration in electrolyte, and also on the electrolysis mode and parameters (Fig. 1).

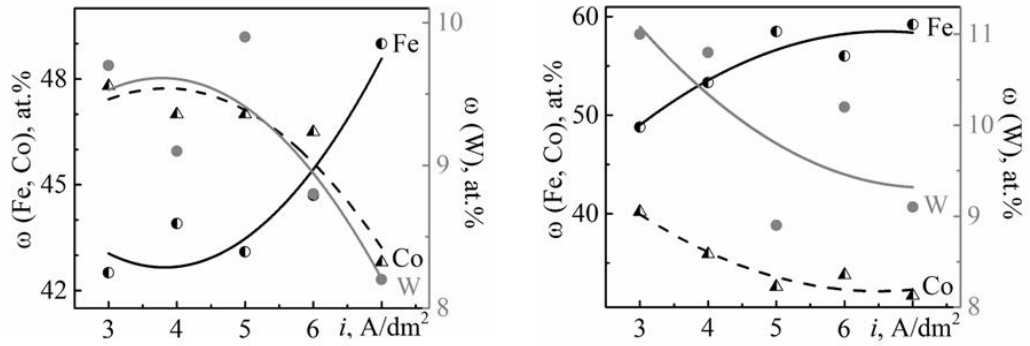

Fig. 1 Current density effect on Fe-Co-W coatings composition deposited from electrolytes: 1 (a) and 2 (b)

With increasing ligand concentration coatings are enriched with a refractory component; however, increasing current density favors a reverse trend. The effect of both current density and pulse on/off time on the quality, composition and surface morphology of the electrolytic alloys were determined. The application of pulsed electrolysis provides increasing tungsten content up to 13 at.%, at current efficiency of 70–75 %. Globular surface of Fe-Co-W coatings is caused by refractory metals incorporation, and crystalline and amorphous parts of structure are visualized by X-ray spectroscopy, including inter-metallic phases Co7W6, Fe7W6 along with α-Fe and Fe_3C. The crystallite size of the amorphous part is near 7–8 nm. Corrosion resistance of the coatings is 1.3–2.0 orders of magnitude higher than the substrate parameters as follows from data of polarization resistance method and electrode impedance spectroscopy.

[1] Yar-Mukhamedova G., Ved M., Sakhnenko N. "Iron binary and ternary coatings with molybdenum and tungsten". Appl. Surf. Sc. **383**, 346-352 (2016).
[2] Yar-Mukhamedova, G.; Ved, M.; Karakurkchi, A." Research on the improvement of mixed titania and Co(Mn) oxide nano-composite coatings" (5th Glob Conf on Polymer and Comp Mater., Japan), pp. 169-174.
[3] Muradov, A. D.; Mukashev, K. M.; Yar-Mukhamedova, G. Sh."Impact of silver metallization and electron irradiation on the mechanical deformation of polyimide films" Techn Phys, 62, 1692-1697 (2017)
[5] Yar-Mukhamedova G., Ved M.et al. "Ternary cobalt-molybdenum-zirconium coatings for alternative energies". Appl.Surf. Sc. **421**, 68-77 (2017).
[6] Yar-Mukhamedova G., Ved M., Sakhnenko N. "Electrodeposition and properties of binary and ternary cobalt alloys with molybdenum and tungsten". Appl.Surf. Sc. **445**, 298-307 (2018).
[7] Yar-Mukhamedova G., Ved M., Sakhnenko Ni. "Composition and Corrosion Behavior of Iron-Cobalt-Tungsten Coatings deposited by pulse current". Eur Chem Techn J. **445**, 298-307 (2017).

Properties of thin cryovacuum deposition films of organic molecules

A. Drobyshev[1], A. Aldiyarov[1], D. Sokolov[1]
Al-Farabi Kazakh National University, Institute of Experimental and Theoretical Physics, 71 al-Farabi Ave., 050040 Almaty, Republic of Kazakhstan
Author e-mail address: yasnyisokol@gmail.com

Abstract: As objects of research in recent decades, cryovacuum deposits, formed from the simplest organic gaseous substances are increasingly being selected [1]. One of the widely used classes of substances in this respect are alcohols and Freon's [2-4], which offer a line of structurally identical substances with different molecular sizes and masses. Such a choice is caused by chance within a particular family study the effect of the degree of complexity of the molecules on the properties of the glassy state [5], including their kinetic stability, as well as astrophysical interest in connection with the frequent detection of these substances in outer space [6].
The results of experimental studies of the IR spectroscopy and refractive index for a series of glass-forming substances - methanol, carbon tetrachloride, and Freon 134a are presented. The choice of temperature range of research from 16 K to 150 K is due to the presence of structural transformations for these substances.

1. Introduction

Mechanisms of glassy states of matter, their connection with the basic properties of the resulting glasses are a set of questions, the answers to which will allow bettering understanding the nature of the formation as a completely deposited state. Having in mind that the concept of the glassy state applies not only to amorphous, but also to the liquid crystal, and even crystalline materials with any type of disorder, the known water glass freezing transition is just one example of a class "glass transition" due to loss of balance, which should occur quite often in condensed matter [7-8]. The same circumstance significantly expands the number of objects of investigation glass-forming states and methods for their preparation and subsequent analysis.

As for the methods for obtaining glass-like materials, in recent decades, the method of physical cryogenic deposition from the gas phase to the cooled substrate has been widely used [9-10], which makes it possible to control the necessary phase-formation conditions-substrate temperature and gas phase pressure (condensation rate). This, in turn, allows the experimental verification of a number of theoretical models for the formation of disordered condensed states. In particular, it can be a test of the model of Ramos [9], in which the influence of the anisotropic structure of molecules on the formation of organic glasses of varying degrees of stability is discussed. The mobility and residence time of molecules in the adsorption layer are considered as the main factors, which is determined by the temperature of the substrate and the rate of cryodeposition, the parameters that can most accurately be maintained in experiments when the samples are obtained precisely by the method of physical cryovacuum condensation. The experimental setup and the measurement procedure were described by us earlier [11].

Based on the data obtained, we determined the glass transition temperatures, which is in agreement with the data of other authors. The temperature range of the existence of the super-cooled liquid phase within the limits is determined. A number of assumptions about metastable states for these substances are made. Cooling of cryocondensates formed at these temperatures leads to changes in the absorption spectra, which indicates structural transformations in them. In general, we can say that at the same temperature value, a cryocondensate sample, in particular methanol, can be in three different states, depending on the temperature history of its formation-direct condensation, heating from a low-temperature state or cooling from a higher condensation temperature. Concluding, we would like to note that the conducted studies have not yet answered to all questions about low-temperature structural changes, which is an incentive for further research.

2. References

[1] M.D.Ediger "Perspective: Highly stable vapor-deposited glasses", The journal of chemical physics 147, 210901 (2017).
[2] A. Drobyshev, A. Aldiyarov, A. Nurmukan, D. Sokolov, A. Shinbayeva, "Structure transformations in thin films of CF3-CFH2 cryodeposites. Is there a glass transition and what is the value of Tg?", Applied Surface Science. V.466, pp 196-200, (2018)
[3] A. Drobysheva, A. Aldiyarov, A. Nurmukan, D. Sokolov, and A. Shinbayeva, "IR Studies of Thermally Stimulated Structural Phase Transformations in Cryovacuum Condensates of Freon 134a", Low Temperature Physics 44, 831 (2018).
[4] A. Drobyshev, A. Aldiyarov, D. Sokolov, A. Shinbayeva, and N. Tokmoldin, Low Temperature Physics/Fizika Nizkikh Temperatur, v. 43, No. 10, pp. 1521–1524, (2017).
[5] S. Ramos, M. Oguni, K. Ishii, and H. Nakayama, "Character of devitrification, viewed from enthalpic paths, of the vapor-deposited ethylbenzene glasses," J. Phys. Chem. B 115, 14327–14332 (2011).
[6] R.L. Hudson, P.A. Gerakines, M.H. Moore, "Infrared spectra and optical constants of astronomical ices: II. Ethane and ethylene", Icarus 243, 148–157, (2014).
[7] Andrea Cavagna, Physics Reports 476, 51 (2009).
[8] H. Suga, S. Seki, J. Non-Cryst. Solids 16, 171 (1974).
[9] Aldiyarov A.; Aryutkina M.; Drobyshev A., Low Temp. Phys. 35, 251 (2009).
[10] Hudson, R. L.; Loeffler, M. J.; Gerakines, P. A., J. Chem. Phys. 146, 024304 (2017).
[11] A. Aldiyarov, M. Aryutkina, A. Drobyshev and V. Kurnosov, Low Temp. Phys. 37, 524 (2011).

A Novel Cryo-controlled Nucleation Method for High Efficiency Perovskite Solar Cells

Annie Ng,[1,2, ¶] Zhiwei Ren,[2, ¶] Hanlin Hu,[2] Patrick W. K. Fong,[2] Qian Shen,[2] Sin Hang Cheung,[3] Pingli Qin,[2] Jin Wook Lee,[4] Aleksandra B. Djurišić,[5] Shu Kong So,[3] Gang Li,[2] Yang Yang[4] and Charles Surya[6,*]

[1] *Department of Electrical and Computer Engineering, School of Engineering, Nazarbayev University, Astana, Kazakhstan*
[2]*Department of Electronic and Information Engineering, the Hong Kong Polytechnic University, Hong Kong SAR*
[3]*Department of Physics, Hong Kong Baptist University, Hong Kong SAR*
[4] *Department of Materials Science and Engineering, University of California, Los Angeles, U.S.A.*
[5]*Department of Physics, the University of Hong Kong, Pokfulam, Hong Kong SAR*
[6]*School of Engineering, Nazarbayev University, Astana, Kazakhstan*
Email: charles.surya@nu.edu.kz, annie.ng@nu.edu.kz

Abstract: A novel cryo-controlled nucleation technique is applied to synthesize organometal halide perovskite for solar cells (PSCs). A rapid reduction in the temperature causes a supersaturation condition in the precursor layer, prepared by solution technique, leading to a uniform nucleation sites for the subsequent crystallization phase. The low temperature condition inhibits the pre-mature crystallization of perovskites in the early stage before a uniform seed layer is formed and, thereby, decoupling the nucleation and crystallization phases. This approach allows the formation of a highly uniform nucleation layer and is crucial for the growth of perovskite films with excellent film quality. A power conversion efficiency (PCE) of 21.4 % for the champion PSC was achieved by using this perovskite growth method.

1. Introduction

Organometal halide perovskite-based solar cells (PSCs) have exhibited rapid enhancements in device power conversion efficiency (PCE) from 3.8 % in 2009 to a recent record PCE of 23.3 %. It is well known that the device performance critically depends on the film quality of the perovskite absorber layer. A variety of methods such as solution processing techniques, thermal evaporation, vapor assisted solution process and hybrid chemical vapor deposition are commonly employed by different research groups to grow perovskites. In this work, we propose a novel cryo-controlled nucleation process for inducing a homogenous nucleation layer without using anti-solvents [1]. Moreover, the approach effectively decouples the nucleation and crystallization phases and, thereby, greatly enhances the control over the growth process, facilitating the growth of highly compact perovskite films with excellent crystallinity. Our champion PSC using the cryo-controlled nucleation technique reaches 21.4 % with 0.80 fill factor. The results will be discussed in the talk.

2. Results

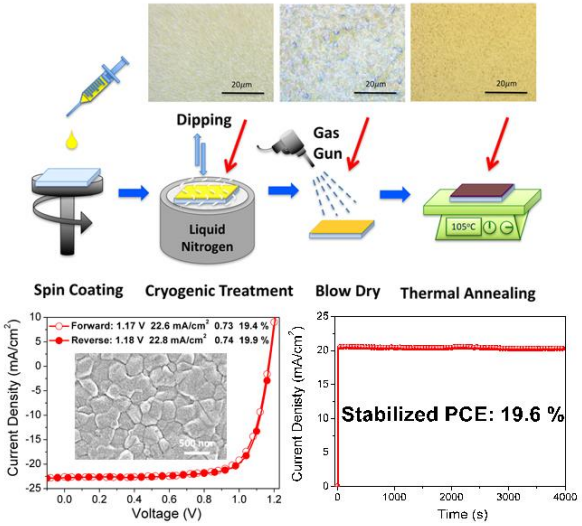

Figure 1. The process of cryo-controlled nucleation method and the performance of the champion perovskite solar cell.

3. References

[1] A. Ng, Z. Ren, H. Hu, P. W. K. Fong, Q. Shen, S. H. Cheung, P. Qin, J.-W. Lee, A. B. Djurišić, S. K. Su, G. Li, Y. Yang, C. Surya, "A Cryogenic Process for Antisolvent-Free High-Performance Perovskite Solar Cells", Adv. Mater. https://onlinelibrary.wiley.com/doi/full/10.1002/adma.201804402.

Dipole-field-assisted Charge Extraction in Metal-perovskite-metal Back-contact Solar Cells

Askhat N. Jumabekov
Department of Physics, School of Science and Technology, Nazarbayev University, Astana 010000, Kazakhstan.
Author e-mail address: askhat.jumabekov@nu.edu.kz

Abstract: Hybrid organic-inorganic halide perovskites are low-cost solution-processable solar cell materials with photovoltaic properties that rival those of crystalline silicon. The perovskite films are typically sandwiched between thin layers of hole and electron transport materials, which efficiently extract photogenerated charges. This affords high-energy conversion efficiencies but results in significant performance and fabrication challenges. Herein we present a simple charge transport layer-free perovskite solar cell, comprising only a perovskite layer with two interdigitated gold back-contacts. Charge extraction is achieved via self-assembled monolayers and their associated dipole fields at the metal-perovskite interface.

We obtained a simple gold-perovskite-gold back-contact perovskite solar cell (bc-PSCs) with a built-in potential and photovoltaic response owing exclusively to collective dipole field of self-assembled-molecular monolayers (SAMs) present at the gold–perovskite interfaces [1]. An interdigitated gold microelectrode array (IDA) on glass forms the back-contact of the solar cell. The SAMs are formed by two para-substituted thiolbenzene derivatives with opposing molecular dipoles. Both molecules are insulators and do not play an active role in the charge transport process. To fabricate the devices, first, selective modification of the two sets of IDA microelectrodes, termed "a" and "b", with the SAM compounds was performed. This modification induces a work function difference between the two microelectrodes of up to 600 mV. The fabrication of bc-PSCs completed by spin-coating a perovskite precursor solution onto the SAM-modified IDAs and heat treatment to form the perovskite thin photo-absorber layer.

The open-circuit potential (V_{OC}) of these bc-PSCs is shown to be equivalent to the work function difference induced by the SAM modification ($\varphi_m^b - \varphi_m^a$). Photocurrent mapping measurements reveal near uniform (less than 25%) charge collection across the cell, giving rise to short-circuit photocurrent densities (J_{SC}) of up to 12.1 mA cm^{-2} despite the large 6.5 μm center-to-center (distance from the center of electrode "a" to the center of adjacent electrode "b") and 4.3 μm edge-to-edge (distance from the edge of electrode "a" to the edge of adjacent electrode "b") electrode distances (Fig. 1).

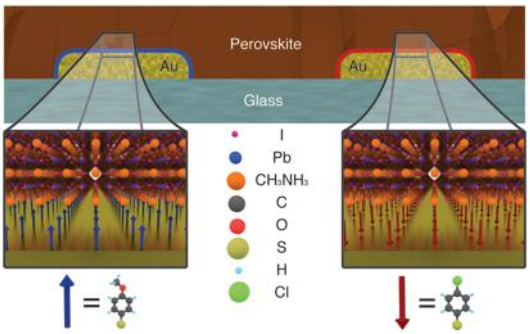

Fig. 1. Back-contact metal-perovskite-metal solar cells. Cross-section diagram of a dipole SAM modified back-contact gold-perovskite-gold solar cell. Electrode "a" (anode, left) is modified with a molecular monolayer of 4-methoxythiophenol (OMeTP) with a molecular dipole of −2.67D. Electrode "b" (cathode, right) is modified with a monolayer of 4-chlorothiophenol (ClTP) with a molecular dipole of + 1.41 D.

This work is the first implementation of a photovoltaic device, in which charge extraction is solely achieved by a dipole field generated via molecular monolayers. We expect this general concept to be adaptable to a wide range of absorber, electrode and molecular dipole materials well beyond the capabilities shown here. Through modelling, we demonstrated that high-performance solar cell devices can be obtained using the back-contact electrode design with a higher work function asymmetry between the electrodes and optimized electrode spacing. A number of important technical advantages arise from abolishing the need for additional CTLs in concert with back-contact designs. This back-contact design concepts combined with scalable low-cost nanofabrication techniques offer the potential for boosting solar cell efficiencies while providing scope for mass-production at low-cost [2,3].

References

[1] X. Lin, A. N. Jumabekov, N. N. Lal, A. R. Pascoe, D. E. Gómez, N. W. Duffy, A. S. R. Chesman, K. Sears, M. Fournier, Y. Zhang, Q. Bao, Y. Cheng, L. Spiccia, U. Bach, "Dipole-Field-Assisted Charge Extraction in Metal-Perovskite-Metal Back-Contact Solar Cells." *Nature Commun.* **8**, 613 (2017).
[2] A. N. Jumabekov, E. Della Gaspera, Z.-Q. Xu, A. S. R. Chesman, J. van Embden, S. A. Bonke, Q. Bao, D. Vaka, U. Bach, "Back-Contacted Hybrid Organic-Inorganic Perovskite Solar Cells." *J. Mater. Chem. C* **4**, 3125-3130 (2016).
[3] X. Lin, A. S. R. Chesman, S. R. Raga, A. D. Scully, L. Jiang, B. Tan, J. Lu, Y.-B. Cheng, U. Bach, "Effect of Grain Cluster Size on Back-Contact Perovskite Solar Cells." *Adv. Funct. Mater.* 1805098 (2018).

Understanding General Relativity after 100 years

Naresh Dadhich

Inter-University Center for Astronomy & Astrophysics,
Post Bag 4, Ganeshkhind, Pune 411 007, India
nkd@iucaa.in

Abstract: I would like to share my own new geometric perspective of general relativity and show that how it naturally arises from inhomogeneity of spacetime. The law of gravity is therefore not prescribed but instead entirely determined by spacetime geometry.

1. The case for a higher dimensional theory of gravity

General relativity is in many ways unique and different from all other physical theories. The first and foremost among them is the fact that, unlike all other forces, relativistic gravitational law is not prescribed but instead it is dictated by spacetime geometry itself.

Spacetime curves or bends like a material object, it should therefore have physical structure – a micro-structure as is the case for any material object. Such a micro structure is also required for vacuum to quantum fluctuate giving rise to vacuum energy. Thus micro structure of space is intimately related to vacuum energy and hence incorporation of the former would perhaps automatically take care of gravitational interaction of the latter. The key question is then how to bring in atoms of space into the fray. A possible avenue could be that vacuum energy may gravitate via higher dimension [1] leaving GR intact in the four dimensional spacetime. It is conceivable that at very high energy gravity may not entirely remain confined to four dimension, it may leak into higher dimension. The basic variable for gravity is the Riemann curvature tensor, for high energy exploration, we should include its higher powers in the action. Yet we want the equation of motion to retain its second order character, then this requirement uniquely identifies Lovelock Lagrangian. Even though Lovelock action is a homogeneous polynomial of degree N in the Riemann curvature, it has remarkable unique property that the resulting equation is always second order. Note that Lovelock gravity includes GR for N = 1, and N = 2 is the quadratic Gauss-Bonnet (GB) gravity, and then cubic and so on. But the higher order terms make non-zero contribution in the equation only in dimensions higher than four. If we want to explore high energy sector of gravity, which should indeed be the case for quantum gravity, we have to go to higher dimensions [2].

Then the question arises, what should be the equation in there? Could it very well be the Einstein equation which is valid in all dimensions larger than two? Yes, that could be the case. However how did we land in four rather than three dimension? This is because in three dimension, gravity is kinematic which means Riemann is entirely determined by Ricci tensor and hence there exists no non-trivial vacuum solution. This translates into the fact that there are no free degrees of freedom for free propagation of gravitational field. This is how we come to four dimension where Riemann has 20 while Ricci has 10 components allowing for non-trivial vacuum black hole solutions. Could this feature be universalized for all odd dimensions in a new theory which reduces to Einstein gravity for dimension, $d \leq 4$? Another desirable feature that one can ask for is existence of bound orbit around a static object like a black hole. It is easy to see that in GR, bound orbits can exist only in $d = 4$ and in none else. If we take these two as the guiding features for gravitational equation in higher dimension, then pure Lovelock gravity is uniquely singled out [3].

[1] V. Soni, N. Dadhich, R. Adhikari, "The cosmological constant from the zero point energy of compact dimensions," arXiv:1509.02156.
[2] N. Dadhich, "A discerning gravitational property for gravitational equation in higher dimensions" Euro. Phys. J. D 78, 1 (2016); arXiv:1506.08764.
[3] N. Dadhich, R. Durka, N. Merino, O. Miskpvic, "Dynamical structure of Pure Lovelock gravity," Phys. Rev. D 93, 064009 (2016); arXiv:1511.02541.

Modified gravities from the nonperturbative quantization of a metric

V. Dzhunushaliev[1,2], V. Folomeev[2,3]
[1]*Dept. Ther. Nucl. Phys., al-Farabi KazNU, Almaty, 050040, Kazakhstan,*
[2] *IETP, al-Farabi KazNU, Almaty, 050040, Kazakhstan,*
[3]*Institute of Physicotechnical Problems and Material Science of the NAS of the Kyrgyz Republic, 265 a,*
Chui Street, 720071 Bishkek, Kyrgyz Republic
e-mail: v.dzhunushaliev@gmail.com

Abstract: Based on certain assumptions for the expectation value of a product of the quantum fluctuating metric at two points, the gravitational and scalar field Lagrangians are evaluated. Assuming a vanishing expectation value of the first order terms of the metric, the calculations are performed with an accuracy of second order. It is shown that such quantum corrections give rise to modified gravity.

The problem of quantizing gravity has been debated frequently during the past decades. In doing so, it was established that the quantization of Einstein's general relativity inevitably results in fundamental problems such as the perturbative nonrenormalizability. This represents a motivation to introduce other, more radical approaches to obtain a quantum theory of gravity, including the consideration of higher-order theories of gravity, string theory, and loop quantum gravity.

According to Heisenberg's non-perturbative quantization technique the classical fields appearing in the corresponding field equations are replaced by operators of these fields. For general relativity, one then has the operator Einstein equations

$$\hat{R}_{\mu\nu} - \frac{1}{2}\hat{g}_{\mu\nu}\hat{R} = \kappa\hat{T}_{\mu\nu} \tag{1}$$

There are no known mathematical tools for solving the operator equation (1). The only possibility to work with such an operator equation is to average the equation (1) over all possible products of the metric operators $\hat{g}_{\mu\nu}(x_1)\ldots\hat{g}_{\mu\nu}(x_2)$, and thus obtain an infinite set of equations for all Green's functions: Dyson – Schwinger equations set.

In accordance with the quantization procedure, a metric in quantum gravity is an operator $\hat{g}_{\mu\nu}$. We consider a system for which the following decomposition is approximately valid

$$\hat{g}_{\mu\nu} \approx g_{\mu\nu} + \widehat{\delta g_{\mu\nu}} + \widehat{\delta^2 g_{\mu\nu}} + \cdots \tag{2}$$

For our approximate nonperturbative calculations, we insert the decomposition (2) into the Einstein-Hilbert action and evaluate it with an accuracy $\langle\left(\widehat{\delta g}\right)^2\rangle \approx \langle\widehat{\delta^2 g}\rangle$. Now we can calculate an expectation value of the Hilbert – Einsten Lagrangian by replacing all classical quantities $\delta g_{\mu\nu}$ and $\delta^2 g_{\mu\nu}$ by the quantum ones, $\widehat{\delta g_{\mu\nu}}$ and $\widehat{\delta^2 g_{\mu\nu}}$:

$$\langle L\left(g_{\mu\nu} + \widehat{\delta g_{\mu\nu}} + \widehat{\delta^2 g_{\mu\nu}}\right)\rangle \approx -\frac{c^2}{\kappa}\sqrt{-g}\left[R - 2RF(R,\cdots) + 3F(R,\cdots)\nabla^\mu\nabla_\mu F(R,\cdots) + G_{\mu\nu}K^{\mu\nu}\right] \tag{3}$$

where $\boldsymbol{K_{\mu\nu}} = \langle\widehat{\boldsymbol{\delta^2 g_{\mu\nu}}}\rangle$.

Let us now perform similar calculations for the matter Lagrangian:

$$L_m + \langle\widehat{\delta^2 L_m}\rangle \approx -\frac{c^2}{\kappa}\sqrt{-g}\left[\frac{1}{2}\nabla^\mu\phi\nabla_\mu\phi - [1 + 2F(R,\cdots)]V(\phi) + T_{\mu\nu}K^{\mu\nu}\right] \tag{3}$$

Thus, we have shown that: (a) Einstein gravity is modified in the spirit of $F(R)$-gravity theories, (b) matter is non-minimally coupled to gravity.

References

[1] V. Dzhunushaliev, V. Folomeev, B. Kleihaus and J. Kunz, ``Modified gravity from the nonperturbative quantization of a metric," Eur. Phys. J. C, 75, no. 4, 157 (2015); [arXiv:1501.00886 [gr-qc]].

FRW cosmology of Myrzakulov gravity with a scalar field

Gulnur Bauyrzhan and Koblandy Yerzhanov
Eurasian International Center for Theoretical Physics and Department of General Theoretical Physics, Eurasian National University, Astana 010008, Kazakhstan)
yerzhanovkk@gmail.com

Abstract: The gravitation of Myrzakulov, generalized with a scalar field, is considered. Several particular cases are considered for this model. The density and pressure of this model were found.

To describe the observed accelerated expansion of the universe, we have generalized the Myrzakulov gravity [1-3] with the k-essence [4-7]. The action of Myrzakulov gravity has the following form:

$$S_{43}=\int d^4x\sqrt{-g}[F(R,T)+L_m], \tag{1}$$

where

$$\mathrm{R} = \varepsilon_1 \mathrm{g}^{\mu\nu}\mathrm{R}_{\mu\nu} + u(a,\dot{a}), \tag{2}$$

$$\mathrm{T} = \varepsilon_2 \mathrm{S}_{\rho}^{\mu\nu}\mathrm{T}_{\mu\nu}^{\rho} + v(a,\dot{a}). \tag{3}$$

Here L_m is the matter Lagrangian that for k-essence we can rewrite as $L_m = K$, $\varepsilon_i = \pm 1$ is signature, R is the curvature scalar, T is the torsion scalar. K includes kinetic term $X = \frac{1}{2}\dot{\varphi}^2$ and scalar field function $f(\varphi)$. For Friedman - Robertson - Walker spacetime, if we will take $F(R,T) = R + T$ and if scale-factor have form $\mathrm{a} = \mathrm{a}_0\mathrm{t}^{\mathrm{n}}$, then:

$$\mathrm{p} = \frac{(2-3\mathrm{n})\mathrm{n}}{\mathrm{t}^2},$$

$$\rho = \frac{3\mathrm{n}^2}{\mathrm{t}^2}.$$

We considered the *F(R,T)* Myrzakulov gravity model with scalar field. Partial solutions were obtained using the Euler-Lagrange equations. Was shown that the general solution for the model with the Lagrangian $L=R+T+X$ is possible.

References

[1] R. Myrzakulov. *Accelerating universe from F(T) gravity* Eur.Phys.J. C71 (2011) 1752
[2] R. Myrzakulov. *Dark Energy in F(R,T) Gravity*. [arXiv:1205.5266]
[3] R. Myrzakulov. *FRW Cosmology in F(R,T) gravity*. The European Physical Journal C, **72**, N11, 2203 (2012). [arXiv:1207.1039]
[4] R. Myrzakulov, K. Yerzhanov, K. Yesmakhanova et al. *g-Essence as the cosmic speed-up.* Astrophysics and Space Science. V.341, I.2 , 681-688
[5] K. Bamba, R. Myrzakulov, O. Razina, K. Yerzhanov. *Cosmological evolution of equation of state for dark energy in G-essence models.* International journal of modern physics D, V. 22 (6), 1350023, 2013
[6] R. Myrzakulov. *F(T) gravity and k-essence.* General Relativity and Gravitation, v.44, N12, 3059-3080 (2012)
[7] E. Gudekli, N. Myrzakulov, K. Yerzhanov, R. Myrzakulov *Trace-anomaly driven inflation in f(T) gravity with a cosmological constant.* Astrophysics and Space Science, (2015) 357: 45

Geodesics in the field of a rotating deformed gravitational source

Kuantay Boshkayev

NNLOT, Al-Farabi Kazakh National University, Al-Farabi avenue 71, Almaty 050040, Kazakhstan,

Department of Physics, Nazarbayev University, Kabanbay Batyr 53, Astana 010000, Kazakhstan

kuantay@mail.ru

Abstract. We investigate equatorial geodesics in the gravitational field of a rotating and deformed source described by the approximate Hartle-Thorne metric. In the case of massive particles, we derive within the same approximation analytic expressions for the orbital angular velocity, the specific angular momentum and energy, and the radii of marginally stable and marginally bound circular orbits. Moreover, we calculate the orbital angular velocity and the radius of lightlike circular geodesics. We study numerically the frame dragging effect and the influence of the quadrupolar deformation of the source on the motion of test particles. We show that the effects originating from the rotation can be balanced by the effects due to the oblateness of the source [1].

Moreover, we consider the kilohertz quasi-periodic oscillations of low-mass X-ray binaries within the Hartle-Thorne spacetime. We show that the interpretation of the epicyclic frequencies of this spacetime with the observed kilohertz quasi-periodic oscillations, within the Relativistic Precession Model, allows us to extract the total mass M, angular momentum J, and quadrupole moment Q of the compact object in a low-mass X-ray binary. We exemplify this fact by analyzing the data of the Z-source GX 5-1. We show that the extracted multipole structure of the compact component of this source deviates from the one expected from a Kerr black hole and instead it points to a neutron star explanation. In view of the recent neutron star model we compute the radius, angular velocity and other parameters of this source by imposing the observational and theoretical constraints on the mass- radius relation [2].

References

[1] K.A. Boshkayev, H. Quevedo, M.S. Abutalip, Z.A. Kalymova, S.S. Suleymanova, “Geodesics in the field of a rotating deformed gravitational source” International Journal of Modern Physics A **31**(2-3),1641006 (2016)

[2] K.A. Boshkayev, J. Rueda, M. Muccino, “Extracting multipole moments of neutron stars from quasi-periodic oscillations in low mass X-ray binaries” Astronomy Reports **59**(6), 441 (2015)

Optical and energetic properties of black holes

Ahmedov B.J.

Ulugh Beg Astronomical Institute, Astronomicheskaya 33, Tashkent 100052, Uzbekistan
National University of Uzbekistan, Tashkent 100174, Uzbekistan

Abstract: We have developed a general formalism to describe the black hole shadow as an arbitrary polar curve expressed in terms of a Legendre expansion. New developed formalism does not presume any knowledge of the properties of the shadow, e.g., the location of its center, and offers a number of routes to characterize the distortions of the curve with respect to reference circles. These distortions can be implemented in a coordinate independent manner by different teams analyzing the same data. It has been shown that the new formalism provides an accurate and robust description of noisy observational data, with smaller error variances when compared to previous measurements of the distortion.

1. A coordinate-independent characterization of a black-hole shadow

Modern astronomical observations on the international level on the ground and space telescopes, and recent discoveries have provided convincing evidence that black holes have a significant impact on nearby objects around, emitting powerful gamma-ray bursts, absorbing the next star, and stimulating the growth of newborn stars in the surrounding areas. Study the photons motion around rotating black holes, in particular, the discovery and analysis of the form of silhouettes of these objects, setting and effective implementation of relevant radiostronomical observations on the proof of the existence of the black hole horizon and retrieval of information events on the central object in our galaxy within the Black Hole Cam (BHC) and Event Horizon Telesop (EHT) international projects is one of the most important tasks of modern astrophysics.

We have developed a new general and coordinate-independent formalism in which the shadow is described as an arbitrary polar curve expressed in terms of a Legendre expansion. It was revealed that the first five coefficients of the polynomial expansion is sufficient to describe the properties of rotating black holes shadow with the accuracy of ~0.1%. Our formalism does not presume any knowledge of the properties of the shadow and offers a number of routes to characterize the properties of the curve. It has been shown that the proposed definition of distortion of black holes shadow are stable under the signal noise.

The analytical expressions for the vacuum electromagnetic fields of the different rotating black holes in the external asymptotically uniform magnetic field has been obtained [2-4]. It has been revealed that the induced electric field around the deformed black hole depends on the deformation parameter linearly, and the magnetic field squared.

An upper limit for the deformation parameter for the rotating non-Kerr black hole has been obtained through comparison of the observable values of the radius of innermost stable circular orbits with the theoretical results obtained in the dissertation as $\varepsilon \leq 22$.

It has been also obtained the silhouettes of the rotating black holes shadow in the presence of an inhomogeneous plasma, which can be used to identify additional asymmetries in the shape of the shadow and retrieve information on the plasma parameters and the central compact object [5].

The gravitational lensing in the vicinity of a slowly rotating massive object surrounded by plasma has been studied. The obtained deflection angle of the light ray in the presence of plasma depends on (i) the frequency of the electromagnetic wave, due to the dispersion properties of the plasma; (ii) the gravitational mass M; and (iii) the angular momentum of the gravitational lens. We have studied photon motion around axially symmetric rotating (i) Kerr black hole, (ii) wormhole in the presence of a plasma with radial power-law density. It is shown that in the presence of a plasma, the observed shape and size of the shadow of rotating (i) Kerr black hole, (ii) wormhole changes depending on the (i) plasma parameters, (ii) gravitational object spin, and (iii) inclination angle between the observer plane and the axis of rotation of the black hole/wormhole.

[1] Abdujabbarov A. A., Rezzolla L., Ahmedov B. J., "A coordinate-independent characterization of a black-hole shadow", Mon. Not. R. Astron. Soc., V. 454, 2423–2435 (2015).
[2] Turimov B., Abdujabbarov A. A., Ahmedov B. J., Bambi C., "Electromagnetic fields of slowly rotating magnetized compact stars in conformal gravity", Phys. Rev. D, V. 97, id. 124005 (2018).
[3] Dadhich N., Tursunov A., Ahmedov B., Stuchlik Z., "On Magnetic Penrose Process and Blandford-Znajek Mechanism", MNRAS Letters, V. 478, Issue 1, L89–L94 (2018).
[4] Toshmatov B., Stuchlık Z., Schee J., Ahmedov B., "Electromagnetic perturbations of black holes in general relativity coupled to nonlinear electrodynamics", Phys. Rev. D 97, id. 084058 (2018).
[5] Abdujabbarov A. A., Ahmedov B. J., Atamurotov F., Dadhich N., "Optical Properties of Braneworld Black Hole: Gravitational Lensing and Retrolensing", Phys. Rev. D, 2017, V.96, id.084017, (2017).

Phenomenology of bouncing black holes

Daniele Malafarina
Physics Department, Nazarbayev University, Kabanbay batyr 53, 010000, Astana, Kazakhstan
daniele.malafarina@nu.edu.kz

Abstract: Dynamical solutions of Einstein's equations in General Relativity (GR) generically lead to the formation of space-time singularities. The possible quantum resolution of such singularities may provide hints about the properties that a final theory of Quantum-Gravity (QG) should posses. In analytical toy models for gravitational collapse the singularity is avoided and replaced by a bounce that depends on the specific behaviour of gravity in the strong field. Such phenomena must have implications for the geometry of the space-time in the weak field region and thus it may alter some observable properties of astrophysical black holes.

1. Removing singularities at the end of gravitational collapse and astrophysical black holes

It is generally accepted that General Relativity (GR) is not a complete theory and that the occurrence of space-time singularities signals the need for modifications in the high energy regime. Also, it is generally believed that a viable theory of QG would not present singularities. Unfortunately, any theoretical attempt to quantize gravitation today must face the problem of the lack of valid experimental tests. It is clear that the energy scales at which QG becomes relevant are beyond the reach of present day particle accelerators. At the same time, the recent detection of gravitational waves from the merger of black holes and neutron stars, shows that Einstein's theory holds well in the regime where $2GM/(c^2r)$ approaches unity.

However, there is still hope that future observations will reveal unexpected phenomena that the classical theory of GR fails to explain. In this context, astrophysical black hole candidates are the most natural targets where to look for QG effects. In recent years, a lot of effort has been put into studying modification of existing collapse models to describe the occurrence of a so-called 'quantum bounce'. The main idea is that QG must induce repulsive effects in the strong field that prevent the formation of singularities and cause the collapsing matter to bounce [1]. In these bouncing scenarios, the removal of the singularity implies that the geometry is never globally described by the Schwarzschild solution and modifications can affect the geometry at the scales of the horizon and farther. Therefore the horizon prescribed by such models can not be the usual event horizon of a classical black hole [2].

Interestingly, many different approaches to modified collapse scenarios produce similar qualitative results, suggesting that there must be some common underlying feature [3]. At the same time, different bouncing models, coming from different theories, provide different predictions, suggesting that it may be possible, at least in principle, to distinguish them experimentally, in the sense that the phenomenological aspects of such bouncing scenarios could be tested with future astrophysical observations [4].

[1] D. Malafarina, "Classical collapse to black holes and quantum bounces: A review", *Universe*, *3*, 48 (2017).
[2] C. Bambi, D. Malafarina, L. Modesto "Non-singular quantum-inspired gravitational collapse," *Phys. Rev. D*, *88*, 044009 (2013).
[3] D. Malafarina, "Gravitational collapse of Hagedorn fluids," Phys. Rev. D 93, 104042 (2016).
[4] R. Carballo-Rubio, F. Di Filippo, S. Liberati, M. Visser, "Phenomenological aspects of black holes beyond general relativity," arXiv:1809.08238 (2018).

Interstellar filaments and interstellar magnetic fields using interstellar dust polarization

Dana Alina[1], I. Ristorcelli[2], L. Montier[2], E. Abdikamalov[1], M. Juvela[3], J.-Ph. Bernard[2]
[1]*Physics Department, SST, Nazarbayev University, Kabanbay batyr ave, 53, 010000 Astana Kazakhstan*
[2]*IRAP, Université de Toulouse, CNRS, UPS, CNES, 9 av. Colonel Roche 31400 Toulouse France*
[3]*Department of Physics, PO Box 64, University of Helsinki, 00014 Helsinki Finland*

Author e-mail address: dana.alina@gmail.com

Abstract:. High precision polarization measurements of the interstellar dust emission offer opportunity to study the interstellar magnetic field, its interplay with the interstellar medium and, in particular, its role in star formation process. The non-linearity in the polarization parameters such as the polarization angle dispersion function, along with the noise in the observational data induces bias that has to be quantified. In this analysis, we quantify the bias depending on the signal-to-noise ratio of the data and the form of the covariance matrix using Monte-Carlo simulations. We determine the limit in signal-to-noise ratio above which one can use the non-corrected estimator for the polarizationa angle dispersion function. We introduce a polynomial estimator and propose a method for the estimation of the bias' upper limit. The method is applicable to any linear polarization data set for which the noise covariance matrices are known.

1. Introduction

The interstellar magnetic field's orientation can be derived using the polarimetric observations of the interstellar dust emission. The derived polarization parameters such as the polarization fraction, angle and polarization angle dispersion function (called S hereafter) are subject to bias [1]. While the bias on the former two parameters has been studied since for several decades, the latter parameter has been used with no correction because of its complexity.

2. Method and results

We quantify the bias on S using Monte-Carlo simulations depending on the form of the noise covariance matrix for different signal-to-noise ratios. We show that it depends not only the noise properties but also on the true value which was not expected (see Figure). We introduce a polynomial estimator of S based on the conventional and dichotomic estimators which shows little bias comparing to the conventional estimator. However, the dichotomic estimator can be calculated only for a limited number of data sets, so that the polynomial estimator can not be applied everywhere. Thus, we propose a method of estimation of the bias' upper limit based on the given noise covariance matrix and signal-to-noise ratio [2].

3. Conclusion

The proposed method has been successfully applied to the real data and allowed to assess the uncertainties on S in studies of interstellar dust polarization and magnetic fields in the interstellar medium [3].

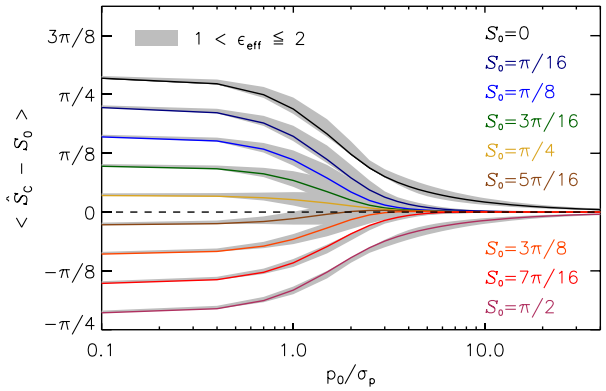

Fig. 1. Bias on polarization angle dispersion function (S) in the case of large asymmetries in the noise covariance matrix for different true values of S as a function of the polarization signal-to-noise ratio.

4. References

[1] K. Serkowski, "Statistical analysis of polarization and reddening of the double cluster of Perseus", Acta Astronomica, 8**,** 135 (1958).
[2] D. Alina, L. Montier, I. Ristorcelli, J.-P. Bernard, F. Levrier, E. Abdikamalov, "Polarization measurement analysis. III. Analysis of the polarization angle dispersion function with the high precision polarization data", Astronomy and Astrophysics, 595, A57 (2016)
[3] Planck Collaboration, "Planck Intermediate Results. XIX. An overview of the polarized thermal emission from Galactic dust", Astronomy and Astrophysics, 576, A104 (2015).

Linear theory of shock-turbulence interaction and its application to stellar explosions

Ernazar Abdikamalov
Department of Physics, School of Science and Technology, Nazarbayev University
Author e-mail address: ernazar.abdikamalov@nu.edu.kz

Abstract: Interaction of shock waves and turbulent flows plays a key role in many scenarios, ranging from applications in engineering to explosive astrophysical phenomena such as core-collapse supernovae. We study the interaction of nuclear-dissociating shocks with hydrodynamic turbulence using a linear perturbation theory. We model the mean flow as a stationary one-dimensional flow, while the unperturbed shock is treated as a planar discontinuity. We decompose the turbulent field into a series of acoustic, entropy, and vorticity waves, each which are then modeled as sinusoidal planar waves. Using the jump conditions at the shock and hydrodynamics equations, we calculate the properties of the turbulent field in the post-shock region. In particular, we calculate the amplification of turbulent kinetic energy across the shock. Finally, we estimate the impact of the incident turbulent perturbations on the explosion mechanisms of core-collapse supernovae [1-3].

1. Introduction

Turbulence plays a pivotal role in determining the outcome of core-collapse supernova explosions. Massive stars with initial masses in range $\sim(8-100)M_{\rm Sun}$ develop electron-degenerate iron cores. Upon reaching their maximum stability mass ($\approx 1.4M_{\rm Sun}$), the iron core collapses to a proto-neutron star, launching a hydrodynamic shock wave into the stellar envelope. This shock wave has the eject the stellar envelope and produce a supernova explosion. The propagation of the shock, however, does not proceed smoothly. The shock loses energy to dissociation of heavy nuclei and to neutrino cooling behind the shock. This turns the shock into a stalled accretion shock. In order to produce an explosion and leave behind a stable neutron star, the shock has to be re-energized and revived within a ~1 second timescale. This is where the turbulence has to play a crucial role. The heating by neutrinos emitted by the neutron star drives turbulent convection in the post-shock region. This exerts *turbulent pressure* behind the shock. In addition, the convective instabilities in nuclear burning shells (e.g., silicon and oxygen burning shells) of the progenitor stars encounter the shock and generate additional turbulence in the post-shock region, creating a more favorable conditions for reviving the shock [1].

2. Results and Conclusion

Using the *linear interaction analysis*, we calculated the generation of turbulence in the post-shock region by incoming perturbations as they cross the shock [1]. Figure 1 shows the amplification of the turbulent kinetic across the shock for incoming vorticity waves. The exact degree of the amplification depends on the angular distribution distribution of the waves, on the shock strength, and on the degree of nuclear dissociated at the shock. Overall, the total kinetic energy is amplified by a factor of ~**2** for the parameters representative of core-collapse supernovae. This leads to a ~12% reduction in the critical neutrino luminosity necessary for driving the explosion. In addition, the entropy waves generated in the post-shock region become buoyant and drive additional turbulence, leading to even stronger reduction of the critical neutrino luminosity by ~24% [2]. The contribution of acoustic waves is found to be less important [3].

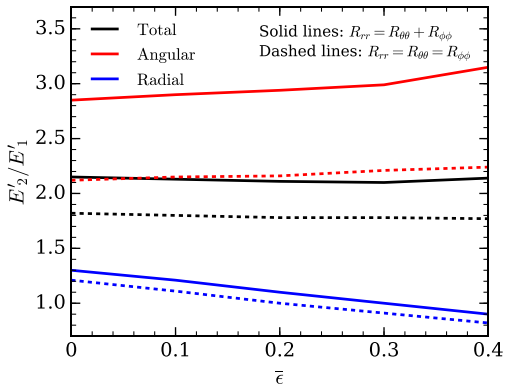

Figure 1. Amplification of turbulent kinetic energy across the shock for incoming vorticity perturbations. The Figure in taken from ref. [1].

3. References

[1] E. Abdikamalov, A. Zhaksylykov, D. Radice, S. Berdibek, *Shock-turbulence interaction in core-collapse supernovae*, MNRAS, 461, 3864, 2016
[2] C. Huete, E. Abdikamalov**,** D. Radice, *The impact of vorticity waves on the shock dynamics in core-collapse supernovae*, MNRAS, 475, 3305, 2018
[3] E. Abdikamalov, C. Huete, A. Nussupbekov, S. Berdibek, *Turbulence Generation by Shock-Acoustic-Wave Interaction in Core-Collapse Supernovae*, MDPI Particles, 1, 7, 2018

Nonlinear solution in Myrzakulov gravity model

P. Tsyba, Zh. Sagidullayeva
Eurasian International Center for Theoretical Physics and Department of General and Theoretical Physics
Eurasian National University, Astana 010008, Kazakhstan)
pyotrtsyba@gmail.com

Abstract: In this article we investigate the Myrzakulov gravity with a fermion field described by a nonminimal action. The cases with a linear and nonlinear interaction of the gravitational and fermion fields are considered. It is shown that in the case of nonlinear interaction, Myrzakulov gravity can describe the accelerated expansion of the universe.

In this paper we consider the $F(R,T)$ theory of gravity that interacts non-minimally with the fermion field. Here, by means of R and T, the torsion scalar and the scalar of curvature are denoted, respectively. In a general form, equations describing the gravitational and fermion fields are obtained. The special case with $F(R,T)=\alpha R+\beta T$ is chosen as the model of $F(R,T)$ gravity cosmological solutions is obtained that describes the accelerated expansion of the universe.

In this paper, we consider the $F(R,T)$ gravity with the non-minimally coupled fermionic field. The corresponding action reads as [1]

$$\mathcal{A}=\int d^4xe\{\tfrac{1}{2}h(u)F(R,T)+Y-V(u)\}, \tag{1}$$

where $Y=\frac{i}{2}[\bar{\psi}\Gamma^{\mu}(\overleftarrow{\partial_{\mu}}-\Omega_{\mu})\psi-\bar{\psi}(\overrightarrow{\partial_{\mu}}+\Omega_{\mu})\Gamma^{\mu}\psi]$ is canonical kinetic term of the fermionic field, $e=det(e_{\mu}^{a})=\sqrt{-g}$ that e_{μ}^{a} is tetrad (vierbein) basis, R is curvature scalar, T is a torsion scalar, ψ and $\bar{\psi}=\psi^{\dagger}\gamma^{0}$ denote the spinor field and its adjoint, with the dagger representing complex conjugation. $h(u)$ and $V(u)$ are generic functions, representing the coupling with gravity and the self-interaction potential of the fermionic field respectively. In our study, for simplicity, we assume that h and V depend on only functions of the bilinear $u=\bar{\psi}\psi$.

Considering the background FRW metric, it is possible to obtain the point-like Lagrangian from action (1)

$$\begin{aligned}L=&\frac{ha^3}{2}(F-TF_T-RF_R+uF_R+vF_T)+3ha\dot{a}^2(F_T-F_R)-\\&-3h\dot{a}a^2\left(\dot{R}F_{RR}+\dot{T}F_{RT}\right)-3h'(\dot{\bar{\psi}}\psi+\bar{\psi}\dot{\psi})\dot{a}a^2F_R+a^3Y-a^3V,\end{aligned} \tag{2}$$

here, because of homogeneity and isotropy of the metric it is assumed that the spinor field depends only on time, i.e. $\psi=\psi(t)$.

Applying the Lagrange equation $\frac{d}{dt}\frac{\partial L}{\partial\dot{q}_i}-\frac{\partial L}{\partial q_i}=0$ to the Lagrangian (2), where $q_i=\{a,\psi,\bar{\psi},R,T\}$, $\dot{q}_i=\{\dot{a},\dot{\psi},\dot{\bar{\psi}},\dot{R},\dot{T}\}$, we obtain the corresponding equations of motion. Then the equation of motion for the scale factor a in terms of the Hubble parameter $H=\frac{1}{a}\frac{da}{dt}$ takes the form

$$\begin{aligned}&(2\dot{H}+3H^2)(F_T-F_R)-\frac{\ddot{h}}{h}F_R+2\frac{\dot{h}}{h}\left[H(F_T-F_R)-(\dot{R}F_{RR}+\dot{T}F_{RT})\right]+2H(\dot{R}F_{RR}+\dot{T}F_{RT}+\dot{R}F_{TR}+\dot{T}F_{TT})+\\&+\tfrac{1}{2}(RF_R+TF_T)-F_{RRR}\dot{R}^2-F_{RTT}\dot{T}^2-2F_{RRT}\dot{R}\dot{T}-F_{RR}\ddot{R}-F_{RT}\ddot{T}-\frac{F}{2}-\frac{Y}{h}+\frac{V}{h}=0.\end{aligned} \tag{3}$$

Energy-momentum tensor

$$3H^2(F_T-F_R)-3H\left(\frac{\dot{h}}{h}F_R-(\dot{R}F_{RR}+\dot{T}F_{RT})\right)+\tfrac{1}{2}(TF_T+RF_R)-\frac{F}{2}+\frac{V}{h}=0. \tag{4}$$

We consider solution in the form $F(R,T)=\alpha R+\beta T, a\sim t^n, h\sim u^n, V\sim u^{n+\frac{1}{3n}}$. Here the interaction expressed by the functions h and V is noninear. Then the pressure p_{eff} and energy density ρ_{eff} we can rewrite as

$$\begin{aligned}p_{eff}&=c^nt^{-3n^2}(3n^3t^{-2}(3\alpha n+2\alpha+\beta)+t^{-1}n^2),\\\rho_{eff}&=c^nt^{-3n^2}\left(9n^3\alpha t^{-2}+c^{\frac{1}{3n}}t^{-1}\right).\end{aligned} \tag{5}$$

In this article researches the $F(R,T)$ theory of gravity in the homogeneous and isotropic spacetime, where R is a scalar of curvature and T is a torsion scalar. Dynamics of the evolution of the universe is described by a power-law solution $a\sim t^n$ and for the case of nonlinear interaction $h\sim u^n$ and $V\sim u^{n+\frac{1}{3n}}$ and certain choice of arbitrary constants, our solution describes the accelerated expansion of the universe.

References

[1] R. Myrzakulov, D. Saez-Gomes, P. Tsyba Cosmological solutions in F(T) gravity with the presence of spinor fields. International Journal of Geometric Methods in Modern Physics Vol. 12 (2015) 1550023 (14 pages)

FRW cosmology of Myrzakulov gravity with *f*-essence

Yerlan Myrzakulov, Nurzhan Serikbayev
L. N. Gumilyov Eurasian National University, Astana 010008, Kazakhstan
ymyrzakulov@gmail.com, znsns@mail.ru

Abstract: In this paper, we consider the Myrzakulov gravity (MG) with the action $S_{37} = \int d^4x\sqrt{-g}[F(R,T)+L_m]$, where R is the curvature scalar and T is the torsion scalar. The particular case, when $F(R,T) = \alpha R + \beta T$ is studied in detail.

1. Introduction to the style guide, formatting of main text, and page layout

Modified theories of gravity have recently attained much attention to explore the dark energy and late accelerated expansion of the universe. The main and well-known examples of such modified gravity theories are $F(R)$ gravity theory and $F(T)$ gravity theory. In this direction, the unification of $F(R)$ and $F(T)$ gravity theories is promised to be the prospective and interesting versions modified gravity theories. One of such unifications of $F(R)$ and $F(T)$ theories was presented by R.Myrzakulov [1,2]. The MG theory is considered as an important gravitational theory which represents, in particular, the evolution of the universe. In this paper, we study the MG with the fermionic matter given by the Myrzakulov fermionic model (M_{33}-model). We consider the particular case of MG, when $F(R,T) = \alpha R + \beta T$, where α and β are real constants.

2. Myrzakulov gravity with f-essence

We consider the MG with f-essence that is some hybrid of the M_{37}-model and the M_{33}-model. Its action reads as

$$S_{37} = \int d^4x\sqrt{-g}[F(R,T)+2K(Y,\psi,\overline{\psi}], \tag{1}$$

where R and T are the curvature and torsion scalars respectively with the expressions

$$R = g^{\mu\nu}R_{\mu\nu}, T = S_\rho{}^{\mu\nu}T^\rho{}_{\mu\nu}, \tag{2}$$

K is some function of its arguments.

3. Particular model for FRW spacetime

To simplify, in this section we make next two simplifications of the problem, namely, we assume that:

1) F has the form

$$F = \alpha R + \beta T, \tag{3}$$

where α and β are some real constants.

2) consider just the Friedmann-Robertson-Walker (FRW) spacetime with metric

$$ds^2 = -dt^2 + a(t)^2(dx^2+dy^2+dz^2). \tag{4}$$

4. Cosmological solution

In this section, we would like to present some simplest cosmological solution of our model. For simplicity, we consider the power law solution that is the scale factor has the form

$$a = a_0 t^n. \tag{5}$$

Next, we get the corresponding expressions for the energy density and pressure

$$\overline{\rho} = 3\frac{n^2}{t^2}, \qquad \overline{p} = \frac{n(2-3n)}{t^2}. \tag{6}$$

The corresponding MFEoS parameter reads as

$$\omega = -1 + \frac{2}{3n}. \tag{7}$$

So if $\lim_{n\to\infty}\omega = -1$ then this model describes the accelerated expansion of the universe with $\omega = -1$. For the matter Lagrangian $\overline{K}$ we have the following expression

$$\overline{K} = C_4 Y^{\frac{2}{2-3n}}. \tag{8}$$

Conclusions

In this paper, we have studied particular case of the MG with f-essence. We constructed some example of exact analytical solution of this model. As the particular solution we considered the scale factor as the power law form. Finally we presented the corresponding form of the K function. The presented results show that the MG with the f-essence can describes the accelerated expansion of the universe.

[1] Myrzakulov R.. Dark Energy in *F(R,T)* Gravity. [arXiv:1205.5266].
[2] Momeni D., Upadhyay S.,·Myrzakulov Y.,·Myrzakulov R. "Cosmic string in gravity's rainbow " Astrophysics and Space Science, vol, 362, 148 (2017).

Plasma-aided ignition and combustion of pulverized coal

V.E. Messerle[1,2], A.B. Ustimenko[3]
[1] *Institute of Thermophysics of SB RAS, Novosibirsk, Russia*
[2] *Combustion Problems Institute, Almaty, Kazakhstan*
[3] *Institute of Experimental and Theoretical Physics of Kazakh National University, Almaty, Kazakhstan*
E-mail: ust@physics.kz

Abstract: This paper presents the results of numerical experiments on plasma assisted ignition of pulverized coal in a plasma-fuel system (PFS). PFS is designed for fuel oil-free start-up of the boilers and stabilization of pulverized coal flame, and represents a pulverized coal burner equipped with plasma torch [1]. Previously via PlasmaKinTherm software which combines kinetic and thermodynamic methods of calculating the processes of motion, heating, thermochemical transformations and fuel mixture ignition in the volume of PFS for two regime parameters of PFS, the power of the plasma torch and ash content of coal, conditions of fuel mixture ignition were determined [2]. Also one of the main regime parameters of PFS providing ignition of the fuel is concentration of coal dust in the fuel mixture. In practice, it varies within a wide range depending on the calorific value of coal, devolatilization, pulverization and transport systems and design of pulverized coal burners. Therefore, conditions for fuel mixture ignition in PFS have been investigated, depending on the concentration of pulverized coal in the fuel mixture in the range from 0.4 to 1.8 kg of coal per 1 kg of air. Numerical simulation was performed for cylindrical PFS of 0.2 m diameter and 2 m of length at fixed consumption of coal (1000 kg/h), the plasma torch power (60 kW) and two values of coal ash content (40 and 70%). The required for coal ignition level of temperature (800°C and above) of the products of thermochemical preparation of fuel for burning (TPFB) and appropriate concentration of combustible components at the PFS output (above 15 vol.%) have been selected as criterions of ignition of the fuel. Distributions of temperature and velocity of coal particles and gas and concentrations of TPFB products along the length of PFS have been obtained. The basic regularities of the TPFB process were revealed, which are in increase of required for ignition the pulverized coal concentration in the fuel mixture with increasing ash content of coal. It is shown that the ignition of coal can be achieved in a wide range of its ash content (20 – 70%) at moderate specific power consumption for the TPFB process (less than 0.06 kWh/kg of coal).

[1] V. E.Messerle, E. I.Karpenko, A. B.Ustimenko, Fuel **126**, 294-300 (2014).
[2] A. V.Messerle, V. E.Messerle, A. B.Ustimenko, High Temperature **55**(3), 352–360 (2017)

Abstracts for Poster Presentations

Perspective Investigations of Physics of Cosmic Rays in Tien Shan Mountain Scientific Station

Sadykov Turlan
Institute of Physics and Technology, Almaty
turlan43@mail.ru

Abstract: The paper presents scientific directions in physics and astrophysics of cosmic rays conducted in the Tien Shan high mountain scientific station. The research program contains the following main sections: at the Horizon-T installation, new processes in cosmic rays are studied at energies above 1017 eV; on the installation of cosmic rays registration, the properties of wide air showers in the region of the fracture of the primary cosmic-ray spectrum (1014-1017 eV) are investigated; the "Hadron-55" installation searches for structures in the particle distributions from the anterior cone of wide air showers at high energies and studies gamma sources of cosmic radiation with energies above 0.5 TeV; Radio-3 installation registers radio emissions from extensive air showers; on the "Groza" installation, a study is being carried out of thunderstorm phenomena at TSHSS; on the "Muon" installation, the degree of tension in the earth's crust of the Almaty seismically active region is investigated with the use of the method of recording cosmic-ray muons of high energies.

[1] Gurevich, AV, Garipov, GK, Sadykov, TK, at all. *Simultaneous observation of lightning emission in different wave ranges of electromagnetic spectrum in Tien Shan mountains*. Atmospheric Research **211**, 73-84 (2018)
[2] A. V. Gurevich, A. M. Almenova, T. Kh. Sadykov at all. *Observations of high-energy radiation during thunderstorms at Tien-Shan*, Physical Review D **94**, 023003 (2016)

Depth profile of aggregate centers and nanodefects in LiF crystals irradiated with swift heavy ions

A. Dauletbekova[1], N. Kirilkin[2], I. Manika[3], J. Manks[3], R. Zabels[3], A. Akilbekov[1], A. Seitbayev[1,4], V. Skuratov[2,5,,6], M. Zdorovets[4,7], M.Baizhumanov[1]

[1]*L.N. Gumilyov Eurasian National University, 2 Satpayev str., 010008 Astana, Kazakhstan*
[2]*Flerov Laboratory of Nuclear Research, Joint Institute for Nuclear Research, Dubna, Russia*
[3]*Institute of Solid-State Physics University of Latvia, Riga, Latvia*
[4]*Astana Branch of Institute of Nuclear Physics, Astana, Kazakhstan*
[5]*National Research Nuclear University MEPhI, Moscow, Russia;*
[6]*Dubna State University, Dubna, Russia*
[7]*Ural Federal University, Yekaterinburg, Russia*
alma_dauletbek@mail.ru

Depth profiles of nanohardness and photoluminescence of F_2 and F_3^+ centers in LiF crystals irradiated with 12 MeV ^{12}C, 56 MeV ^{40}Ar and 34 MeV ^{84}Kr ions at fluences 10^{10} - 10^{15} ions/cm^2 have been studied using laser scanning confocal microscopy, dislocation etching and nanoindentation techniques. The room temperature irradiation experiments were performed at DC-60 cyclotron (Astana, Kazakhstan). It was found that the luminescence intensity profiles of aggregate color centers at low ion fluences correlate with electronic stopping profiles. The maximum intensity of aggregate center luminescence is observed at fluence around 10^{13} ions/cm^2 and rapidly decreases with further increase of fluence (Fig. 1). At the highest ion fluences, the luminescence signal is registered in the end-of-range area only. The depth-resolved nanohardness measurements and dislocation etching data have shown a remarkable hardening effect and increased concentration of dislocations and other nanodefects in the end-of-range region with dominant contribution of defects formed *via* elastic collision (nuclear loss) mechanism[1,2,3].

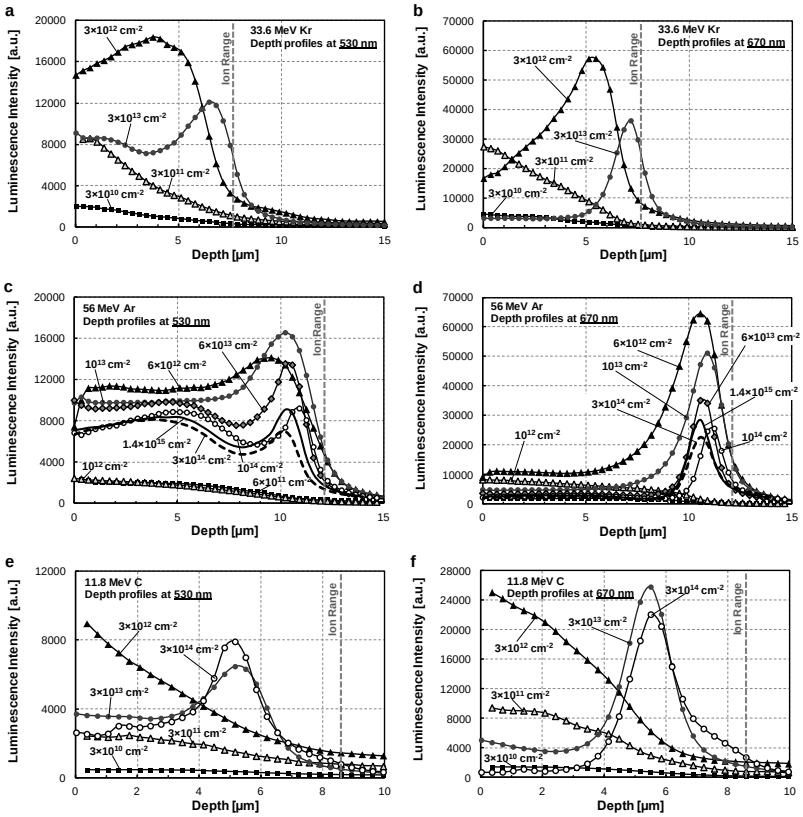

Fig.1. Depth profiles and dose dependence of the luminescence intensity at 530nm and 670 nm for samples irradiated with ^{84}Kr (a, b), ^{40}Ar (c, d) and ^{12}C (e, f) ions. The end of the range is marked with a dashed line.

The observed fading of luminescence intensity at high fluences is related to intense nucleation of dislocations as sinks for aggregate color centers. An activating role of local stress field of dislocations and other extended defects in the evolution of damage structures is suggested.

[1] R. Zabels, I. Manika, K. Schwartz, A. Dauletbekova, M. Baizhumanov, M. Zdorovets "Formation of dislocations and hardening of LiF under high-dose irradiation with 5–21 MeV ^{12}C ions", Appl. Phys. A: 123 (2017)
[2] R. Zabels, I. Manika, K. Schwartz, A. Dauletbekova, M. Baizhumanov, R. Grants, E. Tamanis, M. Z dorovets "MeV-energy Xe ion-induced damage in LiF: The condition of electronic and nuclear stopping mechanisms" Phys. Status Solidi B, 1(2016)
[3] A.Dauletbekova, V. Skuratov, N. Kirilkin, I. Manika, J. Maniks, R.Zabels, A.Akilbekov, A.Volkov, M.Baizhumanov, M.Zdorovets, A. Seitbayev "Depth profiles of aggregate centers and nanodefects in LiF crystals irradiated with 34 MeV 84Kr, 56 MeV 40Ar and 12 MeV 12C ions", Surface and Coatings Technology, In press, corrected proof,Available online 10 April 2018 https://doi.org/10.1016/j.surfcoat.2018.03.096Get rights and content

Fundamental scalar fields and the dark side of the universe

Eduard G. Mychelkin[1] and Maxim A. Makukov[2]
Fesenkov Astrophysical Institute, Almaty, Kazakhstan
[1] mychelkin@aphi.kz, [2] makukov@aphi.kz

Abstract: Starting with geometrical premises, we infer the existence of fundamental cosmological scalar fields. We then consider physically relevant situations in which spacetime metric is induced by one or, in general, by two scalar fields, in accord with the Papapetrou algorithm. The first of these fields, identified with dark energy (DE), has exceedingly small but finite (subquantum) Hubble mass scale ($\approx 10^{-33}$ eV), and might be represented as a neutral superposition of quasi-static electric fields. The second field is identified with dark matter (DM) as an effectively scalar conglomerate composed of primordial neutrinos and antineutrinos in a special tachyonic state.

1. Introduction and outline

In contrast to conventional approaches in cosmology, we do not take any ad hoc scalar fields to describe DE and DM but deduce the first fundamental scalar field from general principles, and only at the last step identify it with DE. This field is represented by neutral superposition of ubiquitous quasi-static electric fields which, in accord with Schwinger's conjecture, should possess their own carriers. These, in our case, should have extremely small but finite mass of about 10^{-33} eV, and might be dubbed "statons". Heuristically, all particles and fields (except gravity) might be comprehended as excited states of the primordial φ-field. Indeed, any particle and antiparticle can annihilate into photons and a photon might be then transformed kinematically (via Doppler effect) into quasi-static state equivalent to φ-field. The entire converse process, from quasi-static field to particles, is, in principle, also conceivable.

Considering cosmological scales in space-flat Friedmannian metric (corresponding to space-conformal symmetry), we supplement the background scalar field with mass- and cosmological term but with no any additional self-interaction potentials. Then, solving the corresponding Klein-Gordon equation, under appropriate integrability conditions, we ultimately arrive at the Gaussian-type cosmological solution for the primordial universe, which allows to identify this antiscalar field with dark energy background.

For the second scalar DM field we propose neutrinos as its constituents, provided that they are tachyons. The discovered effect of neutrino oscillations implies that neutrinos have nonzero masses and thus cannot travel at the speed of light. On the other hand, according to experiments on parity violation in weak interactions, all neutrinos are left (and antineutrinos are right). From heuristic consideration, if neutrino velocities were less than the speed of light, in some reference frames neutrino helicity would swap to the opposite. As this has never been observed (within the accuracy of experiments), the natural conclusion is that neutrino velocities should be greater than the speed of light. Thus, tachyonity of neutrinos can, in principle, be considered as a consequence of the chiral invariance, rather than an ad hoc assumption. If neutrinos are indeed tachyons, there is no necessity to invoke hypothetical right-handed sterile neutrinos to explain the origin of neutrino mass states.

On the scales of galaxies and clusters, for tachyon scalar neutrino–antineutrino conglomerate there are no physical constraints on the value of its density (as opposed to condensate). Thus, this density might be considered as a free parameter and put to be equal to the observed DM density. In quasi-stationary approximation this practically sterile (especially for low energies) neutrino–antineutrino background is distributed all over the universe and produces somewhat denser regions ("smoothed halos") around galaxies and clusters. Tachyonic neutrinos can possess almost stiff equation of state which might be related to the isothermal sphere profile. The latter produces the logarithmic-type potential and leads to the observed flat rotation curves for galaxies.

The structure formation in the early universe is outlined tentatively as follows. Galaxies begin to develop in accord with the standard Jeans instability of baryonic matter. Due to extremely weak interactions with tachyonic neutrinos, small-scale fluctuations of baryonic matter are not washed out. Their subsequent growth accelerates due to permanent background of the surrounding neutrino–antineutrino conglomerate. In turn, only large-scale fluctuations survive in the neutrino conglomerate itself. Therefore, as opposed to bottom-up and top-down scenarios of structure formation, in this case structures at smallest and largest scales develop more or less simultaneously. In this case, observations of very large and relatively early structures such as Huge Large Quasar Group and Hercules–Corona Borealis Great Wall should come as less surprise.

On the whole, in this approach we envisage two well-defined background fields, DE and DM, with comparable densities but drastically different mass scales, making these fields practically noninteracting during almost all of the universe evolution. In this model, there is no necessity to introduce any ad hoc solutions such as self-interaction potentials (except for the mass term), exotic particles unfamiliar to present-day experiments, and modifications of general relativity, to account for the dark side of the universe.

2. References

[1] Mychelkin E.G. & Makukov M.A. (2015) Fundamental scalar fields and the dark side of the universe. *International Journal of Modern Physics D*, **24** 1544025. (*The essay awarded Honorable Mention at 2015 Essay Competition of the Gravity Research Foundation*).

Simpler than vacuum: Antiscalar alternatives to black holes

Maxim Makukov[1] and Eduard Mychelkin[2]
Fesenkov Astrophysical Institute, Almaty, Kazakhstan
[1] makukov@aphi.kz, [2]mychelkin@aphi.kz

Abstract: We seek to compare three distinct physical situations – vacuum, scalar, and antiscalar, which are described by Einstein's equations with vacuum, scalar and antiscalar minimal background (where "anti" is to be understood as in "anti-de Sitter"). We also obtain the exact rotational generalization of the antiscalar Papapetrou spacetime as a viable alternative to the Kerr black hole. The antiscalar metrics appear to be the simplest ones as they do not reveal event horizons and ergospheres, and they do not involve an extra parameter for scalar charge. Static antiscalar field is thermodynamically stable and self-consistent, but this is not the case for the scalar Janis-Newman-Winicour solution; besides, antiscalar thermodynamics is reducible to black-hole thermodynamics. Lensing, geodetic and Lense-Thirring effects are found to be practically indistinguishable between antiscalar and vacuum solutions in weak fields. Only strong-field observations might provide a test for the existence of antiscalar background. In particular, antiscalar solution predicts 5% larger shadows of supermassive compact objects, as compared to vacuum solution. Another measurable aspect is the 6.92% difference in the frequency of the innermost stable circular orbit, characterizing the upper cut-off in the gravitational wave spectrum.

1. Introduction and outline

The field equations of General Relativity relate the energy-momentum tensor $T_{\mu\nu}$ to the Einstein tensor $G_{\mu\nu}$ describing the geometry of spacetime, with the sign of the Einstein tensor to be chosen such that it conforms to observational data at Newtonian limit (the Poisson equation). However, for possible non-Newtonian background media with exotic equations of state the choice of the $G_{\mu\nu}$ sign should be made independently. E.g., the cosmological Λ-term, as a sort of background energy, for a given fixed value might manifest itself in two disguises – de Sitter and anti-de Sitter, both with the same equation of state $p = -\varepsilon$ implying that either energy density ε or pressure p is negative.

Similarly, minimal background scalar field φ with the equation of state $p = \varepsilon$ for timelike gradient $\partial_\mu\varphi$ (or $p = -\varepsilon/3$ for spacelike $\partial_\mu\varphi$) might also be related to positive or negative sign of the Einstein tensor, depending on the conformance to relevant experiments. We refer to these two alternatives as scalar and antiscalar cases. For the scalar case with spherically symmetric boundary conditions one obtains the Janis-Newman-Winicour (JNW) static solution. It reduces to the vacuum Schwarzschild metric in curvature coordinates when the scalar field vanishes; meanwhile, the corresponding rotational generalization of the JNW spacetime reduces to the Kerr metric. For the antiscalar case one obtains the solution first found by Papapetrou and rediscovered by Yilmaz. It stands to reason that changing the sign of the Einstein tensor as discussed above is formally equivalent to changing the sign of the corresponding EMT. Because the scalar EMT is quadratic in field, replacement of the scalar field by its antiscalar counterpart within such interpretation produces the following map: $T_{\mu\nu}(\varphi) \to -T_{\mu\nu}(\varphi)$, i.e. $\varphi \to i\varphi$, implying a similar map for the field source, i.e. the scalar charge σ: $\sigma \to i\sigma$. This interpretation allows us to produce a new algorithm for the transformation of certain scalar-type metrics containing scalar charge into their antiscalar analogs and, thereby, to obtain new antiscalar solutions with subsequent application to observational effects, as covered in this paper [1].

As a whole, we aim to study analytical and observational differences between stationary vacuum, scalar and antiscalar solutions, and pay special attention to the comparison of the Kerr spacetime with the newly obtained exact rotational generalization of the Papapetrou metric [1]:

$$ds^2 = e^{-2\varphi}(dt - a\sin^2\theta\, d\phi)^2 - e^{2\varphi}\rho^2\left(\frac{dr^2}{\Delta} + d\theta^2 + \sin^2\theta\, d\phi^2\right) + 2a\sin^2\theta\,(dt - a\sin^2\theta\, d\phi)d\phi,$$

where $\varphi = Mr/\rho^2$, $\rho^2 = r^2 + a^2\cos^2\theta$, $\Delta = r^2 + a^2$, M and a are the central mass and rotation parameter.

Our new analytical results demonstrate negligible expected observational differences between the two physically distinct situations – for objects in vacuum and in antiscalar background, when considered in weak-field regime. Nevertheless, the differences might be reliably traced in strong fields, e.g., by shadow imaging of the central object in the Milky Way, as undertaken by the Event Horizon Telescope. Our result is that in static case for a fixed mass of compact object the shadow size is about 5% larger in antiscalar approach than in vacuum case. We have also confirmed the 6.92% difference in the ISCO frequency in vacuum and antiscalar case, predicted earlier by Watt & Misner.

When transferring from scalar to antiscalar metrics (static and rotational), the fundamental conclusion is that exactly masses serve as scalar field sources. In the end, the obtained antiscalar solutions are much simpler than their scalar counterparts as they have one free parameter less. At the same time, antiscalar solutions are also simpler than vacuum analogs, as they are deprived of event horizons and ergospheres due to the presence of antiscalar background.

2. References

[1] Maxim A. Makukov and Eduard G. Mychelkin. Simpler than vacuum: Antiscalar alternatives to black holes. *Accepted in Physical Review D, to appear in October issue* (2018). Preprint available at: arXiv:1809.05290 [gr-qc].

Study Resonance Reactions At Heavy Ion Cyclotron DC-60

D.K. Nauruzbayev[1,6], A.K. Nurmukhanbetova[1,2], V.Z. Goldberg[3], G.V. Rogachev[3], M.S. Golovkov[4], A. Volya[5], V.I. Zherebchevsky[6], S.Yu. Torilov[6]

[1]*National Laboratory Astana, Nazarbayev University, Astana, Kazakhstan, 01000*
[2]*Nazarbayev University, Astana, Kazakhstan, 010000*
[3]*Cyclotron Institute, Texas A&M University, College Station, Texas, USA 77843*
[4]*Joint Institute of Nuclear Research, Dubna, Russian 141980*
[5]*Department of Physics, Florida State University, Tallahassee, Florida, USA 32306*
[6]*Saint Petersburg State University, Saint Petersburg, Russia 199034*
E-mail: anurmukhanbetova@nu.edu.kz

Abstract: To study resonance reactions of heavy ions at low energy we have combined the Thick Target Inverse Kinematics Method (TTIK) with Time of Flight method (TF). We used extended target and TF to resolve the identification problems of various possible nuclear processes inherent to the simplest popular version of TTIK. Investigations of the ^{17}O, ^{16}O, ^{15}N, ^{13}C interaction with hydrogen and helium gas targets by using this new approach are presented.

We implemented Thick Target Inverse Kinematics Method [1] for measurements of the resonance scattering at DC-60 cyclotron [2] of heavy ions (2.0 MeV/A maximal energy) at Astana. We added Time of Flight measurements to the conventional TTIK approach as a permanent feature of the studies [3]. In this way, we obtained excitation functions for the interaction of ^{17}O, ^{16}O, ^{15}N, ^{13}C with particles alpha and protons particles using pure helium and hydrogen gas as a target. The measurements were done in a broad range of angles and in the cm energy region of 1.0-5.9 MeV. The experimental excitation functions were analyzed using multilevel multichannel R-matrix code [4] and were compared using cluster-nucleon configuration interaction model [5]. We have a good agreement at low energies between experimental data and theoretical calculations. We were able to make first measurements and analysis of the resonances in ^{17}O+α interaction. The results showed rich cluster structure in ^{21}Ne which deserves a more detailed investigation. Figure 1 presents the 180° degree excitation function for the ^{17}O+α elastic scattering together with a preliminary R- matrix analysis.

Our parameters of the low energy resonances at 1.7-2.1 MeV cm energy are in evident disagreement with the latest ^{17}O(α,n) data [6]. A recent inspection of the data [6] revealed a possible source of an error [7]. This fact stresses out the importance of the complete nuclear information for the analysis of cases of an astrophysical interest.

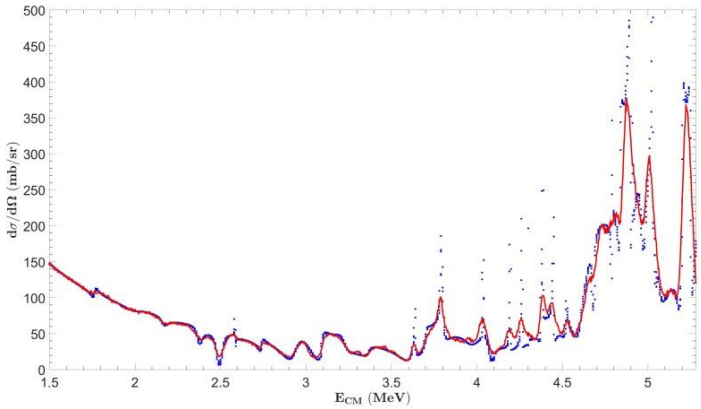

Figure 1.Spectruom of the ^{17}O(α, α) ^{17}O elastic scattering excitation function at 180^0 cm

References:

[1] K.P. Artemov et al., Sov. J. Nucl. Phys., 52 (1990) 406
[2] B. Gikal, S. Dmitriev, P. Apel et al., Physics of Particles and Nuclei Letters 5(7) (2008) 642
[3] A. K. Nurmukhanbetova, et al, NI M in Physics Research Section A: Accelerators, Spectrometers, Detectors and Associated Equipment 847, 125 (2017).
[4] Rogachev G.V. Ph.D. Thysis. Moscow. -Kurchatov Institute.-1999.
[5] A. Volya and V. Zelevinsky, Physics of Atomic Nuclei 77, 969 (2014).
[6] A. Best et al., Physical Review C 87, 45805 (2013).
[7] A. Best, private communication .

Detection of Temperature Profiles with High-sensitivity Chirped Bragg Grating on PMMA Optic Fiber

Sanzhar Korganbayev[a], Madina Jelbuldina[a], Christophe Caucheteur[b], Ole Bang[c], Carlos Marques[d], Daniele Tosi[a]

[a]Nazarbayev University, School of Engineering, 010000 Astana, Kazakhstan; [b]Electromagnetism and Telecommunication Department, Universite de Mons, 31 Boulevard Dolez, Mons, 7000, Belgium; [c]DTU Fotonik, Department of Photonics Engineering, Technical University of Denmark, Denmark; d Instituto de Telecomunicacoes, Campus of Santiago,3810-193 Aveiro, Portugal (8-point type, centered, italicized)
Presenting author e-mail address: madina.jelbuldina@nu.edu.kz

Abstract: In this work we demonstrate a linearly chirped fiber Bragg grating (CFBG) inscribed in a microstructured polymer optical fiber (mPOF) for detecting temperature profiles during thermal treatments. A CFBG of 10 mm length and 0.98 nm bandwidth has been inscribed in a mPOF fiber by means of a KrF laser and uniform phase mask. The CFBG has a high temperature sensitivity of -191.4 pm/°C. The CFBG has been used as a semi-distributed temperature sensor, capable of detecting the temperature profile along the grating length during radiofrequency thermal ablation (RFA). The result is that the higher sensitivity of the CFBG supports the detection of spatially nonuniform temperature fields by means of spectral reconstruction.

1. Introduction

Fiber optic sensors, in particular, linearly chirped fiber Bragg grating (CFBG) sensors have a potential of temperature monitoring during biomedical procedures, thanks to their biocompatibility, miniature size and a possibility to reach a sub-centimeter spatial resolution. A drawback of a standard CFBG on a glass fiber is its low temperature sensitivity of typically 10 pm/°C. In order to increase the sensitivity, recent works showed promising results on the fabrication of CFBGs on polymethyl methacrylate (PMMA) polymer optical fiber (POF), resulted in a thermal sensitivity increase of about one order of magnitude, which allows spectral detection technique to be more effective, and allow the measurement of temperature patterns with a better accuracy [1], [2].

2. Sensor fabrication, experiments and results

A microstructure PMMA polymer optic fiber (mPOF) with sensitivity -191.4 pm/°C was used for detection of temperature patterns during radiofrequency thermal ablation. A 248 nm wavelength pulsed Coherent Krypton Fluoride (KrF) excimer laser system was employed for the inscription of 1 cm length chirped Bragg grating into mPOF. In a first experiment, the mPOF CFBG has been located on a heating plate, detecting a linear temperature profile. Then, the mPOF CFBG has been used for detecting the temperature in proximity of the ablation thermal peak, with a profile close to Gaussian.

For the experimental analysis, we used a Luna OBR4600 optical backscatter reflectometer (OBR, Luna Inc., Roanoke, VA, US) as an interrogation setup to detect the mPOF CFBG spectrum with 1525-1610 nm wavelength range and 33 pm wavelength resolution. The use of an OBR instead of a standard interrogator of FBG analyzer allows the detection of a smaller amount of power, since the PMMA fiber and its connector are lossy devices. In addition, the OBR can measure the group delay.

A demodulation technique for the mPOF CFBG is introduced, which allows converting the CFBG spectrum into the temperature measured in each section of the grating, with 1 mm spatial resolution. The results of thermal reconstruction are shown in Fig. 1. The proposed results represent an important benchmark for application of PMMA CFBG in healthcare for detection of thermal maps with narrow spatial resolution, with immediate application in thermos-therapies.

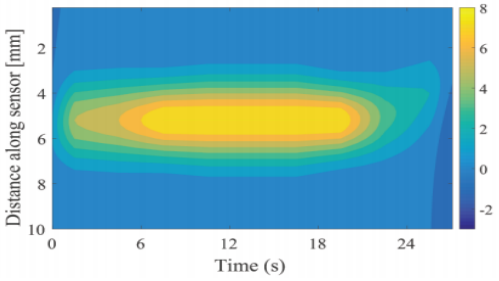

Fig. 1. Measurement of Gaussian temperature gradient with a mPOF CFBG: thermal profile reconstructed with the CFBG as a function of distance along grating and time during ablation. The colorbar shows temperature in °C degrees.

4. References

[1] D. J. Webb, "Fibre bragg grating sensors in polymer optical fibres," Meas. Sci. Technol. **26**, no. 9, p. 092004 (2015).
[2] S. Korganbayev, M. Rui, M. Jelbuldina, X. Hu, C. Caucheteur, O. Bang, B. Ortega, C. Marques, D. Tosi, "Thermal profile detection through high-sensitivity fiber optic chirped Bragg grating on microstructured PMMA fiber," J. Light. Technol., vol. **36**, no. 20, pp. 4723-4729 (2018).

Distribution of concentrations along the length of the channel in the ternary gas system during diffusion mixing

Asembaeva M.K., Moldabekova M.C., Mukamedenkyzy V., Fedorenko O.V.

Al-Farabi Kazakh National University, Almaty, Kazakhstan
050040, Almaty, al-Farabi Ave. 71, Kazakhstan
mukameden@inbox.ru, fedor23.04@mail.ru

Abstract: The distribution of the concentration along the diffusion channel under isothermal diffusion in a ternary gas mixture of different initial composition is considered. It is shown that in systems where the "diffusion-convection" transition takes place, it is possible the appearance of nonlinear concentration distributions along the diffusion channel.

The study of isothermal diffusion in three-component gas mixtures with different compositions [1, 2] has shown the possibility of the appearance of concentration convection, which greatly intensifies the total mass transfer. For ternary gas mixtures, a solution of the system of diffusion equations was obtained, which showed the possibility of nonlinear concentration distributions along the diffusion channel of the two- flask method [3]. As the initial concentration of the component with the highest molecular weight increases, the nonlinearity of the distributions in the diffusion channel increases. The solution of the diffusion equations for the partial concentration values contains exponential terms of the coordinate. This leads to a non-linear distribution of concentrations along the length of the channel, where special mixing regimes appear [4].

The purpose of this work is to study the distribution of concentrations along the channel length in a ternary gas system under diffusion mixing, where the "diffusion-convection" transition takes place.

Fig. 1 shows the distribution of the concentration along the length of the diffusion channel for the ternary gas system H_2 (1)+CO_2(2)–Ar(3) with different initial concentrations. Significant non-linearity of the concentration distribution have to be observed in the conditions $D_{23} << D_{12}, D_{13}$. For the considered system $D_{12} = 0{,}68 \times 10^{-4} m^2 \sec^{-1}$, $D_{23} = 0{,}149 \times 10^{-4} m^2 \sec^{-1}$, $D_{13} = 0{,}85 \times 10^{-4} m^2 \sec^{-1}$.

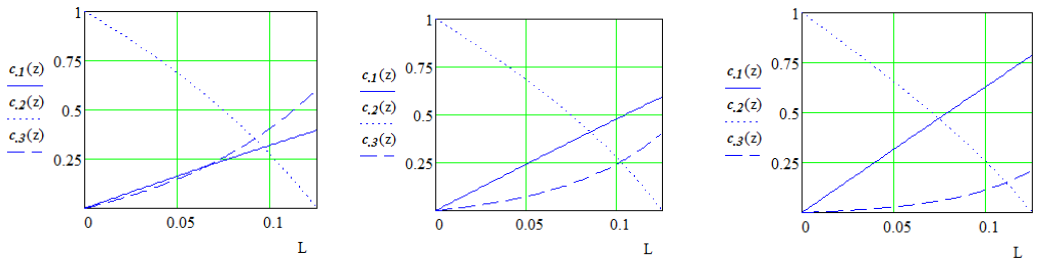

a) b) c)

Fig. 1. Distribution of concentrations along the channel length for the system H_2 +CO_2 – Ar at T = 298,0 K, $L = 70{,}05 \cdot 10^{-3}$ м, $r = 3 \cdot 10^{-3}$ м. a) 0,369H_2+0,604CO_2 –Ar, b) 0,594H_2+0,406CO_2 –Ar, c) 0,786H_2+0,216CO_2 –Ar.

As can be seen from Fig. 1, the nonlinearity of concentration distribution for carbon dioxide and argon is observed along the length of the channel. The presented distributions of the concentrations of the components along the length of the channel confirm the manifestation of special modes of mixing gases, while convective instability is accompanied by gravitational concentration convection.

Thus, the research shows that the feature of quasistationary isothermal three-component diffusion is the possibility of the existence of a nonlinear distribution of the concentrations of components along the length of the diffusion channel.

References

[1] Kosov V N, Kul'zhanov D U, Zhavrin Yu I, Fedorenko O V. Emergence of Convective Flows during Diffusional Mass Transfer in Ternary Gas Systems: The Effect of Component Concentrations. 2017 Russ. J. Phys. Chem. A 91 984.

[2] Zhavrin Yu.I., Kosov V.N., Fedorenko O.V., Akzholova A.A. Some features of the multicomponent gas transfer in the convective instability of gas mixture // Theoretical Foundations of Chemical Engineering. – 2016. – Vol. 50, No. 2. – P. 171-177.

[3] Moldabekova M.S., Asembaeva M.K., Akzholova A.A. Experimental investigation on the stability of the mechanical equilibrium of a four-component mixture with ballast gas // Journal of Engineering Physics and Thermophysics. – 2016. Vol. 89, No. 2. – P. 417-421.

[4] V N Kossov, S A Krasikov, O V Fedorenko, D B Zhakebaev and M K Asembaeva. Experimental and numerical study of the peculiarities of the multicomponent gas mixtures separation under natural gravity convection. Journal of Physics: Conference Series. PTPPE-2017 IOP Publishing IOP Conf. Series: Journal of Physics: Conf. Series 891 (2017) 012113 doi :10.1088/1742-6596/891/1/012113

Spectra of light charged particles from interaction of the 3He ions of energy 50 MeV with construction materials

T.K. Zholdybayev, B.M. Sadykov
Institute of Nuclear Physics, Almaty, Kazakhstan;

Obtaining of new experimental nuclear data from double-differential and integral cross sections of the reactions initiated by stable isotopes of helium for updating the data base required for the design of safety systems of power reactors, development of advanced nuclear technologies, in particular, hybrid nuclear energy systems. Consequently, it is extremely important to obtain experimental cross sections of the reactions used as benchmarks in constructing and development of models of nuclear reaction mechanisms, and to improve their predictive power. Experimental information about the reactions induced by ^{3}He ions is extremely small.

The experiment was performed using a beam from the isochronous cyclotron U-150M of the Institute of Nuclear Physics (Almaty, Kazakhstan). The energy of the incident ^{3}He ions was 50.0 MeV. Self-supporting foil was used as the target. The reaction products were registered by ΔE-E telescope. The double-differential cross sections of the reactions with light particles in exit channels were measured in the angular range 305-135^{o} with angle increments of 15°. The energy distributions integrated over angle were determined on the base of these experimental results.

The experimental results were analyzed using Griffin's model of exciton nuclear decay, which reflects the dynamics of the formation of an excited system and its transition to the equilibrium state. Despite all the ambiguities, the exciton model remains one of the most powerful tools for describing inclusive spectra. It is essentially a statistical model, where the excited states of a compound system are characterized by the number of excited particles and holes. In the two-component exciton model, the proton and neutron degrees of freedom are considered separately. A satisfactory agreement between experimental and calculated values has been achieved.

The main results were published in [1-3]. The work was supported by the Program of Grant funding of scientific researches under Ministry of Education and Science of Republic of Kazakhstan - Grant 0335/GF4.

1. Duisebayev A., Duisebayev B.A., Zholdybayev T.K., et al // Bulletin of the Russian Academy of Sciences: Physics. – 2016. – Vol. 80. – P.894.

2. Duisebayev A., Duisebayev B.A., Zholdybayev T.K., // Bulletin of the Russian Academy of Sciences: Physics. – 2017. – Vol. 81. – P.1170.

3. Zholdybayev T.K., Duisebayev B.A., Sadykov B.M., et al // Acta Physica Polonica B. – 2018. – Vol.49. – P.693.

Estimating Cosmic Curvature with Strong Lens Systems

Mikhail Denissenya[1], **Eric V. Linder**[2,3], **Arman Shafieloo**[4,5]
[1]*School of Science and Technology, Nazarbayev University, Astana, 010000, Kazakhstan*
mikhail.denissenya@nu.edu.kz
[2]*Energetic Cosmos Laboratory, Nazarbayev University, Astana, 010000, Kazakhstan*
[3]*Berkeley Center for Cosmological Physics & Berkeley Lab,*
evlinder@lbl.gov
[4]*Korea Astronomy and Space Science Institute, Daejeon, Korea*
[5]*University of Science and Technology, Daejeon, Korea*
shafieloo@kasi.re.kr

Abstract: Cosmic spatial curvature is a fundamental geometric quantity of the Universe. We develop a model independent geometrical approach to measure spatial curvature directly from cosmological observations. The curvature is determined by employing measurements of strong lensing time delays and supernova distances. We propose two complimentary curvature estimators K and Ω_k which differ by error propagation characteristics and redshift dependence. Our simulations of redshift distributions and distance measurements of lenses and sources showed that the model independent methods can constrain the curvature to ~ 0.006 with next generation measurements.

1. Introduction

Spatial curvature is one of the two fundamental quantities defining the Robertson-Walker (RW) metric of a homogeneous and isotropic spacetime. Unlike spacetime curvature, which depends on the second derivative of the scale factor $a(t)$ entering the metric, spatial curvature k is a purely geometric quantity. The most popular theories of early universe inflation predict spatial flatness $k = 0$, so any detection of nonzero spatial curvature would have significant impact on our understanding of the early universe and cosmic evolution.

2. Cosmic curvature and distances

The curvature can be determined by measuring the distance to a gravitationally lensed source, r_s, to the object doing the lensing, r_l, and the distance between the two along the null geodesic followed by the light ray, r_{ls}. The following relation

$$r_{ls} = r_s\sqrt{1+\Omega_k r_l^2} - r_l\sqrt{1+\Omega_k r_s^2}, \tag{1}$$

which comes from the properties of null geodesics in Robertson-Walker space-time, does not depend at all on the Friedmann equations. The distance r_{ls} between lens and source can be found through strong gravitational lensing, The distances r_l and r_s relative to the observer can be measured through geometric probes such as Type Ia supernova distances or baryon acoustic oscillations (BAO).

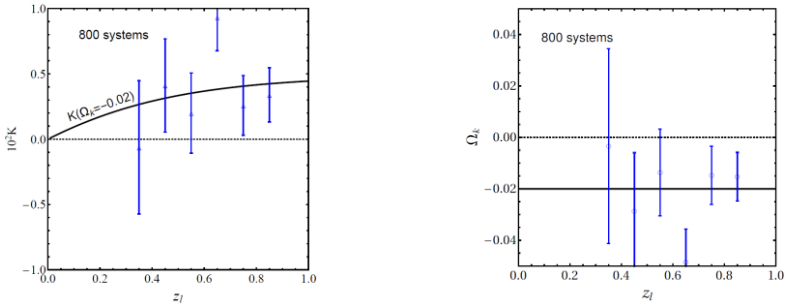

(a) (b)

Fig. 1. (a) The K curvature estimator gives a specific redshift dependence at non-zero curvature; (b) the estimation of the value of the curvature Ω_k and its consistency with redshift independence. The solid black curve shows the input value $\Omega_k = -0.02$. Blue points with error bars show the results of our simulated measurements.

3. Curvature estimation

We express the curvature Ω_k in terms of observables and propose the so called "K test"

$$K = \frac{1}{D_{\Delta t}} - \frac{1}{r_l} + \frac{1}{r_s}, \tag{2}$$

where $D_{\Delta t}$ is the time delay distance from the strong gravitational lensing. We consider ensembles of measurements over a range of redshifts such as would be delivered by next generation surveys. Fig.1. shows that two quantities, K and Ω_k, provide an accurate estimate of cosmic spatial curvature and the redshift dependence without taking derivatives or extrapolations of data, see [1] for more details.

4. References

[1] M. Denissenya, E. V. Linder, A. Shafieloo Cosmic Curvature Tested Directly from Observations, Journal of Cosmology and Astroparticle Physics 1803, 041 (2018).

Stimulated Emission of Laser Dyes with Plasmon Nanoparticles in Porous Aluminum

Aimukhanov A. K., Ibrayev N. Kh., Zeinidenov A.K.
Institute of Molecular Nanophotonics, Buketov KarSU, Karaganda
a_k_aitbek@mail.ru

Abstract: The properties of stimulated emission of laser dyes dye in the pores of PAO were studied. Stimulated emission of laser dyes molecules in the pores of alumina was obtained at the maximum of fluorescence band. The parameters of stimulated emission of molecules laser dyes in the pores of alumina were determined. It is shown that low-Q generation of stimulated emission in the film $Q \geq 1 * 10^2$ relates to the fact that the ray geometry of in the pores is not approximate to the ray geometry for the case of total internal reflection, resulting in the increase of radiative losses. The presence of plasmon nanoparticles in PAO results in the increase in fluorescence intensity and lowering of the generation threshold of dye stimulated emission.

1. The results and their discussion

The morphology of the surface and transverse cleavage of the film obtained on a scanning electron by microscope MIRA 3LMU is shown in Fig. 1 (a, b). The measurements were carried out at accelerating voltage of 7 kV, with a working distance of 7 mm in a high vacuum. On the film surface, same ~ 60 nm diameter pores and with pore distance of 80 nm are observed.

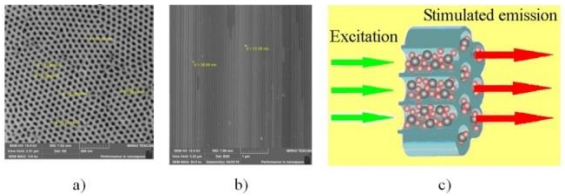

Fig. 1. SEM image of the surface (a), of the transverse cleavage of the porous film (b) and the scheme of generation of the stimulated emission of the dye with NPs in the PAO (c)

The absorption spectrum of plasmon nanoparticles in the PAO matrix is overlaps well with the absorption and fluorescence spectra of laser dyes, indicating that the resonance conditions between the plasmon nanoparticles and laser dyes spectra are met. The fluorescence of the dye in porous alumina with plasmon nanoparticles depends on the concentration of plasmon nanoparticles. The luminescence intensity increases up to the critical concentration of plasmon nanoparticles, and a further increase plasmon nanoparticles results in quenching of the fluorescence.

The maximum of the stimulated emission of laser dyes molecules in the PAO matrix is observed at the wavelength of the fluorescence spectrum maximum. Such low-quality generation of stimulated emission is due to the fact that in the case of a cylindrical resonator on a nanometer scale, ray geometry in the pores is not approximate to ray geometry for the case of total internal reflection, and as a result, radiative losses increase. Comparison of experimental data for the samples with plasmon nanoparticles and without them demonstrated a correlation between changes in the emission intensity and half-width emission spectrum. The presence of plasmon nanoparticles in porous alumina results in the increase in fluorescence intensity and lowering the threshold of dye stimulated emission. In pores with plasmon nanoparticles, reduced pulse duration of stimulated emission is observed.

2. References

[1] A. K. Aimukhanov, N. Kh.Ibrayev Influence of gold nanoparticles on the properties of stimulated emission of 6-amino-1h-phenalen-1-one in the pores of anodized aluminum oxide // J. Lum., 204, pp. 216-220 (2018).
[2] A. K. Aimukhanov, N. Kh. Ibrayev, A. M. Esimbek. Properties of stimulated emission of the PM567 dye in pores of anodized aluminum oxide // Russian Physics Journal – 2018. – Vol. 60, No. 10. P. 1667-1673.
[3] Ibrayev N.Kh., Zeinidenov A.K., Aimukhanov A.K., Napolskii K.S. Stimulated emission from aluminium anode oxide films doped with rhodamine 6G // Quantum Electronics. 2015. – V.5, No. 7, – P. 663 – 667.
[4] Zeinidenov A.K., Ibrayev N.Kh., Aimukhanov A.K. The laser active element based on dye on porous aluminia // Eurasian chemico–technological journal. – 2014. – Vol. 16, № 1. – P. 73–78.
[5] Ibrayev N.Kh., Zeinidenov A.K. Plasmon–enhanced stimulated emission of Rhodamine 6G in nanoporous alumina // Laser Physics Letters. – 2014. – Vol. 11, №. 11. – P. 1–4.
[6] Ibrayev N.Kh., Zeinidenov A.K., Aimukhanov A.K. The influence of silver nanoparticles on the stimulated luminescence of Rhodamine 6G solutions // Optics and Spectroscopy. – 2014. – Vol. 117, № 4. – P. 540–544.

Photoinduced Electron Processes in Nanocomposite Materials for Photovoltaics

Niyazbek Ibrayev, Evgeniya Seliverstova, Dmitriy Afanasyev, Aitbek Aimukhanov
Institute of Molecular Nanophotonics, Buketov KarSU, Universitetskaya str. 28, Karaganda 100028, Kazakhstan.
Author e-mail address: niazibrayev@mail.ru

Abstract: Currently organic-based solar cells are the one of the promising converters of solar energy to electrical. In this work the results of studies of photostimulated electron processes in heterogeneous systems based on metal oxides, semiconductor polymers, complex organic molecules and plasmon nanoparticles in order to create scientific and technological foundations for the production of functional materials for photovoltaics are presented and discussed.

Currently, the dye-sensitized solar cells (DSSC) are the one of the promising converters of solar energy to electrical [1-3]. The explanation for this is their low cost and ease of production of this type of solar cells. The technology of manufacturing of DSSC is much easier and cheaper in comparison with silicon solar cells. Most DSSC research based on TiO_2 and ZnO is concentrated on two main problems: (1) development of simple methods for synthesizing semiconductor nanostructures that have good electrically conductive properties and (2) the search for suitable dye sensitizers. However, little detailed research has been done to study the mechanism of injection, electron transport, and recombination of charge carriers in DSSC.

In this paper, we present the results of studies [1–12] of photostimulated electron processes in heterogeneous systems based on metal oxides, semiconductor polymers, complex organic molecules and plasmon nanoparticles in order to create scientific and technological foundations for the production of functional materials for photovoltaics.

As a result of this work, technologies for obtaining of arrays of nanostructures of oxide semiconductors were developed and the processes of electron transfer at the semiconductor-organic chromophore interface were studied. The influence of the morphology of nanostructures, the chemical nature of the organic molecule, the multiplicity of the electronic state on the photovoltaic and electrotransport properties of nanocomposite materials were studied. Technologies for manufacturing organic solar cells with a planar arrangement of the donor/acceptor layers and with a bulk heterojunction based on semiconductor polymers and fullerenes have been developed. Structural, optical and electrical characteristics of solar cells are determined. Methods for depositing of plasmon silver nanoparticles in various functional layers of an organic solar cell have been developed. It is shown that a significant increase in the cell efficiency was observed when silver nanoparticles are deposited on the ITO surface. The technology of synthesis of organo-inorganic halide perovskite films has been optimized and the processes of generation and transport of charge carriers have been studied. The characteristic times of migration and recombination of electronic excitations are established. As a result of the work, new data on the effect of the structure of the medium on the physicochemical properties of organic and inorganic nanocomposite materials have been obtained. This will make it possible to create scientific basis for obtaining new materials with prescribed properties for organic photovoltaics, molecular electronics and hydrogen energy.

[1] N. Ibrayev, E. Seliverstova, N. Nuraje, "FRET–Designed Dye–Sensitized Solar Cells to Enhance Ligt Harvesting," Mat. Sci. Semiconduct. Processing **31**, 358 (2015).
[2] B. Ilyassov, N. Ibrayev, N. Nuraje, "Hierarchically assembled nanostructures and their photovoltaic properties," Mat. Sci. Semiconduct. Processing **40**, 885 (2015).
[3] D.A. Afanasyev, N.A. I.I. Davidenko, Davidenko, N.Kh. Ibrayev, "Photovoltaic Properties of Films of Polyvinyl Alcohol–Xanthene Dye Composites," High En. Chem. **49,** 255 (2015).
[4] D.A. Afanasyev, N.Kh. Ibrayev, T.M. Serikov, A.K. Zeinidenov, "Effect of the titanium dioxide shell on the plasmon properties of silver nanoparticles," Rus. J. Phys. Chem. A **90,** 833 (2016).
[5] A. K. Zeinidenov, N. Kh. Ibrayev, V. K. Gladkova, "Effect of Silver Nanoparticles on Spectral–luminescent and Generation Properties of Rhodamine 6G in Aqueous Alcohol Solutions," Rus. J. Phys. Chem. A **12,** 2441 (2016).
[6] A.K. Aimukhanov, N. Kh. Ibrayev, T. M. Serikov, "Effect of Formulas of Titanoxide Compositions on the Photovoltaic Characteristics of Solar Cells," Rus. J. Phys. Chem. A **90,** 2489 (2016).
[7] N.Kh. Ibrayev, B. R. Ilyassov, D. A. Afanasyev, "Influence of the Morphology of ZnO Nanostructures on Luminescent and Photovoltaic Properties," Optics Spectrosc. **122,** 462 (2017).
[8] N. Ibrayev, E. Seliverstova, A. Ishchenko, M. Kudinova, "The effect of sulfonate groups on spectral-luminescent and photovoltaic properties of squarylium dyes," J. Photochem. Photobiol. A **306,** 570 (2017).
[9] Md. Moniruddin, B. Ilyassov, E. Seliverstova, Y. Shabdan, N. Bakranov, N. Ibrayev, N. Nuraje, "Bioinspired Study of Energy and Electron Transfer in Photovoltaic System," J. Exp. Nanosci. **10,** 1 (2017).
[10] Gadgil T., Ibrayev N., Nuraje N., "Photocatalytic Water Oxidation" in *Heterogeneous Photocatalysis: From Fundamentals to Green Applications*, J. C. Colmenares, Yi-Jun Xu, ed. (Springer Berlin Heidelberg, Berlin, 2016).
[11] N. Ibrayev, E. Seliverstova, D. Afanasyev, A. Nurmakhanova, I. Davydenko, N. Davydenko, "Features of deactivation of excited states of cationic polymethine dye in the matrices of halogen-containing derivatives of poly-N-epoxypropyl carbazole," J. Lum. **124,** 349 (2018).
[12] Md. Moniruddin, B. Ilyassov, X. Zhao, E. Smith, T. Serikov, N. Ibrayev, R. Asmatulu, N. Nurage, "Recent progress on perovskite materials in photovoltaic and water splitting applications," Mat. Today En. 7, 246 (2018).

Thermalization Effects on Temperature Changes in Magnetic-Inertial Fusion Devices

Zh.Seksembayev[1], **S.Sakhiyev**[2]
[1]*L.N.Gumilyov Eurasian National University, Satpayev str., 2, 010008 Astana, Kazakhstan*
[2]*Abai Kazakh National Pedagogical University, Dostyk ave., 13, 050010 Almaty, Kazakhstan*
jandos_s90@mail.ru

Abstract: The fusion device with magnetic-inertial confinement is considered. As a fuel DD, as well as DT mixtures taken and the burning kinetics of such dense hot plasma are studied. Energetic nuclear reaction ion products are supposed to leave their energy in local burning areas leading to temperature rise of it. Using kinetic equations of thermonuclear burning and modern refined nuclear reaction rate data, the burning scenarios of the mentioned fuel types obtained in recent studies. As the result, burning properties of plasma in thermonuclear devices with inertial-magnetic confinement of plasma estimated.

1. Introduction

For the traditional fusion fuel types DD and DT, main reactions that take place and define the burning nature of the fuel can be found in [1]. One of the scheme of realization of magnetic-inertial fusion described in [2]. There the authors propose to use combination of Z-pinch with laser pulse to ignite fuel and start self-supporting fusion process. In this kind of device, the fuel is contained in extreme conditions allowing the nuclear reactions actively take place. The temperature of plasma due to strong shock waves and electromagnetic forces is brought up to several keV values. At these values, the rates of fusion reaction are very high. The reaction rate is maximum for D+T reaction among the other main reactions in thermonuclear burning [1].

2. Thermalization of energetic particles

The interaction between ions in hot dense plasma described in [3]. Fast reaction products in hot plasma should interact with bulk particles. The energetic particle gets temperature equalized with the bulk, the exceed energy is stored as overall kinetic energy of local burning zone, i.e. rising its average temperature. Since at such conditions the confinement times are several orders much higher than the thermalization times, then we can consider that thermalization occurs immediately and one should observe temperature rise of local thermonuclear burning volume.

3. Results

Within the described approach, we obtain the temperature changes, considering the initial conditions of fusion fuels shown in [2]. The energy release in time is described using kinetic equations from [2, 3]. Here also we take into account radiation losses in the form of bremsstrahlung. The results for energy release, losses, and also local burning zone temperature changes are given in recent studies [4], and shown here in Fig. 1. The approach for fast nuclear reaction products thermalization and temperature change evaluations described and justified.

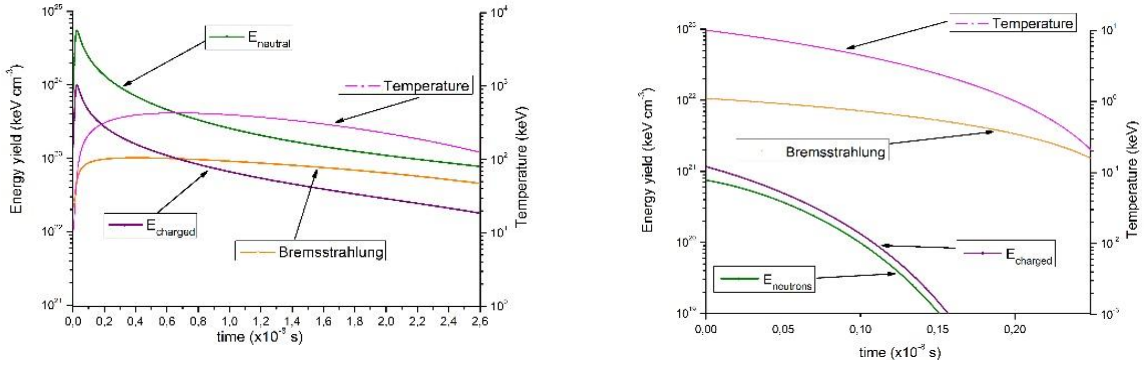

Fig. 1. Energy release and temperature change for DT and DD fuels burning, respectively [4].

As the result, we obtain energy efficient fuel to be DT, while DD fuel observes no temperature rise due to prevalence of radiation losses over energy output.

4. References

[1] V.T. Voronchev, V.I. Kukulin, Yadernaya Fizika, 63, 12 (2000), p.2147-2162.
[2] V.T. Voronchev, V.I. Kukulin, Yadernaya Fizika, 73, 1 (2010), p.41-61.
[3]. D.V. Sivukhin, “Kulonovskie stolknoveniya v polnostyu ionizovannoi plasme,” in Voprosy teorii plasmi, V.4, №,5 (1964), pp.81-187.
[4] Zh. Seksembayev, V.Kukulin, S.Sakhiyev, Phys. Scr. 93 (2018), 085602.

Complex-Range Gaussians as a Basis for Treatment of Charged Particle Scattering

D.A. Sailaubek[1*], O.A. Rubtsova[2], V.I. Kukulin[2]

[1] *Faculty of Physics and Technical Sciences, Gumilyov Eurasian National University, 010000 Astana, Kazakhstan*

[2] *Skobeltsyn Institute of Nuclear Physics, Moscow State University, 119991 Moscow, Russia*

**s.dinmuhamed@gmail.com*

We suggest a new technique towards solving scattering problems with charged particles [1]. The method is based on the Wave-Packet Continuum Discretization (WPCD) approach and Coulomb wave-packet (CWP) formalism [2]. CWPs are constructed as integrals of regular Coulomb wave functions over discretization intervals and thus represent normalized states in continuum. An evident advantage of the CWP formalism is a possibility to adjust a discretization mesh to the problem in question[†]. On the other hand, exact CWPs can be evaluated only numerically which represents some inconvenience in practical calculations. Thus, we employ here some special representation for the Coulomb wave-packets, the so called complex- range Gaussian basis (CRGB) [4]. The real-valued functions of this basis are constructed from Gaussians with complex scale parameters, so that they oscillate in coordinate space and very well suited to approximate wave functions of excited and continuum states (see Fig. 1).

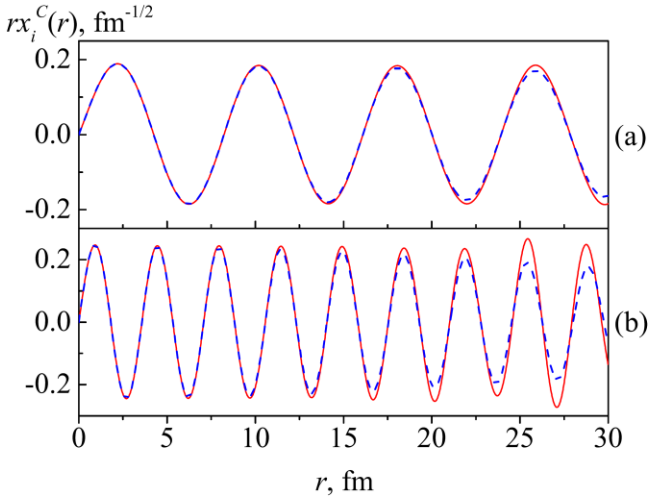

Figure 1: Coordinate behavior of the exact Coulomb wave-packets (dashed curves) and their approximations (solid curves) in the CRGB at $E = 10.15$ MeV (a) and $E = 50.6$ MeV (b).

With the developed technique, off-mass-shell elements of the Coulomb-nuclear T-matrix can be found in a wide energy region from a two-fold diagonalisation procedure for the total and Coulomb Hamiltonian matrices on the CRGB. The efficiency method is illustrated with calculations of partial phase shifts for nucleon and deuteron elastic scattering off alpha particles where its accuracy and convenience is demonstrated clearly.

References

[1] D.A. Sailaubek, O.A. Rubtsova, V.I. Kukulin, Eur. Phys. J. A, **54** 7 (2018) 126

[2] O.A. Rubtsova, V.I. Kukulin, V.N. Pomerantsev, Ann. Phys. **316**, 613 (2015).

[3] I. B. Abdurakhmanov, A. S. Kadyrov, I. Bray, Phys. Rev. A **94**, 022703 (2016).

[4] E. Hiyama, Prog. Theor. Exp. Phys. 01A204 (2012).

[†]For example, recently CWPs has been successfully employed for a calculation of cross sections for the antiproton impact ionization of the hydrogen atom at very low antiproton incident energy (few keV) in the close-coupling approach [3].

Inhomogeneous fluids for warm inflation

Myrzakul S.R.[1,2], Sebastiani L.[1], Myrzakulov R.[1]
[1]*Department of General & Theoretical Physics and Eurasian Center for Theoretical Physics, Eurasian National University, Astana 010008, Kazakhstan,*
[2]*Al-Farabi Kazakh National University*
srmyrzakul@gmail.com

Abstract: Inhomogeneous fluid models for warm inflation are investigated. The early-time acceleration is supported by inhomogeneous fluid whose coupling with radiation leads to the radiation dominated era after inflation (this thesis is based on the article [1]).

Accelerated cosmology is the result of repulsive gravity in our universe. Standard matter and radiation cannot play this role. To describe inflation, an (effective) fluid which violates the Strong energy condition (the ratio between pressure and energy density must be smaller than -1/3) has to be introduced in the theory. This effective fluid can be given by a scalar field with potential, can be the result of some modifications to the gravitational action of Einstein's theory or can be merely an exotic "dark" fluid with an (effective) negative pressure. Generally speaking, it is clear that, in order to exit from inflation, the fluid must have an inhomogeneous Equation of State (EoS) parameter,

$$\omega(\rho) = \frac{p}{\rho}, \tag{1}$$

depending on the energy density. Here, p, ρ are the pressure and the energy density of the fluid.

Our aim is to study fluid cosmology in the warm inflation scenario, generalizing the results of scalar field inflation. The Friedmann equations are

$$\frac{3H^2}{\kappa^2} = \rho_{rad} + \rho, \quad -\frac{1}{\kappa^2}\left(2\dot{H} + 3H^2\right) = p_{rad} + p, \tag{2}$$

where the radiation contribute has been also considered, and the conservation law leads to

$$\begin{aligned} \dot{\rho} + 3H\rho(1+\omega(\rho)) &= -\Upsilon f(\rho), \\ \dot{\rho}_{rad} + 4H\rho_{rad} &= \Upsilon f(\rho), \qquad 0 < \Upsilon, f(\rho). \end{aligned} \tag{3}$$

Here, $f(\rho)$ is a general (positive) function of the energy density of the fluid with the dimension $[f(\rho)] = [\rho]$, and therefore $[\Upsilon] = [1/\kappa]$ is a friction coefficient and it is assumed to be positive to produce positive energy density for radiation. Up to now, the only requirement is that $3H\rho(1+\omega(\rho)) \sim \Upsilon f(\rho)$ during inflation, $3H\rho\,|(1+\omega(\rho))| < \Upsilon f(\rho)$ corresponding to strong dissipation regime, but $\Upsilon f(\rho) \ll H\rho$ to avoid radiation contribute to the dynamics.

The (quasi) de Sitter solution of inflation evolves with the (positive) Hubble flow functions

$$\varepsilon_1 = -\frac{\dot{H}}{H^2}, \quad \varepsilon_2 = -\frac{2\dot{H}}{H^2} + \frac{\ddot{H}}{H\dot{H}} \equiv \frac{\dot{\varepsilon}_1}{H\varepsilon_1}, \tag{4}$$

which have to remain small until the end of inflation, when acceleration finishes end $\varepsilon_1 \ll 1$ (note that $\dot{H} < 0$). By assuming $H^2 \gg \kappa^2\rho/3$, we get for these functions,

$$\varepsilon_1 = \frac{3(\omega(\rho)+1)}{2} + \frac{\Upsilon}{2H}\left(\frac{f(\rho)}{\rho}\right), \quad \varepsilon_2 = \frac{3H\dot{\omega}(\rho) + \Upsilon\left(\dot{f}(\rho)/\rho\right)}{3H^2(1+\omega(\rho)) + \Upsilon H\left(f(\rho)/\rho\right)} + \frac{3\Upsilon f(\rho)}{2H\rho}. \tag{5}$$

When $\Upsilon = 0$ we recover the formulas for classical inflationary scenario. Thus, the spectral index n_s and the tensor-to scalar ratio r read

$$n_s = 1 - 2\varepsilon_1 - \varepsilon_2, \quad r = 16\varepsilon_1. \tag{6}$$

More in-depth studies are presented in our papers [1-4], where various examples of viable inflation with inhomogeneous fluids are considered, which are consistent with the latest cosmological data from the Planck satellite [4] constrain indexes as $n_s = 0.9603 \pm 0.0073(68\%CL)$ and $r < 0.11(95\%CL)$.

References

[1] Myrzakul S.R., Sebastiani L., Myrzakulov R. Inhomogeneous fluids for warm inflation Astrophys.Space Sci. 357 (2015) 2, 168.

[2] Myrzakul S.R., Sebastiani L., Myrzakulov R. Inhomogeneous viscous fluids in FRW universe and finite-future time singularities. Astrophys.Space Sci. 350 (2014) 845-853.

[3] Myrzakul S.R., Sebastiani L., Myrzakulov R. Warm inflation in Horndeski gravity. Gen.Rel.Grav. 49 (2017) 7, 90.

[4] Myrzakul S.R., Sebastiani L., Myrzakulov R. Reconstruction of k-essence inflation in Horndeski gravity The European Physical Journal Plus (2017) 132: 433.

[5] Ade, P.A.R., et al. (Planck Collaboration): arXiv:1303.5076 [astroph.CO] (2013).